AD_____

THREE-DIMENSIONAL COMPUTER GRAPHICS BRAIN-MAPPING PROJECT

Annual/Final Report

Robert B. Livingston, M.D.

March 24, 1988

Supported by

U.S. ARMY MEDICAL RESEARCH AND DEVELOPMENT COMMAND
Fort Detrick, Frederick, Maryland 21701-5012

Contract No. DAMD17-86-C-6093

University of California, San Diego
La Jolla, CA 92093

The views, opinions and/or findings contained in this report are those of the author and should not be construed as an official Department of the Army position, policy or decision unless so designated by other documentation.

SECURITY CLASSIFICATION OF THIS PAGE

REPORT DOCUMENTATION PAGE

Form Approved
OMB No 0704-0188
Exp. Date Jun 30, 1986

1a. REPORT SECURITY CLASSIFICATION Unclassified	1b. RESTRICTIVE MARKINGS
2a. SECURITY CLASSIFICATION AUTHORITY	3. DISTRIBUTION/AVAILABILITY OF REPORT Approved for public release; distribution unlimited
2b. DECLASSIFICATION/DOWNGRADING SCHEDULE	
4. PERFORMING ORGANIZATION REPORT NUMBER(S)	5. MONITORING ORGANIZATION REPORT NUMBER(S)
6a. NAME OF PERFORMING ORGANIZATION The University of California, San Diego 6b. OFFICE SYMBOL (If applicable)	7a. NAME OF MONITORING ORGANIZATION
6c. ADDRESS (City, State, and ZIP Code) La Jolla, California 92093	7b. ADDRESS (City, State, and ZIP Code)
8a. NAME OF FUNDING/SPONSORING ORGANIZATION US Army Medical Research & Development Command 8b. OFFICE SYMBOL (If applicable)	9. PROCUREMENT INSTRUMENT IDENTIFICATION NUMBER DAMD17-86-C-6093
8c. ADDRESS (City, State, and ZIP Code) Fort Detrick, Frederick, Maryland 21701-5012	10. SOURCE OF FUNDING NUMBERS PROGRAM ELEMENT NO. / PROJECT NO. / TASK NO. / WORK UNIT ACCESSION NO.

11. TITLE (Include Security Classification)
(U) Three-Dimensional Computer Graphics Brain-Mapping Project

12. PERSONAL AUTHOR(S)
Robert B. Livingston, M.D.

13a. TYPE OF REPORT	13b. TIME COVERED	14. DATE OF REPORT (Year, Month, Day)	15. PAGE COUNT
Annual/Final	FROM 3/10/86 TO 12/24/87	1988 March 24	140

16. SUPPLEMENTARY NOTATION
Annual covers period of time March 10, 1987 - December 24, 1987

17 COSATI CODES			18. SUBJECT TERMS (Continue on reverse if necessary and identify by block number)
FIELD	GROUP	SUB-GROUP	Keywords - Brain Mapping, Neuroanatomy, Computer Graphics, Image Processing, Data bases, anatomical models (AT)

19. ABSTRACT (Continue on reverse if necessary and identify by block number)

In response to the AMCRDC Broad Agency Announcement, we assembled a core group at UCSD and the Scripps Clinic and Research Foundation, which, together with participating national advisors, could solve problems that stand in the way of engaging computer graphics and database management more effectively in the solution of neurosciences problems. Labor-intensive, data-laden problems abound for image acquisition, image editing and manipulation, data storage and retrieval, 2-D and 3-D reconstructions, and the display and analysis of whole animal and human brains at microscopic levels of detail. We aimed at improving the interface between neuroanatomy and computer graphics systems so that the groundwork for accurate quantitative morphology will be satisfactory from the neurosciences viewpoint in proceeding to achieve whole brain reconstructions. We have succeeded in developing sound methods for preparing whole brains for sectioning and microscopic analysis, with controls for reducing brain distortions in three dimensions and for correcting the inevitable distortions that accompany slicing brain tissue at microscopic intervals, for combining structure/function data, and for beginning an analysis of whole brain tissue sections at microscopic levels of detail.

20. DISTRIBUTION/AVAILABILITY OF ABSTRACT	21. ABSTRACT SECURITY CLASSIFICATION
☐ UNCLASSIFIED/UNLIMITED ☒ SAME AS RPT ☐ DTIC USERS	Unclassified
22a. NAME OF RESPONSIBLE INDIVIDUAL Mary Frances Bostian	22b. TELEPHONE (Include Area Code) 301-663-7325
	22c. OFFICE SYMBOL SGRD-RMI-S

DD FORM 1473, 84 MAR — 83 APR edition may be used until exhausted. All other editions are obsolete.

SECURITY CLASSIFICATION OF THIS PAGE

Table of Contents

INTRODUCTION

The central aim of the Brain Mapping Project is to contribute to the solution of an exceedingly important and refractory problem: how to go from a whole human brain to an accurate computer graphics representation of its three dimensional structure/function organization at microscopic levels of detail.

To comprehend how human brains govern multi-factorial processes like sensory processing, decision making, and behavior, it is necessary to be able to analyze and to compare brain structure/function relations in whole human brains.

Brain structure and function are two sides of the same coin. Yet little is known about brain structure/function relations except piecemeal, in small-scale and scattered circuits. Brain functions, however, are globally integrated: this mandates integration of innumerable lower order integrative processes.

"Mapping" the human brain is further complicated by the fact that there are gross morphological differences among individual human brains. Techniques such as we are developing are essential to begin acquiring normative data that can reflect the range of differences in gross and microscopic neuroanatomical form and function among so-called "normal" individuals. Establishment of such a database requires accurate mapping and comparison of a great many brains. This is a technically and quantitatively formidable task for which there presently exists no adequate conceptual framework and no sufficiently competent hardware or software to acquire, manipulate, display and analyze the necessary images.

Whole human brain structure/function representations have not been feasible heretofore because of the enormously labor-intensive, computation-intensive requirements of the task. There are five major challenges: (1) acquisition and identification of data that are desirable for three dimensional whole brain mapping; (2) intelligible and efficient management of the massive amounts of data (measured in giga- and tera-bytes) necessary to represent whole human brains at microscopic levels of detail; (3) morphometric manipulations necessary to de-deform microscopically thin whole brain tissue sections--which are inevitably deformed in the process of sectioning--to conform to their pre-sectioned form, and to re-de-deform sequences of sectional images to conform to three dimensional requirements, some of which are not determinable two dimensionally; (4) display, comparison and analysis of brain mapping data including statistical analysis; (5) creation and maintenance of a widely sharable

neurosciences database that includes neuro-anatomy, -physiology, -pharmacology, -pathology, -psychophysics and -psychological correlates of normal and abnormal brain organization.

The Brain Mapping Project addresses how to overcome to a modest degree the first of these five challenges, while paying due regard to the requirements imposed by the other four challenges on the first.

INTRODUCTORY COMMENTS: THE IMPORTANCE OF THREE-DIMENSIONAL COMPUTER GRAPHICS DISPLAY AND ANALYSIS TO UNDERSTANDING THE INTEGRATIVE ACTIONS OF THE HUMAN BRAIN

The purpose of this section is to present a few heuristic reflections which argue that to understand integrative action of the nervous system, the brain must be investigated as a whole. The nervous system is continuously integrative for the body as a whole. [Details of these reflections are found in twelve chapters on Neurophysiology in Best and Taylor's Physiological Basis of Medical Practice, Eleventh Edition, edited by John B. West, pages 969-1312, 1985, authored by the Principal Investigator.] If the reader is already convinced, or wishes to sally forth without conviction, he/she should proceed to the section called "Scope of Work," which documents the ways in which the Brain Mapping Project has responded to the detailed requirements of the U.S. Army Medical Corps Research and Development Command Contract DAMD17-86-C-6093. These "reflections" are entered here because, if one isn't convinced of the urgent need to examine structure/function relations of the nervous system as-a-whole to be able to comprehend human perception, judgment, and behavior, there is no need to make such an extraordinarily difficult research and development effort.

The nervous system integrates visceral activity, consciousness, perception, memory and behavior. Remove any part of the brain and the remainder continues pursuing overall integration. When Sherrington wrote The Integrative Action of the Nervous System, in 1906, in accordance with contemporary insight, he assumed that the nervous system is informed by message passing, a cognate operation which, in a Cartesian sense, can be disassembled and reassembled, like clockwork parts. Although that view has a popular appeal, it is more appropriate at present to consider motor and sensory systems as functioning adaptively together as a coordinated selective system in the pursuit of a dynamic integration of both short- and long-range central satisfactions.

The brain uses massive parallel processing, "degenerate" mapping of body parts on brain parts, and mapping of

environmental features and events on brain parts via body parts. Degenerate refers to structurally/functionally abundantly overlapping processes, functionally closely equivalent, but neither structurally nor functionally strictly redundant.

Central responses to external objects and events pass via parallel channels to multiple internal mappings, and these communicate reentrantly with one another. This organizes what Edelman (1987) calls "global maps," that interweave central combinations of endowed and acquired capabilities. Global maps, according to Edelman provide continuous dynamic programs which integrate and govern experience and performance. Both perception and behavior are thus creative functions, destined to follow internal needs. Furthermore, the shaping of brain maps is mainly by population selection. Various mapping systems: motor, sensori-motor, sensory, limbic, etc., connect reentrantly with other mapping systems, including what are thought of as association areas, often reciprocally, back and forth, establishing reentrant mapping which provides for a global or gestalt organization of brain functions.

Initial mapping as well as reentrant mapping is capable of considerable adjustment when the body changes or when presumably corresponding maps get out of alignment. Global mapping appears to facilitate perceptual generalization and categorization and may be fundamental to conventional learning.

Selection of secondary repertoires is based on systematic conditioning of partially overlapping large domains of synaptic populations. On this foundation, conventional learning and social interactions are organized. Social interactions contribute to information processing which enhances conventional learning and possesses the advantage of social transmission.

To comprehend integrative actions of the human brain adequately, we need access to accurate three-dimensional computer graphics display and analysis of whole brains. Adult brains exhibit extraordinary variations at gross as well as microscopic levels of detail. Relatively surprising is the extent of variation in gross morphology; anyone who teaches a course in gross neuroanatomy can vouch for this observation. We tend to assume more uniformity in gross neuroanatomy than our experience actually warrants because of the repetition of diagrammatic images carried over from the nineteenth century, and also because our observations during dissection and surgery are ordinarily both partial and non-quantitative. Quantitative neuroanatomical analysis is ordinarily confined to small tissue blocks which are dislocated from overall organization of the brain.

We have sliced at microscopically thin intervals and carefully reviewed serial cinemorphology sequences through more than seventy whole human brains. We found each brain to be unique at the level of gross neuroanatomy. There are major differences in gyral formations on the surfaces of each hemisphere, including multiple asymmetries between the two hemispheres in addition to those identified recently by Geshwind and Levitsky (1968) and Gazzaniga (1970) in areas of speech and language representation.

There are also conspicuous differences and asymmetries in the dimensions of subcortical structures, in the gross morphology of thalamus, hypothalamus, basal ganglia and cortical and subcortical organization of the cerebellum. These are not trifling differences but range in scale among individual anatomical parts from ten to a hundred percent of volumes, and manifest distinctiveness in shapes that enable easy familiarity in specimen recognition: "This is the brain with a relatively squared-off thalamus, not so smoothly rounded as as in most other brains;" "This is the brain with a two-to-one L/R asymmetry in volumes of heads of the caudate;" "This is the brain with extraordinarily large dentate nuclei in the cerebellum;" etc.

In a 28-minute composite motion picture film, produced in 1976, The Human Brain: A Dynamic View of Its Structures and Organization, we demonstrated gross neuroanatomical differences in seven of these specimens and showed one specimen in its entire cinemorphology sequence. Images of that specimen were then employed in the creation of a dynamic three-dimensional computer graphic display which exhibited twenty neuroanatomical structures moving in their correct relative orientations in three-space, and portrayed their participation in different composite functional systems.

From these experiences we became convinced that development of a "normative data bank" for gross human brain neuroanatomy will require very sophisticated specimen selection, slicing, imaging, digitizing, and quantitative morphometric and statistical analysis. We have no notion which of the seventy human brains we have sliced or what kind of an amalgam of them might be suitable to establish a "standard human brain" although several groups have used our morphological data as their standard for PET-scanning localization, and other purposes.

In the past couple of decades it has become possible to "map" neural circuits that have distinctive neurotransmitter patterns. Some neurons utilize more than one neurotransmitter and some exhibit changes in neurotransmitter during the course of development.

Some neurotransmitter-specific circuits have been

identified with certain disease categories--parkinsonism, schizophrenia, Alzheimer's disease, manic-depressive disorders, tardive dyskinesia, etc. They have been associated with dopamine, norepinephrine, serotonin, enkephalin and other naturally-occurring opioid products, and a large number of distinctive oligopeptides. Certain behavior patterns have also been identified with monoamine transmitters and modulators: exploratory pursuit (dopamine), active avoidance (serotonin), resistance to extinction (norepinephrine), and the like. Many of these circuits are distinctively and diversely far-reaching and complicated in their distributions. Obviously, neuropharmacological patterns are likewise neuroanatomically specifically and elaborately distributed.

Finally, neurological studies find, for example, that such phenomena as directed attention and unilateral neglect have multiple, distributed, interdependent functional localizations. Mesulam (1981) observed that unilateral neglect reflects disturbances in the spatial distribution of directed attention. Four cerebral regions constitute an integrated network for the guidance of directed attention into extrapersonal space: a frontal component coordinates motor programs for bodily and gestural exploration, and for eye-scanning and fixation; a posterior parietal component provides an internal sensory map and apparently varies the dimensions of the map for specific portions of the external world; a reticular component generates the level of arousal and vigilance; and a limbic component in the cingulate gyrus conveys motivational valence. Lesions in only one locality in this network yield partial unilateral neglect syndromes. There is asymmetry here, too, in that unilateral neglect syndromes are more frequent and severe following disorders in the right hemisphere.

It is therefore becoming increasingly obvious that the nervous system needs to be examined, structurally and functionally, in its entirety. The interdependence of parts and functions cannot be adequately appreciated unless there is knowledge of the relative dimensions, specific connections, neurotransmitters and other agents which exist in relationship with one another in terms of feed-back, feed-forward, reciprocity and linked sequential circuitry.

The Importance of a Comprehensive Neurosciences Database

Assuming that a normative database is established for display and analysis of the human brain at, say, 40 microns cubic resolution, and similar standards are created for common laboratory animals, then the structure/function data from a wide variety of laboratory and clinical research sources can be evaluated and introduced into the maps, or filed with reference to specific 3-D parts of established

whole brain maps. By such means, structure/function relations can be accumulated and assembled in relation to whole brain maps in a disciplined and instructive fashion.

Not everyone would need to have the sophisticated equipment necessary to acquire whole brain maps at microscopic levels of detail. Rather, optical discs could be used to transport three-dimensional maps and "standard atlases" to practically all neuroscientists. This would encourage collaborative sharing of data, accelerate the accumulation of structure-function-literature correlations and documentation, and improve the teaching of neuroanatomy and the application of three-dimensional computer graphics data for display and analysis. By this means, data could be made available to clinical neurosciences research and patient care. This will be useful for controlling spatial localization and comparing normal parameters in a variety of scanning procedures and will contribute to both research and clinical neuroanatomical interpretations.

There is no question that it is highly desirable to pool information on neurotransmitters, connectivity, electrical phenomena and morphological plasticity in adequate recognition of the great amount of high quality work that is being accumulated. In significant respects three-dimensional graphics will contribute to a database that is complementary and supplementary to other forms of neurosciences communication and sharing.

BACKGROUND REFERENCES CITED IN INTRODUCTION

Edelman, Gerald M., Neural Darwinism: The theory of neuronal group selection, New York, Basic Books, 1987.

Gazzaniga, M., The Bisected Brain, New York, Appleton-Century-Crofts, 1970.

Geschwind, N. and W. Levitsky, Human brain; left-right asymmetries in temporal speech region, Science 161: 186-187, 1968.

Mesulam, M-M. A cortical network for directed attention and unilateral neglect, Annals Neurol., 10:

Sherrington, Charles, The integrative action of the nervous system, New York, Charles Scribner, 1906.

* * *

RATIONALE, EXPERIMENTAL METHODS, RESULTS, AND DISCUSSION FOLLOW SECTION-BY-SECTION IN THE "SCOPE OF WORK"

S C O P E O F W O R K

1. DEVELOP AND IMPROVE BRAIN MAPPING TECHNOLOGY/METHODOLOGY

Between 1967 and 1976, UCSD developed Cinemorphology. This involves photography, in registration, of each successive surface of whole human brains sectioned at microscopically thin intervals. Qualitative examination of seventy such Cinemorphology sequences, all from "normal" adult brains, showed each of them to be unique. They differed conspicuously one from another in various gross neuroanatomical components. Neurosciences peeked into a box labeled "Endophrenology."

In 1975-76, one of these brains was hand digitized. It was then reconstructed three dimensionally, using an Evans and Sutherland Picture System 2. This provided a dynamic three dimensional display of the whole brain. The digitization had to be done by hand, however, and therefore the three dimensional reconstruction was achievable only at macroscopic z-level intervals (1.1mm).

To permit the analysis of enough brains in enough detail to answer interesting scientific questions, it is necessary to overcome the time and labor consumed by hand digitization. There is no existing alternative to developing efficient systems for image acquisition, three dimensional reconstruction, and computer graphics display and analysis.

We are convinced that within a few years computer graphics technology directed toward this goal will prove tremendously powerful as well as labor-saving. Computers will bring new objectivity and sharability to neuroanatomical interpretations. They will also enable database developments that combine structure/function and source information. This will revolutionize the quality and applicability of neurosciences research. Of course, similar computer techniques for combining structure/function/information can be applied to all of biology. New analytic and synthetic power will become available for the investigation of evolution, development and disease.

We believe three dimensional reconstruction of whole brains must conform as closely as possible to the three-space organization of the same brains when they were functionally intact. With support through this Contract, we developed innovative methods for preparing rat, monkey and human brains and tissues: they provide (1) accurate spatial integrity for whole brain 3-D reconstruction, and (2) specific localization of structure/function relations.

The Brain Mapping Project (BMP) organized collaboration between UCSD and the Scripps Clinic and Research Foundation (SCRF), with the latter group operating under the leadership of Floyd E. Bloom.

The BMP benefitted greatly from scheduled contributions in La Jolla and continuing remote consultations by three National Co-Directors: Dean Hillman from New York University; Larry Stensaas from the University of Utah; and Arthur Toga formerly from Washington University at Saint Louis, now from UCLA; and by a European Consultant, Wolfgang Rauschning from the University of Uppsala.

The BMP also gratefully appreciates the engineering and computer science advice provided at the beginning of the Project by Wesley Clark, BMP's "Dutch Uncle Engineer" from New York City, and Jerome Cox and Charles Molnar, both from Washington University at Saint Louis. They provided extremely cogent advice during the period when the Army was asking UCSD to lead a national program to construct a prototype computer system within four years that is capable of mapping in three dimensions and displaying the entire human brain at microscopic levels of detail. When that prospect was abandoned by the Army, the need for organizing engineering and computer science talent relaxed in urgency.

The BMP hosted a four-day National Task Definition Workshop which assembled experts in fields of computer science, engineering, database management and neurosciences (See List of Workshop Participants in Appendix A). The Workshop evaluated technical opportunities and provided guidelines for a collaborative, multi-university National Brain Mapping Program.

This "Final Report" describes BMP considerations relating to acquisition of equipment, research and development in quantitative morphology, and systematic fulfillment of the four-part "Scope of Work" required under Contract with the U.S. Army Medical Corps Research and Development Command. The Report is also written with the objective of specifying some of the most important brain mapping contributions, for the benefit of future brain mapping enterprise.

The BMP wishes to express very sincere appreciation for the generous support of the U.S. Army Medical Corps Research and Development Command, and particularly for the thoughtful personal attention given the BMP by many Officers and Staff of the USAMCRDC.

1.1. Improve Accuracy and Speed of Histological Data Acquisition

(a) Computer-Assisted Cryomicrotomy and Registration Control Image Acquisition

(i) Selection of Major Items of Equipment

Criteria for selection of major items of equipment have been identified in Quarterly Reports. Here we consider equipment selection in the context of contributions to general strategies for brain mapping.

For computing purposes we selected two DEC VAXstation II/GPX Graphics Workstations composed of a MicroVax II processor and advanced graphics capabilities. A medical student, Sheldon Furst, who had installed DEC equipment professionally, skillfully organized the BMP computing environment. This enabled double team pursuits in parallel at SCRF and UCSD, for image acquisition, software development, and neurohistological analysis. The two systems were linked telephonically to support complementary research activities being pursued simultaneously by investigators working in separate buildings. Similar networking could be used on a larger scale for national coordination of collaborative brain mapping progress.

Warren Young and Phil Mercurio analyzed four image acquisition hardware-software systems, including Kontron/Zeiss IBAS 2; Gould IP 8500; Recognition Concepts Trapix 5500; and MegaVision 1024 XM. Discussions were held with high-level technical personnel from each vendor and hands-on experience was obtained. MegaVision was selected as the system within our price range best qualified for brain mapping purposes.

MegaVision systems under control of MicroVAXes were installed for brain mapping purposes in the two settings. The MegaVision at SCRF is primarily engaged in localization of specifically labeled neurotransmitters and other functionally significant brain components in the three-space of monkey brains. The MegaVision at UCSD is primarily engaged in image acquisition of Registration Control Images (RCIs) from the surface of brain blocks, and in two dimensional reconstruction of whole tissue section composite images obtained by means of a new Tissue Section Image Microscope, the TSI Microscope.

We estimated the comparative accuracy and speed of several data acquisition instruments and components. These included film and digital cameras for image acquisition through microscope columns, for imaging the cut surface of whole brain blocks, and for imaging neuroanatomical slides on light boxes. Don McEachron at Drexel University

established criteria for testing cameras, helped in the selection of types of cameras and tested specifications and performance of the Circon CCD camera and MegaVision vidicon-type camera utilized in the Project.

We compared and analyzed equipment specifications and tested other hardware including different assemblies of microtomes, cameras, microscopes, stages, condensors, nosepieces, drawing tubes, oculars, objectives, optical filters, image intensifiers, fluorescent and other light sources, etc.

Harvey Karten, John Morrison, and Charles Wurtz conscientiously investigated designs and specifications, ran tests and selected three research microscopes. These reflect a conscientious BMP effort to establish neurological structure/function relations and to acquire digital images for quantitative two and three dimensional brain mapping.

A Zeiss Axiophot Widefield Research Microscope, with a Maerzhauser computer-driven stage, mainly for BMP research by John Morrison, Floyd Bloom, Warren Young and their colleagues, has been devoted to quantitative three dimensional brain tissue mapping of neurotransmitters such as somatostatin, substance p, dopamine, norepinephrine, and other important stereospecific molecules in monkey cortex. These studies have been made possible by the use of EMMA, a powerful software development by Warren Young that enables efficient computer-aided quantitative morphological display and analysis.

A Leitz Orthoplan II Microscope, including equipment for epifluorescence, with Nomarski optics and a Maerzhauser stage, modified for visualization with three different fluorescent module cubes, interchangeable stages, a video port and microdensitometry, has been utilized by Harvey Karten and his colleagues for quantitative spatial analysis of the architecture and biochemical diversity of cell populations in the retina--the most accessible part of the brain.

This microscope is equipped with an OPELCO image intensifier which permits the examination of single tissue sections stained with three different fluorophores. The output of the image intensifier is captured by means of a CCD Cohu solid state camera, and the image is directly copied onto a Mitsubishi video copy processor, permitting the acquisition of images rapidly enough to prevent loss of data due to decay of fluorescent sources in the tissue. Alternatively, the image can be piped to a microcomputer which has a dedicated frame grabber for digital image processing. This allows Karten and his colleagues to capture alternative images showing the pattern of receptor staining for each fluorophore. From this, clarification of the relationships between cholinergic amacrine cells in the retina and neurons

which contain nicotinic acetylcholine receptors was established.

A Tissue Section Imaging Microscope (TSI Microscope) was designed by Charles Wurtz in collaboration with William McBain of Pacific Precision Laboratories (See Figure 1b). The TSI Microscope presents a very large computer-driven stage for "mosaic mapping" or "strip mapping" of whole brain tissue sections. Images are acquired in strips or squares and composed into a single large synthetic image which combines the strips or squares in exact order so as to create a large synthetic image that combines the strips or squares into a "seamless" image of large regions or the entirety of whole brain tissue sections. Computer control of camera and stage allows for either "strip map" or "mosaic map" options.

Mark Shin wrote an easy mosaic program that permits automatic TSI acquisition and reconstitution for 2x, 4x, 10x and 20x magnifications to secure synthetic images up to 16 Mb in detail. This permits whole rat brain TSIs to be obtained at each of the three lower magnifications. The images are stored in memory with indicators of where they fit into the magnified, reconstituted TSI.

Compression of the synthetic TSI images is necessary for display of the images on limited graphics systems. This technology can be expanded with larger memory and more powerful graphics management computers and it promises to provide a radically new opportunity for neurohistological study. When robust warping machines become available, the large synthetic TSI can be subjected to automatic de-deformation to compel the inevitably distorted thin tissue section to conform to the registration control image (RCI).

(ii) Research for Registration Control Imaging

It was necessary to establish a system for obtaining Registration Control Images (RCIs) from each successive cut surface of whole brain blocks undergoing serial sectioning. The LKB giant cryomicrotome was selected as the most rugged, accurate and and versatile programmable microtome (See Figure 1a). The MegaVision system was installed and software programs were designed expressly to facilitate imaging the cut surface of whole brain blocks.

A scaffold was built to fasten the MegaVision vidicon-type camera joined to a Tamron 70-210mm macro-zoom lens and special Examatron lamps in a precisely fixed relationship to the angle and distance of the cutting plane of the microtome (See Figure 2). The scaffolding was mounted on the pillars on which the microtome knife is supported so that as the knife descends the camera and lights maintain an exact and fixed relationship to the block surface. Cynthia Lemere constructed a tailored black shroud to protect the specimen

surface from spurious light reflections within the cryomicrotome. Spectral sensitivity of the cameras was tested carefully before their selection and tested again in situ in the environment of image acquisition (See Figure 3).

Whole rat brains, perfused, stained and embedded in CMC by Lemere, destined for acquisition of RCIs, were sectioned in the LKB cryomicrotome at -30°C with a 35° angle to the knife. Section thickness was 5μm, with RCIs acquired at 40μm intervals. Later, methylene blue-stained albumin-gelatin embedded rat brains were used for RCI acquisition and for extensive operator experience with tissue section removal. These brains were sectioned at -10°C with a lower knife angle setting. Section thickness was 50μm, with RCIs acquired at 200μm intervals. The cutting was smoother and the tissue section integrity was better with the second set of sectioning parameters.

(b) MegaVision Image Acquisition, Editing, Contouring, and Storage

Sectioning and image acquisition software created and adapted to the MegaVision by Warren Young is called SLICE. This software package provides an easy interface for users operating the MegaVision system under UNIX control. Commands are specific to RCI acquisition (See Figure 4).

Version I of SLICE provided a primitive repertoire for image processing and proved successful for acquisition of images from the blockface at selected intervals during automatic cryomicrotome slicing. Version I was used to develop and refine procedures and it provided the first computer-aided automatic acquisition of digitized blockface images. SLICE was also important as a test for μMIPS, showing that μMIPS has been designed by Warren Young and Mark Shin so that innovative applications can be easily and flexibly constructed to enable progress toward specialized image processing objectives.**

**Footnote: μMIPS refers to UNIX Multiuser Image Processing Software. μMIPS constitutes a series of command programs designed to control the image processing environment, including any number of users or 1024XM (MegaVision) systems, and the Maerzhauser stage on any number of microscopes. μMIPS is implemented as an applications software and is now implemented on three separate operations contexts. The programs are UNIX-based, therefore highly flexible and callable from nearly any level of the UNIX software hierarchy. The internal structuring of the programs is written so that embellishments do not involve extensive rewriting of the code.

SLICE now includes methods for automatic filenaming of images, automatic correction of non-uniform shading across the image field, and automatic processing of images through a variety of user-selected sequences available through the MegaVision system.

Analysis of blockface images (RCIs) and Tissue Section Images (TSIs) is achieved by a series of routines called MAPPER. The MAPPER sequence represents a cascade of procedures to generate boundary contours from gray level digitized images. Contours consist of coordinates that characterize a series of linked points having vector dimensions that are defined according to the gray level values of neighboring points. Contours can be labeled to identify a set of coordinates that circumscribe any relatively differentiable object in a given section.

The sequence of MAPPER operations uses MegaVision routines to optimize contrast in the image and then define the edges (See Figure 5). One of first operations subtracts an image of the background taken without the specimen. This eliminates some unevenness of illumination inherent in the cryomicrotome environment. The process includes image normalization which reschedules density values from low contrast images so that they can span the full 256 gray level range.

Once the blockface image has been normalized, edge detection and thresholding routines are run. The threshold is then mapped to a binary overlay channel to compare threshold level with boundaries of structures represented in the image. MAPPER offers an option which allows editing of the image after thresholding and before contouring.

An edge detector is applied to the binary image to generate a set of vectors that characterize the boundary. This edge follower tracks the boundary from an arbitrarily selected point to extract a serial set of pixel coordinates that comprise the contour (See Figure 6).

(c) Additional Specialized Software Developments for Contouring Neurohistological Structures

Our goal is to design and implement edge-detection and boundary extraction software that will define contours that have substantial neuroanatomical interest, among the subtle and confusing patterns reflected from the cut surfaces of whole brain blocks, and as seen by TSI Microscope transmission through tissue sections.

We find that with present histological and software techniques, there is precious little neuroanatomical material that is amenable to "unambiguous contouring." Not surprisingly, as has been learned through studies of

artificial intelligence, some things that seem incredibly obvious to human observers are loaded with ambiguities when it comes to machine segmentation. An old "Rule for Scheduling Software Development" has been reinforced: "No matter how long it is predicted that software development will require, it will actually take twice that long."

MAPPER contouring remains to date the most applicable software. BRAINMATE was developed at UCSD by Donal Hurley, of Ireland. It is specialized for neuroanatomical tissue analysis and is based on CELLMATE, developed earlier by Hurley at New York University, under the guidance of Dean Hillman. CELLMATE enables an operator to contour neurons for two and three dimensional reconstructions. BRAINMATE enables an operator to trace neuroanatomical boundaries onto the digital image of a tissue section. BRAINMATE is also employed for correcting and amending machine-generated contours.

A number of innovative approaches to the software extraction of image boundaries have been undertaken and vigorously explored and improved during the period of the Contract. Developments in boundary detection software include a series of novel and evolving algorithms known as ROTATING BAR, FACET-MODEL, HARALICK, and CONTOUR FOLLOWER. Shankar Chatterjee provided considerable understanding of the art of computer graphics image interpretation and general guidance for these software developments.

Detection of subtle neuroanatomical boundaries within widely variable pixel densities manifested in digital images of whole brain blockfaces remains a profoundly difficult image analysis problem. A roughly approximated rapid edge-detection and boundary generation program is available in the standard software provided by MegaVision. However, it suffers from many inaccuracies and inadequacies and is not robust against laboratory actualities, including factors such as non-uniform illumination across the image field and electrically noisy circumstances that accompany image collection.

ROTATING BAR and FACET-MODEL are edge detectors that use local intensity derivatives to discover edges, assuming that an edge is nothing more than a chain of relatively consistent local variations in pixel intensity (See Figure 7). Both algorithms are implemented in C language under the MicroVax UNIX operating system. Both algorithms generate an "edgel" file that contains edge magnitudes and edge directions for each pixel in the image. This information is then used by an "intelligent" CONTOUR FOLLOWER to produce a contour file in vector format, where the contour lists are described in terms of three spatial values.

The main design problem in CONTOUR FOLLOWER is the

successor function, which at any given point along the contour selects the function that is most likely to prolong an existing contour. The choice is guided by the magnitude and direction associated with each edge pixel, and by such parameters as the look-ahead depth, tolerance in direction, and closest permitted distance to neighboring contour data.

Work is currently in progress to design a refined edge-detector (single pixel-width edges) that will detect all points on the boundary accurately and pass them to a 3-D graphics routine which will generate the three dimensional reconstruction display. We are continuing research on edge-detection algorithms that will be sufficiently robust to detect edges within both high and low contrast gray level ranges.

(d) Three Dimensional Reconstructions From Registration Control Images

Registration Control Images (RCIs) are images taken from the cut surface of a brain block. They are images of the as yet undistorted plane of the tissue section which is the next one to be removed by the cryomicrotome. Since the microtome considerably deforms the microscopically thin tissue section during the process of cutting, it is necessary to have a corresponding Registration Control Image (RCI) for de-deforming the synthetic image made from the distorted thin tissue section, the Tissue Section Image (TSI).

RCIs do not have much blockface contrast and the gray levels do not contrast sufficiently for sharp digital image analysis. Nevertheless, they do contain considerable information, enough to be able to define a number of landmarks, which are then used as an RCI "x, y, Truth Base" to which homologous landmarks on the TSI are to be matched as the basis for guiding the algorithm for de-deformation of the TSI. Methods for both RCIs and TSIs must be pushed to the optimum for locating and circumscribing data that are of interest and value to the population of neuroscientists, neuroanatomists, neurophysiologists, neuropharmacologists, neuropathologists, and clinicians.

The RCIs, taken off the block surface, as they are now, are rich and reliable enough in data to enable contouring of the whole brain for purposes of creating a wireframe "atlas." The same information can be used, with CONTOUR VIEW, developed in Philadelphia by Anthony Reynolds, and specifically adapted by him to run on our system with our data, to display solid surfaced, shaded images. See Figure 8 for examples of three dimensional wireframe reconstructions and solid surface renderings.

(e) Three Dimensional Reconstructions from Tissue Section Images

Many neuroscientists would like to obtain a robust software package that requires minimal specialized operator discrimination in the course of mapping whole brain tissue sections. They would then like to create three dimensional reconstructions from such stacked tissue section maps. Such software does not exist, but its potentialities are implicate in the three dimensional reconstruction that has been accomplished from tissue sections by Larry Stensaas. Using serial sections selected by him as the best in the Yakovlev Collection at the Armed Forces Institute of Pathology, Stensaas has personally invested the extraordinary time and effort to discriminate neuroanatomical structures, section-by-section, throughout the brain stem and telencephalon, exclusive of neocortex (See Appendix B for a list of the names of neuroanatomical structures identified and contoured by Stensaas). This means that Stensaas has differentiated almost all the important structures in the whole brain, by hand. More information on Stensass' contribution is presented later in this report.

This is exactly what is hoped can be accomplished in the near future automatically or semi-automatically with the aid of TSI-Microscope-like computer systems. Such software must be adaptable to a wide variety of types of neurological tissues and exotic stain applications (including molecularly stereospecific labels, fluorescent [i.e., transient duration] antibody markers, radioactive tracers to be identified in photographic plates, etc.).

Explicit expectations were expressed during the Task Definition Workshop relating to special kinds of software that could be developed for computer-aided microscopic analysis of neuroanatomical tissues. This expectation includes being able to detect and localize in x, y, z, coordinates, and count specialized neurons, characterize them by class iconically, trace neuroanatomical structural boundaries, and distinguish the borders among different cytoarchitectural regions of cortex.

(f) Comparison Between Registration Control Images (RCIs) and Tissue Section Images (TSIs)

It is essential for purpose of accurate three dimensional whole brain reconstructions, that we compare RCIs, obtained from the blockface, which are taken to be TRUTH Images, with TSIs, obtained as composite mosaics through the TSI Microscope. The two images need to be compared for purposes of correction of deformations that occur to the thin tissue sections during microtomy. Homologous landmarks are located in each image; the RCI landmarks are considered to be undeformed, hence the TSI landmarks must be made to conform to the RCI landmarks. This is necessary for two dimensional "de-deformation" of the TSIs.

Even after all the TSIs have been de-deformed in this way, to compell conformation among as many landmarks as can reasonably be identified in the corresponding RCI/TSI pairs, there will still remain three dimensional deformations which will be evident only when the TSIs are assembled into some measure of z-depth tissue or brain reconstruction. Therefore, it is necessary to identify the individually discrepant TSIs and to "re-de-deform" them iteratively, until the entire three dimensional reconstruction is clearly correctly aligned. The re-de-deformation of each discrepant TSI must always be referred for its re-alignment to the corresponding RCI.

For the purpose of both (2-D) de-deformation and (3-D) re-de-deformation, it is essential that the two images (RCI and TSI) overlie one another in a display so that each of the images can be presented independently, in different colors, and that they also can be separately "blinked" on demand. To make a reasonably accurate two dimensional correction, it must be possible to identify a sufficient number of homologous landmarks that can be located on both images. [Although we refer to them as homologous landmarks, they are really the same landmarks, the TSI landmarks being more or less displaced.] The TSI landmarks must be differentially deformable with linear extrapolations among the landmarks in order to match the homologous landmarks of the corresponding RCIs. Then they must be checked visually, by image overlay, for satisfaction of correspondence of the entire TSI to the RCI. Both images need to be examined and the TSIs de-deformed on a high resolution monitor that is not troubled by weak sensors, electric overload, nonlinearity, and that shows comparatively little flare.

It is generally agreed that information obtained from the cut surface of a block, the RCIs, aided by prior perfusion of coloring material, should be as detailed as single frame imaging can provide. Our methodological research suggests that in continuation of the Brain Mapping Project we may want to convert RCI acquisition to photographic camera images which can document at least an order of magnitude more information than is presently obtainable by digital systems. RCI information is so desirable and useful that we will probably eventually forego digital imaging of RCIs in favor of large format, fine-grained color photography. Exactly this, in fact, was advocated from the beginning by our Swedish Consultant, Wolfgang Rauschning, who has considerably improved images obtainable for Cinemorphology by introducing superior photography. Photographic images provide an abundance of fiduciary information for comparison purposes in the processes of de-deformation and re-de-deformation of TSIs. Finally, photographic images are familiar and reassuring. They can easily be preserved indefinitely to serve as a stable reference and registration control series for each brain. There may be a further

advantage in being able to have smooth-flowing Cinemorphology images of the same brain, to supplement its three dimensional computer graphics reconstruction.

The saving grace is that RCIs themselves are never to be de-deformed: there is therefore no requirement that they be digitized. We have shown that digital images can be compared to photographic RCIs by projection means, and homologous landmarks can be identified on both images and specified in x, y, space in the RCIs for definition of the required 2-D de-deformation of the corresponding TSIs.

TSI images can be de-deformed and re-de-deformed as much as may be required to complete a satisfactory three dimensional whole brain reconstruction. Note: Reference control must always be made back to the original RCIs. The tissue section, of course, has been obtained from that particular anatomical plane, although, depending on translucency of the specimen, the RCI will detect some structures that may be discernible beneath the thickness of the tissue section.

It is our considered opinion that the TSI images should be as highly detailed as TSI microscopy allows. At the Task Definition Workshop, Bud Tribble III suggested that 8 bits per pixel is not enough. He recommended 12, or better, 16 bits. Three colors are considered to be useful and Bud thought that additional colors, including UV might prove to have discriminative advantages in the analysis of histological materials.

It may prove advantageous also to capture an image of each TSI before it is stained. We planned for this but couldn't afford the design and construction of the necessary low-distortion Macroscope. That image would be visually more akin to the corresponding RCI and therefore it is likely to be especially useful in identifying homologous landmarks.

An appropriate de-deformation algorithm to make the TSI match the corresponding RCI would be applied to such image pairs, (or triplets, if simultaneous comparison with the unstained section is desired). TSI images in deformable format must be preserved long enough to be helpful in the conduct of 3-D re-de-deformation. Ultimate three-dimensional re-de-deformation (to accommodate displacements visible on 3-D which may not be detected on 2-D) await algorithm developments intended by Fred Bookstein.

At the BMP Innsbrook meeting it was decided that for a minimum scale rat brain "atlas" 512 x 512 pixels would be sufficient information for 3-D reconstruction purposes. Functional data obtained from other sources at higher magnifications e.g., from specially stained sections in another

laboratory--intended to be added to the correct three-space of the "atlas," could be readily compressed to conform to the dimensions of the remainder of the "atlas."

(g) Cameras on Microscopes

2048 x 2048 video CCD MOS solid state well-tested cameras appear to be a reasonable future choice for TSI Microscopy. The TSI requirement is to be able to define boundaries, locate cell clusters, fiber tracts, boundaries between fiber tracts, etc., to outline and envelope anatomical objects, and to assemble these objects in 3-D reconstructions at microscopic levels of detail.

Bob Nathan advocated Perk and Elmer systems which have microscopes with a built-in halogen light source and 3-color filters. They can do 10"x10" scans to within 5 microns, thus providing considerable geometric fidelity plus pixel depths with multiple spectra. Unfortunately, these systems are extremely slow for whole human brain reconstructions. They would require about 6 hours to render an image of one human brain section, i.e., 36,000 hours to scan the 6,000 sections needed to represent a whole human brain by its least thick axis--in horizontal sections. Moreover, they cost $0.25 million. Their speed is to be compared with 1/8 seconds for Iconics, pixel by pixel analysis, i.e., needing a few minutes to scan a whole human brain section. Optimally, TSIs need microscopic magnification to permit resolution into the few micron range. For such resolution, human TSIs will probably require laser scanners operating at 1000 lines/inch.

1.2. Develop Methods for the Computer-Aided Acquisition of Tissue Images

(a) The Tissue Section Image Microscope

High quality digital Tissue Section Images (TSIs) are required in order to be able to de-deform tissue two-dimensionally to conform to the undistorted reference images taken from the cut surface of the block, the RCIs. Charles Wurtz worked out the design and had constructed a Tissue Section Image (TSI) Microscope. It arrived only a few days before the end of the Contract. Nevertheless, it has now been put to work, largely through the efforts and skill of Mark Shin (See Figure 1b).

The development of whole tissue section imaging microscopy is proving to be one of the most innovative and exciting contributions of the Brain Mapping Project to date. The TSI Microscope is stabilized on a large granite block. It is highly adaptable for camera mounting, drawing tube access, nose piece and turret for objectives. It supports a

computer-controlled stage that is large enough to hold whole human brain sections (and sections of the even larger brains of whales). It has an especially wide field illumination light source and condenser, although still not sufficiently uniform over the whole field. The stage has position control registers in both x and y axes, with digital display in microns, all under control of the MicroVAX and coupled to the MegaVision system.

This microscope constitutes a simple but useful exploratory tool for rapid, accurate, computer-operated digital image reconstruction of whole tissue sections. We put up a modest Circon CCD camera which we can modify to serve as a line camera for continuous section sweeping in a horizontal or vertical direction, to make a "strip map," or we can use it with a square pixel array to make a composite mosaic.

The center of the camera image through the microscope is displayed on a black and white monitor that is useful to the operator for purposes of scanning whole sections, using a variable speed toggle switch, and for focussing the image. This is in addition to the field of view which is accessible to the operator directly through the normal operator viewing port of the microscope.

The MegaVision system is used to acquire, store in sequence, create and display composite mosaic images of whole or partial tissue sections. The main shortcoming of the present *TSI Microscope design* is that the light source cannot provide a sufficiently uniform field of illuminaion for low power magnification tissue section reconstruction. This leads to a "patchwork quilt" appearance of the composite synthetic image. This is especially objectionable with low magnification images (See Figure 9).

This difficulty of illumination was anticipated from the beginning and the best system that was considered to be possible was engineered into the microscope. The roughly circular unevennesses in uniformity of illumination do not interfere with good quality imagery patch-by-patch. They are hardly noticeable to the viewer because the eye quickly adapts. They become noticeable when multiple patches are arranged into a large mosaic composition. Then the variations in illumination stand out; they are made perceptually more obvious because of their alignment along the x and y axes. In this way a "postage stamp" appearance becomes obvious. Of course these effects are reduced to virtual disappearance when higher magnifications are used. Then the field of view is reduced to the "sweet" part of the optical column and the center of the field of illumination (See Figure 10).

With the MegaVision it is possible to subtract for

uneven elimination and we are presently working on a protocol to gain this advantage for TSI Microscope imaging.

Mark Shin did an excellent job of eliminating seams between patches in the composite mosaic reconstructions. There is such close tolerance for the computer control of the stage that he is able to keep the seams between adjacent images down to about a single pixel level.

It was noted earlier that the Circon CCD camera has a 525 x 480 line chip. This presents a problem because the MegaVision T scanner digitizer tries to map this awkward dimension into 525 x 525 scan lines. The difference of 45 scan lines manifests in presenting that number of blank lines in the upper margin of the digitized image. Shin has the computer control the movement of the stage so that that blanked strip is occupied with the adjacent rank of the mosaic image. The stage control is sufficiently accurate that patches can be made to abut one another uniformly and precisely so that a square pattern of mosaic images is reconstructed.

(b) Improvements in Brain Specimen Preparation

For most laboratory purposes, when animal and human brains are prepared for histology, three dimensional spatial integrity of the entire brain is not required. For purposes of whole brain mapping at microscopic levels of detail, however, spatial integrity must be preserved as far as possible. This must be maintained through all procedures required for brain processing, from the living brain, in the case of animals, and from the fresh cadaver in the case of humans, to the condition of the same brain embedded in block form ready for sectioning. This is the only way, too, by which proper database standards can be created that will appropriately serve the research and applications requirements of various neurosciences communities.

The brain is served by a blood supply that is about ten times greater in volume than that of other organs. It is suspended in cerebrospinal fluid, and is subject to relatively abrupt shrinking and swelling. When removed from the brain's fluid bath, its relative weight is increased three hundred-fold. Its own weight then imposes plastic deformity and even dehiscence. Maintaining spatial integrity through every procedure from the living brain to completed graphic reconstruction is no simple problem.

The BMP requires creation of accurate whole brain reconstructions, and accurate comparisons between brains, gross and microscopic, so it was essential to develop and test entirely new and stricter brain and tissue preparatory methods.

These new methods constitute one of the major contributions of the BMP. They ensure that reliable Registration Control Images (RCIs) can be obtained prior to sectioning and that Tissue section Images (TSIs) represent tissue well preserved for microscopic study.

Spatial integrity is particularly difficult to maintain throughout the agonal period of perfusion. The brain must again be especially carefully protected against deformity during the process of removal from the skull and subsequent handling. We were uncertain of being able to accomplish this and began with the assumption that we would have to slice whole brains within the meninges and skull. [That the LKB giant cryomicrotome could do this was one of the attributes in its favor for our selection.] There could be no better mold to hold the brain than its natural cradle. Even there, there is still considerable room for distortion. A better technique had to be worked out. An unexpectedly reliable method was discovered by Charles Wurtz with the technical assistance of Cynthia Lemere. Their novel techniques for rat brain preparation, differ in three important respects from state-of-the-art methods with which we began.

First, they established that when a rat is allowed to cease respiration for a few seconds prior to perfusion-fixation, the brief period of asphyxia dilates the cerebral vasculature and enhances both perfusion and staining.

Second, they found that while lithiumcarmine staining *in vivo* was better for digital image acquisition than any other of some twenty carmine formulae, it still yielded sub-optimal white matter/gray matter differentiation. Carmine dyes produce a red/yellow spectral contrast. Each of these colors is poorly resolved by digital imaging cameras.

Wurtz and Lemere tried to solve the spectral sensitivity problem by perfusing with low concentrations of osmium tetroxide. When delivered by vascular perfusion, cacodylate buffered 0.5% osmium tetroxide preferentially stains gray matter a light brown, while leaving white matter relatively unaffected. This osmium-brown has a broad spectral reflectivity, and it was felt that good anatomical differentiation could be achieved by this method. While the preparation yielded the expected coloration, the contrast proved insufficient for adequate digital image analysis.

To circumvent this problem they turned to methylene blue. This dye stains gray matter dark blue-green, and white matter yellow-green. These colors are satisfactorily separated by the MegaVision camera. Methylene blue penetrated tissues best when perfusion of the dye preceeded fixation (See Figure 6).

Third, they learned how to remove the brain especially

carefully from the skull and meninges, after fixation and without deformation. The guarantee of dimensionally stable removal of the brain depended on development of non-distorting perfusion techniques that stabilize the brain as a whole preparatory to its removal and final embedding.

Wurtz and Lemere also prevented brain edema and shrinking by carefully adjusting osmolarity of the perfusion solutions. Their chain-linked histological protocols combined thorough fixation using paraformaldehyde and glutaraldehyde. Brain removal from skull and meninges improved brain outline contrast in the RCIs. It facilitated software application during digital image processing, and reduced difficulties in removing and handling the delicate tissue sections. It also saved microtome blade damage which can scar the block face and spoil the quality of RCIs. Blade sharpening and replacement is expensive and takes a long time for blade turnaround. Bone cutting means that a large stock of expensive blades must be kept on hand.

To increase the cutting speed of the microtome and to increase the quality of tissue sections, they introduced embedding with egg-albumin polymerized with glutaraldehyde, as suggested by Dean Hillman. This medium, when blackened with a mixture of India ink and carbon (lamp-black), allowed sectioning of exceptional quality at 50 to 100 μm, and provided an excellent optical contrast with a minimum of back reflectance. This combination greatly improved the quality of the RCIs.

Furthermore, this improved method of preparation allowed sectioning at +5 ^{o}C rather than at sub-freezing temperatures. This provided a further increase in the permissible speed of the cutting stroke of the cryomicrotome (See Figures 11 and 12).

1.3. Improve Accuracy of x-y Coordinates of Histological Sections--I

A major contribution to computer-assisted analysis of tissue sections was the development of techniques for composite, whole-section synthetic image acquisition and reconstruction of tissue sections done by TSI Microscope and computer. This is another first in the history of computers and microscopy. More importantly, it is applicable to morphological studies throughout all the life sciences. This software can be built upon for neuroanatomical feature detection and texture analysis.

(a) Development of Stage Control to Match Digital Image Dimensions

The computer driven stage is powered by two precision indexers which control the x and y axes. A library of routines was written in C language by Mark Shin to control the indexers. Communication linkage is established by a high level program by calling an initialization routine in the stage library. Thereafter, the program has direct access to the indexers and can precisely control movement of the stage platform.

The TSI Microscope with its computer driven stage and computer controlled imaging technology was developed de novo for the BMP, to create whole tissue section computer graphic mosaic image reconstructions. With this instrument, it is possible to digitize individual frames from the microscope-mounted solid state camera. The program controls the microscope stage so as to move step-wise across a stained, microscopically thin tissue section in an orderly fashion so that a mosaic of squares is sequenced and imaged with single-pixel accuracy in camera placement in both x and y dimensions.

The image on the microscope is scanned in mosaic fashion, digitizing each frame on station between moves of the computer controlled stage. The requirement here is to create a square "patch" for mosaic reconstructions of whole tissue sections.

Mark Shin established stage motion that corresponds to the dimensions of one frame of 512 x 512 pixels for each specified microscope objective. Thus, as magnification increases the number of patches increases, but each patch contains the same number of pixels.

Shin created a database containing the scale factors for each of the microscope objectives allowing the computer-controlled stage movements to match the camera magnifications precisely. Application programs consult this database. Depending on the magnification, the stage is moved an appropriate amount to capture the next tissue image without overlapping the previous frame or leaving a gap between frames.

We have devoted this new technological development to imaging monkey and human tissue sections (See Figures 9 and 10). Success with these monkey brain mosaics indicates that applications to tissue section imaging in the rat brain will be entirely straightfoward [2.1.2].

Whole rat brain wireframe fiducial "atlases" contain sufficient information to allow the 2-dimensional de-warping of both the macro-registration thin-section unstained images (macro-TSI) and the stained mosaic composite reconstruction of stained sections, the microscopic TSI (micro-TSI) images [SOW 2.1.5].

Inasmuch as the rat brain is less than 10% of the volume of the monkey brain, whole tissue section mosaic mapping can be achieved at correspondingly higher magnifications. The MegaVision image display system, however, is limited to 1 Mb per image. Therefore, storage can be complete but display requires compression of data to fit the 1 Mb format.

A whole monkey brain tissue section can marginally be accommodated in one mosaic image reconstruction at 2x magnification. It, too, has to be considerably compressed for purposes of display. Only about one-tenth of a whole human brain section can be accommodated at a similar level of magnification. We will need much more capacious image display systems to accommodate composite mosaic image reconstructions made up of an assembly of 1 Mb mosaic image reconstructions.

The accuracy of control of the TSI Microscope stage allows seamless junctions to be reconstructed in the course of assembling very large mosaic reconstructions. The storage of mosaic patches in proper order in our system can be accommodated for every mosaic image acquisition. With limited memory capacity our computer would have to dump the information to tapes repeatedly, and the sequencing would still be appropriate to make an immense composite mosaic reconstruction. Unfortunately, there is no place to manipulate or display such a composite image, not at UCSD or at the San Diego Supercomputer Center.

A practical financial hitch has influenced us to forego completion of the whole rat brain tissue section mosaic reconstruction [2.1.2] at this time. A simple, practical difficulty is this: A 20x objective needs to be closer to the tissue than cur present coverslips permit. Coverslips of the requisite thinness are about ten times more expensive. Moreover, they have an average 80% rate of loss through breakage on slides that have enough space to hold four rat tissue sections. We consider, however, that the technical challenge has been successfully met.

A tissue section mosaic reconstruction of the rat brain at 2x magnification does not require full use of the power of the MegaVision 1024 x 1024 pixel imaging capability. The MegaVision however is not capable of accommodating magnifications higher than 2x when applied to whole tissue sections of whole monkey brains. And, the power of the MegaVision is trivial with respect to requirements for imaging whole human brain sections. The accumulation of synthetic images from whole human brain serial sections runs into many terabytes of data storage and manipulation.

1.3.1. Improve Accuracy of x-y Coordinates of Histological Sections--II

The problem of tissue distortions with sectioning at microscopically thin intervals has never been solved by histologists. Integration and de-distortion is done by their brains and hands. There is often some sacrificing of sections, too.

When one is integrating small pieces of tissue this does not much matter. Without having the task of accurate, quantitative 3-D reconstructions an histologist can assume that distortions between successive slides are inconsequential. Optimal choices of embedding material, careful, uniform motion of the microtome, exquisite care in removal of the delicate section, etc., are carefully practiced by histologists, and yet compression, dilation, differential translation, breaking away, overlapping and gapping of tissue, all occur.

The MegaVision system purports to have up to twelve differentially moveable points for warping purposes. We found, however, that if you use only two or three differential points the sections become more patently skewed than before. If you put in more than about three points for differential warping, MegaVision simply gives up and does not solve the algorithm.

This is one of the hardest problems we must solve to achieve accurate three dimensional brain mapping. Building "de-deformation" algorithms of high differential complexity is difficult. We would like to have implemented what we call a "pushbroom" whereby a certain tear or fold or a piece that remains intact but may have floated away from the rest of the section can be rotated, translated and properly replaced.

(a) Rationalizing Images for Two and Three Dimensional Reconstructions

Requirements for brain mapping have two subordinate problems that deserve consideration. The first, alluded to already, is that RCIs include some data that lie at variable depths beneath the relatively translucent surface of the frozen block face. Thus RCIs contain some pixel data that do not correspond to the plane of the TSI. Because of the depth of focus, analysis of the RCI does not reveal such z-axis complications. This does not usually constitute a complication for the location of homologous landmarks in the two images.

There is a further problem that was addressed extensively in the Task Definition Workshop. What are to be

taken as the most appropriate fiduciary marks for the registration of images in the process of three dimensional reconstruction. Introduction of fiduciary fine needles that penetrate the brain tissue interfere with blood flow and produce serum leakage from injured capillaries. Because of the normally low oncotic pressure of extracellular and cerebrospinal fluid, leaked serum proteins induce rapid local and regional tissue edema. Similar damage is done by the heat created by penetrating brain tissue with laser or particle beams. Tissue marking is actually accomplished by tissue vaporization.

When thin sections are sliced by the microtome, the fiducal marks so laboriously introduced are themselves differentially displaced within the tissue as a consequence of the slicing. Matching up the fiducial marks does not then match corresponding parts of the tissue; one has a false sense of correct alignment. Proper placement of fiduciary marks does not ensure that the tissue sections are in proper registration.

After examining a number of possibilities, we concluded that biological fiducials are more plentiful, more useful, and available at practically any scale in any part of the tissue, to well below the level at which such marks can be identified in RCIs.

We plan at present to take advantage of large and moderate sized blood vessels when they are cut at close to right angles by the microtome, for marking TSI alignments. Eventually software can be developed for machine recognition of such vessels, and a semiautomatic alignment procedure to rationalize between RCI's and TSI's.

When the x, y, and rotational aspects of the overall synthetic TSI image has been matched to the outlines of the brain, ventricles, and other gross morphology of the RCI, and finer details rationalized using blood vessels as markers, then the images can be differentiated by subtraction so that what does not lie on the surface z plane of the RCI can be eliminated from that image.

A more difficult problem lies in 3-D de-deformation. Even when individual TSIs and RCIs have been matched as closely as may be feasible, and even when the alignment provided by the successive RCI images has been ensured for three dimensional reconstruction, there will remain discrepancies in 3-D organization that are only discoverable when the three dimensional object can be inspected through the use of a volume rendering device such as is being built by Charles Molnar and Fred Rosenberger at Washington University at Saint Louis. Then it will be recognized that some nuclear groups, fiber tracts, and blood vessels are "stair-stepping" in a way that does not obtain in reality. Then a

three dimensional de-deforming algorithm must be applied. This has not yet been developed, and we look to Fred Bookstein to build software to solve this problem. Adequate three dimensional re-de-deformation of the TSI is by no means a trivial problem. It's robust solution is essential for purposes of the Brain Mapping Project.

(b) Clinical Scanning Already Benefits Brain Mapping and Will in Its Turn Benefit from Brain Mapping

We have used both computed tomography scans (CT-scans) and magnetic resonance scans (MRI-scans) for purposes of control of the premortem and postmortem three dimensional condition of animal brains before sectioning, as detailed elsewhere in this Report (See Figure 13). We have done both CT and MRI scans for whole human for heads prepared for atlas development, and have established protocols for obtaining such scanned images for each of the three species. The animals are imaged premortem under anesthesia as well as postmortem, prior to perfusion and after perfusion. The three dimensional reconstruction of scan images serve as templates for comparison of scans from living specimens. As data accumulate, this reflexive system of comparison and analysis will become increasingly useful.

It is terribly time-consuming (measured in weeks) and expensive (measured in thousands of dollars) to slice a single human head. It is also very desirable to obtain a broad database for assessment of what may be taken as "normal" gross human neuroanatomy. We have begun to develop a database and to acquire data from other sources involved in scanning large numbers of living human brains. This database will contribute to very much needed knowledge for estimating the limits of normal variations in gross neuroanatomy. It will also help to define some of the morphological phenomena encountered among classic neurological conditions. With the help of John Hesselink, Medical Director, Magnetic Resonance Institute, at UCSD, and Terry Jernigan at the Veterans Administration Hospital, we intend making three dimensional reconstructions from clinical scans already made for us in the course of human brain preparation for the BMP. These scans have the advantage that they can be verified neuroanatomically, in detail. Gradually, an important clinical database can be established, with appropriate controls. This is also not a trivial problem. For example, every time an MRI magnet is put into action it sets up a somewhat different field: there may be "pillow" or "hourglass" distortions or other field deviations which occur in all three planes of projection. To obtain an undistorted MRI, it is necessary to put in a suitable model of the head with gelatin-salt in glass tubes in three orientations the image of which can be used to de-deform the image of a human head put into the same field in the same location on the same day.

Clinical scanning can be useful to the BMP and, in turn, the BMP will increasingly contribute to clinical scanning, both by providing quantitative brain models and by increasingly demonstrating what may be considered "normal limits." In making whole brain reconstructions from clinical scans we have received encouragement and help from William Oldendorf.

(c) Side Contributions to Brain Development and Brain Evolution

The Brain Mapping Project has sparingly allowed utilization of its hardware, software and conceptual developments to help advance fields of investigation closely related to quantitative morphology and three dimensional computer graphics reconstruction. This has been done by the PI in non-BMP time, on the basis of strict non-interference with BMP activities and progress, by way of becoming acquainted with a few important related research puzzles. We have learned some new applications and improvements for BMP software and have confronted an unusual assortment of tissues and stains as well as other challenges to digitization, in respect to the following problems: (1) attempts at quantitative resolution of the gap between macroscopic and microscopic domains of brain mapping; (2) reckoning the reciprocal relations between clinical scanning (computed tomography and magnetic resonance scanning) as controls for brain mapping purposes, and seeking better interpretations of clinical scans through utilization of primitive brain maps generated in this Project; (3) mapping three dimensional growth of the human embryo, using slides from the Carnegie Laboratory for Human Embryology, at the University of California Davis; (4) three dimensional morphometric analysis of experimental brain infarctions in monkeys; (5) reconstruction of serial sections of a human temporal bone; and (6) three dimensional reconstruction of an important fossil skull.

Given the powerful potential of brain mapping systems, it is desirable to utilize the evolving computer graphics capabilities to deal with display and analysis of morphometric change over time, i.e., adding the fourth dimension. We already have four human embryos (stages 13, 15, 17 and 19) digitized for cerebral ventricles, outline of brain and spinal cord, and outline of the body as a whole. The four embryos were obtained, thanks to Ronan O'Rahilly, Director of the Carnegie Institute of Embryology, at the University of California Davis. The specimens are accurately dated and superbly cut and stained. It will be possible to utilize (i) neuraxial levels; (ii) the midline; (iii) external contours, dorsal and ventral midline profiles and circumferential profiles at successive neuraxial levels; and (iv) localizing features such as the Vth cranial nerve to establish homologous landmarks as a framework by which to

manifest differential growth in dynamic computer graphics. This will contribute to embryology in ways that have heretofore not been practicable.

By the same token, there are a number of fossil skulls that are clear of stony material from which close CT-scans can be obtained to allow three dimensional reconstruction of the "fossil brain". We have already done this on a fossil skull of a werewolf recovered intact from the LaBrea Tar Pits in Los Angeles, through the efforts of Harry Jerison, with close scanning (1 mm) provided by William Glenn and Michael Rhodes.

With hominid skulls obtained from museums, it should be possible to estimate the dimensions of the brain stem, the sizes and intervals of the cranial nerve foramina, the tentorium and dimensions of the hemispheres. In some specimens it is possible to measure some gyral markings which provides additional clues to evolving brain morphology. Whereas previously only a few measurements could be made in such specimens and endocasts, it is now possible to obtain relatively credible data on brain evolution. We are assured cooperation of several key people for such endeavors, and progress really awaits the development of improved algorithms for three dimensional reconstructions and for demonstration of dynamic measures of changes in three dimensional shape.

1.4. Improve Alignment of x-y Whole Section Images With z Axis

The technical requirement here is to obtain accurate RCIs, with fixed camera in relation to the cut surface of the block, that is, the camera-blockface spatial relationships including both verticality (that is, the film plane to be exactly parallel to the plane of section) and distance must be rigid and constant. Through the entire length of human brains cut coronally, for example, there is sufficient distance to produce a skewed reconstruction if these conditions are not satisfied precisely.

Charles Wurtz worked out how the movement of the LKB sledge could be stopped precisely at a fixed station in relation to the scaffolding that holds the camera. The scaffolding itself is borne by the pillars that rise and fall with the microtome, hence the distance, and thereby the magnification to the camera is kept constant throughout cutting the whole thickness of a human brain block. He also used precise physical instruments to measure the uniformity of distance of rise and fall and repositioning of the knife blade during each stroke and between successive sectioning strokes, as well as over a long continuing series of strokes. He built a housing to cover the block specimen to

prevent sublimation from the surface when the specimen had to be left for more than several minutes between strokes. By such means it is possible to ensure that each RCI maintains stable x - y relations to the specimen throughout all sections.

From the RCIs, outlines of the hemispheres, brain stem and cerebellum are derived. These are automatically in perfect registration. They are used to create wireframe three dimensional whole brain reconstructions (See Figure 8).

For synthetic images derived from already cut sections, such as the whole human brain material from the Yakovlev Collection, we use the Evans and Sutherland Picture System 2 which we have been employing for this purpose for a dozen years. Its virtue is that it can scale, rotate and translate 50,000 points in three-space in real time. An algorithm for alignment, implemented by Phil Cohen, allows the operator to see a succession of sections simultaneously in three orthogonal planes, en face, vertical and horizontal and to select and move any given section to ensure its alignment. Moreover, numbers relating to spatial alignment, direction and amount of rotation or translation can be identified and used for control purpose. There are some problems in interpreting some motions of three dimensional objects in free space, hence these data can be useful. This system allows us to take any vector images and align them to one another. Thus, wireframe images in vector form can be aligned usefully on the E&S system. It is somewhat cumbersome to transform raster images from the MegaVision and MicroVAX systems to vectors and, after E&S alignment, reconvert them back to raster data. To simplify the problem, at some sacrifice in precision, Kathy Drinkard, a medical student volunteer, implemented software that allows operator to control parameters of alignment of a raster to a vector system and back again. We used the E&S to align all the sections for the human brain "Atlas" depicted in the skillful neuroanatomical drawings of Larry Stensaas.

Cynthia Lemere made digital images of three whole monkey brain serial sections, cut along the three classical orthogonal planes. Using MegaVision and making black and white silhouettes via thresholding she was able to get the MegaVision system to outline the whole hemisphere, brain stem and cerebellum (See Figure 14). These provided three wireframe "atlases" of the monkey. The mounted sections, however, could not be controlled by RCIs and therefore were only approximately aligned. There was not time to do all three monkeys via the E&S which would have assured an even closer approximation.

There is no hesitancy in our conviction to insist that RCIs are an absolute necessity if we are going to be able to create accurate, three dimensional reconstructions of whole

human brains. We can easily appreciate the difficulties that obtain otherwise.

Arthur Toga has done an exceptionally fine job in the alignment and reconstruction of his monkey brain and is to be commended for the adroit algorithms he has devised for this purpose. In short, what is needed is more automation in acquisition of undistorted brain blocks, RCI imaging during careful sectioning, and powerful computer systems for TSI matching to RCIs and three dimensional algorithms to ensure internal alignment throughout the entire reconstruction.

Fred Bookstein has been eager to apply himself to this attractive mathematical problem of three dimensional shape measurement and manipulation, but we have not yet found the funding for this purpose.

1.4.1. Superimposition of Block and Slice Images

We are still a long way from being in a position to superimpose TSIs with their corresponding RCIs. There is the necessity ahead, given the powerful 2-D and 3-D alignment algorithms we anticipate, with reducing operator time so that the machine can be given intelligence or acquire intelligence to recognize corresponding landmarks by itself.

a *Program Warping of Images to Remove Distortion*

There is, as noted above, only very primitive capacity for program warping to remove complex distortions. At best, now, they can rotate and translate and perhaps manipulate a few simple geometric distortions. Our experience indicates that this is a profoundly difficult problem.

b Program Warping With Operator Intervention

The MegaVision system is the only one with which we are familiar. Judging by the difference between their claims (of up to 12 differential warping loci) and their performance (2 or 3 at the most), we are inclined to be skeptical. Most engineers are not familiar with the complexity of differential distortions that are commonplace with microscopically thin tissue sections.

c Investigate Three Dimensional Registration

We know absolutely nothing about this. Bookstein claims that it is not too difficult mathematically and

requires only a few tens of thousands of dollars for completion. How readily such an approach can be built to work with relatively primitive imaging systems and whether it can be built in hardware is an open question.

We visualize that as three dimensional reconstruction at microscopic levels of detail become more commonplace, operators will be able to distinguish boundaries more readily by eye when "moving through" a three dimensional display. It should look something like swimming through a kelp bed in the ocean.

Perhaps, according to Robert Barnhill, with interactive linkage between operators and large-scale computer graphics systems, we can look forward to three dimensional boundaries being computer drawn, corrected, and compared, under general operator surveillance.

1.4.2. Intra-Sectional Deformations

This problem has been thoroughly dealt with in the discussions throughout SOW Sections 1.3 and 1.4.

We consider that mapping the whole human brain at microscopic levels of detail deserves one of the highest priorities in contemporary goals of scientific endeavor. We believe that it deserves a priority equal or better than that for sequencing the whole human genome. In fact, these two now technically feasible opportunities will reinforce one another and provide a combined significance that is greater than the sum of their separate contributions.

2. ACQUIRE AND CREATE MORPHOMETRICALLY CORRECT LARGE SCALE BRAIN MAPS

This is perhaps the most innovative and exciting part of the Brain Mapping Project to date. It introduces a systematic method for acquiring magnified images in a sequence. From this sequence, the images can be reconstituted into a morphometrically correct large scale map. It involves computer-assisted operation of a custom made Tissue Section Imaging Microscope, the TSI Microscope (Figure 1b). The microscope employs the Circon CCD camera for image acquisition, and the MegaVision system for image editing, management, storage and retrieval. All microscope and image management functions are under control of the MicroVAX.

The operation of tissue image acquisition for creation of large scale brain maps involves capturing, filing and accessing sequential square "patch" images and assembling them into exact re-order for the creation of large-scale, multi-patch synthetic "mosaic" maps. With the TSI Microscope, synthetic maps can be created from any size brain section, up to 20 x 20cm, at 2x, 4x, 10x, and 20x magnifications. The data accumulated during this process are so enormous that they tax the memory capacities of a small computer system such as ours. And the amount of data contained in large scale tissue maps are too massive to display on a modest computer graphics system, such as the 1024 x 1024 MegaVision system.

Although designed and commissioned many months previously, by Charles Wurtz, various components of the TSI Microscope began arriving during the last month of the Contract. The microscope could not be fully assembled until beyond the end of the Contract. Nevertheless, during the period of Contract Extension, Mark Shin implemented software that controls the stage and acquires digital images stepwise in accordance with simple instructions presented to the operator.

The operator uses a variable speed toggle switch with which to position the stage in any desired location in relation to visualizing the tissue section through the microscope. The operator then selects the light and contrast values to use in acquiring magnified images from a particular specimen. The location of the image sequence is then roughly bounded, and the computer executes the sequence by placing the tissue section correctly in the microscope field, acquiring each image (in 1/30 second), and moving on to precisely station the section for the next and subsequent images to be acquired. The microscope scans a given number of mosaic elements of the magnified section along a horizontal row and proceeds with a second third and subsequent rows, etc., all aligned so that individual patches of the

final synthetic mosaic reconstruction are in perfect order and juxtaposition. A full tissue section or an area of a tissue section can be acquired in this way, according to the operator's wishes. Any rectangular array of any size can be acquired: the present limit is in image memory storage capacity. Even so, by filling MicroVAX memory and emptying it on tape repeatedly, any desired large scale image file can be acquired. The limitation is on how that large an image can be outwardly expressed.

On request, then, the computer delivers a synthetic image made up of mosaic patches captured by the CCD camera and composed into a single panoramic representation of the tissue section as reconstructed by the MegaVision system.

Each frame is reduced and stored on disk is 64 x 64 bytes plus 2048 bytes for header and color table, totalling 6,144 bytes. Each frame, as displayed on the MegaVision is 262,144 bytes. This means that even a given frame can't be displayed without compression. Since the MegaVision can display only 1 Mb, this means that even with compression, we can only display a mosaic made up of 16 x 16 mosaic patches. In principle, the TSI Microscope, in one operation, could acquire images from a given tissue section, up to the maximum size of the microscope stage, but one would have to be repeatedly unloading memory in excess of the capacity of the MicroVAX onto tape in order to keep up with image acquisition by the microscope. It is a case of the Sorcerer's Apprentice.

Then there is the problem of representation of the reconstituted synthetic mosaic tissue section images.

The computerized stage operates with two precision indexers which monitor the x and y axes. A library of routines was written in C language to control the indexers. The communication link is established by a high level program that calls for an initialization routine in the stage library. Once initialization is achieved, the program has a direct link to the indexers and can precisely control movements of the stage over the whole area of the stage, 20 x 20 centimeters. The stage is large enough to accommodate not only whole human brain sections but sections of the somewhat larger-brained whales. A right-angle registration plate has been affixed to the stage so that individual tissue section slides can be inserted against the margins of that plate. This ensures that each slide can be restored to exactly the same stage position when it is inserted repeatedly onto the TSI Microscope stage again for imaging purposes.

The digitizer of the MegaVision has a limited resolution of 525 by 525 lines. The image obtained from the TSI Microscope must be scanned in a square-patch mosaic fashion for the acquisition of single frames. The whole tissue

section is composed of square patches which are systematically reconstituted into a whole composite tissue section image.

Successive square patches must be acquired stepwise with computer control of motion of the indexers. The rectangular shape and limited size of the MegaVision digitizer is accommodated by establishing the exact stage movement that corresponds to the width of one frame of a given, specified microscope objective. An appropriately scaled database containing the scale factors for each of the microscope objectives was developed by Shin. Application programs consult this database and, depending on the magnification, move the stage an appropriate amount so that the frames seamlessly abut one another on four sides, without overlapping or leaving gaps with frames adjacent in the same rank or with frames adjacent in the ranks directly above and below.

2.1. Prepare Whole Rat Brain Atlases

We have not completed this objective, and the reasons are simple. As noted in the section above, the TSI Microscope has the capacity to conduct the whole operation without difficulty. We are satisfied that the technical capability for making such an "atlas" is at hand: this includes computer-controlled tissue section image acquisition and large scale synthetic tissue section mosaic image reconstruction. We have satisfied ourselves that these two achievements can be applied to "atlas" production for rat, monkey and human brains.

What is technically not yet satisfied includes: sufficiently uniform full field illumination in the TSI Microscope to eliminate the "patchiness" of the synthetic image. We do not yet know whether this problem can be solved for low level magnifications in this microscope, or perhaps any affordable microscope. More importantly, we do not have computer memory capacity adequate for producing a whole brain atlas. Producing segments of such an atlas and reconstructing the segments into a "quantitatively spatially equivalent atlas" can be done and reproduced with photography or paper printout, but it cannot be displayed as a whole in three dimensional graphics form in any equipment available to us, including that in the San Diego Supercomputer Center.

What is more fundamental is that we do not have the necessary algorithms or hardware capabilities to de-deform tissue section images to conform to the corresponding registration control images. Therefore, any "atlas" prepared at this time would carry with it all of the idiosyncratic individual tissue section distortions that were imposed by the

sectioning procedure. We not only need to de-deform an appropriate number of landmarks on the TSIs to conform to the truth-bearing landmarks of the corresponding, undistorted RCIs, but we do not have the monitor equipment necessary to compare and warp the images to achieve and demonstrate satisfactory correspondence of TSIs to RSIs.

We have so far dedicated the TSI Microscope to proving the technical prowess of the computer TSI imaging system for making "atlases," using monkey and human tissue section material predominantly, rather than making the actual "atlases" themselves.

We have established: (1) that putting together a complete whole brain synthetic tissue section reconstruction can be accomplished entirely under computer control, using this microscope; (2) that sequential RCIs already taken from the cut surface of whole rat brain blocks of several rats serially sectioned in their entirety in different planes of section are in ideal registration, perforce of the fixed relations between RCI camera and blockface. We have thus concentrated on solution of the methodological problems rather than on executing a specific "atlas" that would, at this time, be both two dimensionally and three dimensionally deformed.

Within the duration of the Contract such an "atlas" production, even with geometric shortcomings, would have turned out to be impossible because of the late arrival of the equipment for the TSI Microscope. We shall have to be satisfied that certain methodological problems for image aquisition and image synthesis have been satisfied, and that the registration control images are have provided geometrically correct wireframe "atlases."

2.1.1. Three Dimensionally Accurate Alignment

Only the external morphology, as interpreted by the RCIs, is three dimensionally accurately aligned at this time. We await two dimensional de-deformation and three dimensional re-de-deformation algorithms and the requisite monitors for display and warping performance purposes.

2.1.2. Tissue Section Image Maps

Here, we can rejoice in what we have to report and demonstrate. This can be appreciated from what we have already said, and particularly, from Figure 15.

2.1.3. Generally Agreed Upon Structure Maps (Wireframe Outlines)

We have succeeded in constructing wireframe and solid surface renderings of whole rat brains (See Figure 8 a, b, c), whole monkey brains (See Figures 16 a, b, and 17 a, b) and combinations of wireframe with accurate internal mapping of identifice structural organization in the whole rat brain (See Figures 18 a, b; 19 a, b).

2.1.4. Prepare One or More Rat Brains

Three whole rat brains were sliced through full dimensions of the specimens, RCIs were taken of each section, and contours were drawn using the MegaVision system, by Cynthia Lemere. These contours were reconstructed three dimensionally and presented graphically as wireframe and solid modeled figures (See Figures 8 a, b, c). Additional rats were similarly sectioned, digitized for wireframe "atlasing" and for internal structure/function manifestation, by Dean Hillman (See Figures 18 and 19). Due to improvements in specimen staining and embedding quite good computer interpretation of outside boundaries can now be achieved with the MegaVision system. Some difficulties remain to be overcome when thresholding the captured RCIs in order accurately to distinguish and contour by computer discrimination, white matter and ventricles.

A series of whole rat brains were prepared according to a protocol for systematic exploration of various dyes, mordants, embedding material, etc., including the following:

> Ammonium carmine (RCIs) 1; Boracarmine (stained, not sectioned) 1; Lithium carmine (trial sectioning on one) 3; Picrocarmine (trial sectioning on two) 21; Osmium (RCIs on one) 7; Methylene blue (sectioning on four; RCI and wireframe reconstructions on three) 9; Neutral red (trial sectioning on two) 2; Luxol fast blue (trial sectioning on one) 2; Unstained (trial sectioning) 2. Outcome of image analysis: Methylene blue has reasonable advantages. Trials with various embedding media: outcome: preferential advantages for Egg albumin with gelatin, blackened with India ink and carbon (See Figure 12).

2.1.5. Test Bed for Two and Three Dimensional Warping Algorithms

By the 5th quarter we had completed three satisfactory whole rat brain wireframe fiducial "atlases" in precise registration. Their contours are three dimensionally

accurately aligned. They constitute an appropriate test bed for two- and three-dimensional de-deformation. The appropriate algorithms await the mathematical genius of Fred Bookstein for whom we have as yet not been able to obtain the requisite funding.

2.2. Prepare Whole Monkey Brain Atlas

We prepared, according to a similar protocol followed in humans, a single whole monkey brain, stained with Methylene blue and embedded in black egg albumin and gelatin (See Figure 20). This is properly vapor-locked in a frozen state and held in storage until we can be confident enough of both automatic cryomicrotome tissue section capture and simultaneous automatic RCI acquisition with the MegaVision system, techniques that are under continuing development, using rat brains.

Arthur Toga was successful in developing methods by which to create computer graphic three dimensional reconstructions of a whole monkey brain (See Figures 16 and 17). His data are derived from a single animal. The serial sections were scanned and digitized as detailed in the Toga References. The sections were re-aligned using several methods. They were either aligned manually by indicating translational rotational correction factors, or they were aligned automatically using a registration tool set. This tool set is comprised of algorithms which are based upon the notions of: centroid of the mass, principal axis, best fit, and fiducial alignment. The algorithms are executed iteratively such that the results of one are fed into the other. The process continues until the increment of change is smaller than a pre-set level.

Although Toga is not entirely satisfied with the results of the alignment procedure we have developed so far, we believe that his work represents a major advance toward a completely accurate solution of a very difficult problem. It reasonably satisfies the requirement for three dimensional accuracy in whole brain mapping and three dimensional computer graphic reconstruction, display and analysis.

Until now, these algorithms have been applied only within a single brain and have not yet been tested on different brain data sets. Moreover, the multiple brain database on which it had been intended to test these algorithms for interbrain registration and comparison purposes has not yet been implemented. The time to complete the database and interbrain registration algorithms is greater than the time allowed.

2.2.1. Prepare a Minimum of One Complete Monkey Brain

Toga prepared one complete monkey brain, complete with an "atlas." The sequence of its preparation and reconstitution of its three dimensional volume are illustrated in Figures 16 and 17.

2.2.2. Three Dimensionally Accurate Alignment

The accuracy of section alignment is evidenced by the fact that the sulci and other cortical landmarks in the monkey brain appear realistic and correspond to the locations of gross morphological landmarks on the surface of the original specimen. If the alignment algorithms did not produce excellently registered sections, you would see obviously skewed and distorted sulci and gyri following the surface modeling.

2.2.3. Tissue Section Image Maps

The tissue section image maps are depicted in Figure 17 b. Three dimensional volumes of the whole brain can be resectioned along any arbitrary plane to illustrate the tissue section used in the original data collection, or along any arbitrarily devised plane. In this case, these maps depict functional activity, specifically, cerebral glucose utilization.

2.2.4. Generally Agreed Upon Structure Maps (Wireframe Outlines)

The structure maps which are delineated by wireframe outlines have not yet been completed for an exhaustive list of structures. However, the algorithms which were used to generate the surface of the whole brain are appropriate and competent for depicting substructure modeling to be rendered deep to the cortical surface. If the work continues, the database application and substructure wireframe maps will be completed in parallel and in the same brain three-space as whole monkey brain three dimensional wireframe and solid contouring reconstructions.

2.3. Prepare Preliminary Atlas of Whole Human Brain

Creation of a cytoarchitectural and myeloarchitectural reference "atlas" of the human brain was carried out using material from a single, serially-sectioned, celloidin embedded brain from the Yakovlev Collection at the Armed Forces Institute of Pathology (AFIP) in Washington, D.C.

Subcortical structures were mapped on photographic enlargements having a magnification of 12.5x, of whole brain Nissl and myelin stained sections using a dual stage microscope that permits optical superposition of adjacent serial sections. Adjacent Nissl and myelin sections could thus be superimposed, and next-sequential myelin to myelin or Nissl to Nissl could be similarly compared.

Mapping of cells constituting the subcortical cytoarchitectural units was carried out under the microscope at 40x, 100x and 200x, and photographic documentation of each of the anatomical features of interest was provided on 35mm color transparencies.

Serial tracings of the brain cytoarchitecture were created at 0.7mm intervals to demonstrate the location of subcortical nuclei which were all named in accordance with conventions found in recent literature. (See Appendix B for Neuroanatomical List of Human Brain Subcortical Structures depicted in this "atlas" by Stensaas). Serial maps of brain myeloarchitecture were created at a similar 0.7mm interval using 35μm sections adjacent to the Nissl sections used for cytoarchitectural analysis. The principal myeloarchitectural units were identified on tracings in the maps.

Photographic documentation of the cytoarchitecture and myeloarchitecture in the form of several hundred 35mm slides has been described earlier in this Report.

2.3.1. Prepare One Preliminary Human Brain

BMP, mainly Charles Wurtz and Cynthia Lemere, with demonstrations and consultative advice from Wolfgang Rauschning, and with the special facilities provided by John Sykes and Bill Collins of the UCSD Willed Body Program, prepared eight intact human heads according to a careful, experimentally designed new protocol (See Figure 20). Most of these heads were imaged with Computed Tomography, thanks to Clint Stiles of Picker Corporation, or Magnetic Resonance Imaging, thanks to John Hesselink of the Magnetic Resonance Institute at UCSD, (or with both of these scanning procedures). These procedures were undertaken for purposes of three dimensional clinical image reconstructions. The reconstructions will be used for comparison with serially sectioned whole brain computer graphics reconstructions obtainable from studying the anatomical material. The BMP goal was to generate a small number of "normal" whole human head preparations and to delineate them with state-of-the-art clinical scanning techniques prior to sectioning them in the LKB giant cryomicrotome for production of complete RCI sequences and selected tissue section image analysis. Several "ideal normal" heads were selected and prepared in order to benefit from inter-specimen comparisons, and so

that we could section through whole normal heads in each of the three classical orthogonal planes of reference. Methods for selection and preparation of these specimens were detailed in BMP Quarterly Reports and summarized in the Annual Report.

2.3.2. Three Dimensionally Accurate Alignment

Using data from Cinemorphology sequences, captured earlier, which were acquired using a Mitchell, 35mm pin-registered motion picture camera, using camera-blockface alignment procedures similar to those for MegaVision system RCIs, we were confident of three dimensionally accurate alignment to proceed with the following:

2.3.3. Generally Agreed Upon Structure Maps (Wireframe Outlines)

BMP created a single whole human brain wireframe reconstruction and rendered the same with solid surfaces. We also created wireframe reconstructions and rendered solid surfaces on twenty subcortical parts of that brain in correct dimensionally accurate whole brain three-space. For the solid rendering, we used the Reynolds solid surfacing software to produce solid models comparable to the wireframe outlines we had made of the same structures (See Figures 21 and 22).

3. ACQUIRE AND CREATE SELECTED SUB-STRUCTURE BRAIN MAPS

3.1. Prepare Neurochemical Structure/Function Maps of Whole Rat Brain

Recent production of high titer polyclonal antibodies against choline acetyltransferase, the acetylcholine biosynthetic enzyme, together with technical improvements in immunolabeling procedures in David Armstrong's laboratory, permitted localization of cholinergic neurons within regions of the brain where they had not previously been detected (hippocampus, cortex, and hypothalamus). In BMP studies, Armstrong and his colleagues employed light microscopic immunocytochemical techniques to the whole rat brain in serial sections and reexamined the anatomy of the entire rat brain cholinergic neurotransmitter system. BMP work was conducted with technical help by Susanne Almstrom.

The Armstrong group generated accurate two dimensional maps of the distribution of cholinergic perikarya throughout the whole rat brain. Two dimensional tissue section maps of ChAT were prepared for insertion into one of the BMP three dimensional whole rat brain wireframe "atlases" reconstructed from RCIs acquired with the MegaVision system. Armstrong provided enough landmarks in his "atlas" to be able to make a reasonable fit of his data into the wireframe "atlas."

ChAT localization in three dimensions was complemented by other studies in Armstrong's laboratory involving characterization of the quantitative morphology of cholinergic neurons in the aged rat the brain and in brains of specifically lesioned animals. BMP Progress in Armstrong's laboratory has been published, or is in process, in five papers (See References in Appendix) which include quantitative morphometrics of cholinergic neurons in normal, denervated, and aged rat brains.

3.1.1. Maps Will Be Based On Cells Labeled By Neurotransmitter Specific Markers:

a Acetylcholine

In addition to the work, cited above, in Armstrong's laboratory on acetylcholine, Dean Hillman created additional three dimensional reconstructions of the rat brain. Using BRAINMATE, developed at UCSD for the BMP Contract by Donal Hurley, a former student of Hillman's, external contours of the brain were digitized and reconstructed three dimensionally. Using monoclonal antibodies for

acetylcholinetransferase, each of the cells that manifested receptors was located in correct x, y, coordinates on each section. Then, all the sections were assembled three dimensionally and aligned in the form of a three dimensionally accurate wireframe "atlas." This illustrates structure/function relations for acetylcholine systems of the rat brainstem and telencephalon (See Figures 18 a, b; 19 a, b), with cell aggregations in three-space alone and with external boundaries of the brain stem and telencephalon added in stereospecific spatial relations.

b Substance P

Antibodies for substance p have been obtained, characterized and tested in John Morrison's laboratory, using monkey cortex for three dimensional localization in whole monkey brain mapping protocols. There have been no conclusive experiments to date with substance p as the labeling target for three dimensional mapping of the whole rat brain.

c Catecholamines

Both dopamine and norepinephrine have been extensively mapped three dimensionally in monkey cortex by John Morrison and his colleagues, but these techniques have not yet been applied to the whole rat brain.

3.1.2. Maps Will Be Based on Wireframe Imaging

The BMP has produced a few whole rat brain wireframe "atlases." Note the localization of specifically labeled neurons, e.g., Dean Hillman's work noted above (See also the relevant figures 18 and 19).

3.2. Prepare Neurochemical Structure/Function Maps of Monkey Neocortex

3.2.1. Produce Quantitative Regional Profiles for at Least 80% of Cortex

Somatostatin has been identified and localized in all neurons which reacted with the receptor label, in the full-thickness three dimensional space of monkey cortex throughout most of occipital, parietal, frontal, and temporal brain regions.

The total aggregate of completed somatostatin localization represents 80% plus of the entire monkey neocortex.

This large-scale undertaking demonstrated the practical utility of these pioneering computer assisted methods for three dimensional mapping of an important brain structure/function relationship. This important task was conceived and executed by John Morrison, Warren Young, and their colleagues. Throughout most of the Contract period, they were obliged to us a more primitive, less efficient hardware system. The BMP Zeiss Axiophot Widefield Research Microscope was delivered late, but nonetheless proved its capability and efficiency in the completion of the somatostatin mapping, although the Maerzhauser stage still lacks a shim that had to be remanufactured to conform to the original specifications.

For purposes of accurately and quantitatively localizing somatostatin throughout so much neocortex, Morrison and his colleagues depended on the EMMA software package designed by Warren Young and Mark Shin.

A three dimensional representation of somatostatin, together with a specifically identified beta amyloid polypeptide associated with familial Alzheimer's Disease, also found in monkey cortex, was created by Morrison and his colleagues, using these same methods for three dimensional reconstruction. An example of this clinically important structure/function analysis was published as a cover of Science, volume 235, 22 February 1987. It served as the herald for four accompanying articles on the beta amyloid polypeptide and its genetic linkage in familial Alzheimer's Disease. The Legend to the BMP-assisted cover illustration states: "A color graphic display of an optical density scan of prefrontal cortex from a cynomolgus monkey, hybridized with an RNA probe transcribed from complementary DNA clone lambda-Am4 coding for Alzheimer beta amyloid polypeptide. Each color represents an optical density range of grain clusters, with red as highest, green as intermediate, and blue as lowest density. See p. 873. Graphic provided by John H. Morrison, Gerald A. Higgins, David A. Lewis and Michael C. Wilson, Scripps Clinic and Research Foundation, La Jolla 92037; and Sina Bahmanyar, Dmitry Goldhaber, S.K. Shankar and D. Carleton Gajdusek, National Institutes of Health, Bethesda, Maryland 20205; Computer software (E.M.M.A.) by Warren Young and Mark Shin, Scripps Clinic and Research Foundation."

Copies of this Science cover were sent to the US Army Medical Corps Research and Development Command shortly after publication.

3.2.2. Structure/Function Maps Shall Be Prepared for Two Neurochemicals

Using same these techniques, Morrison and his

colleagues have recently carried out similar three dimensional localization of all cells bearing dopamine receptors, throughout most of parietal and temporal cortex (comprehensively surveying about 35% of total neocortex), and for all cells bearing norepinephrine receptors throughout occipital, parietal and temporal cortex (comprehensively surveying about 60% of total neocortex).

3.2.3. Maps Shall Be Based on Wireframe Imaging

Arthur Toga has produced both wireframe and solid rendering reconstructions of the whole monkey brain, and has inserted functional data such as metabolic rate, spread of seizure activity, etc., into both wireframe and solid rendered representations of the monkey brain (See below SOW 4), we have not yet inserted neurochemical structure/function data into three dimensional wireframe reconstructions.

All structure/function related data we have are available in in computer graphics displays as individually digitized sections bearing both neurochemical and neuroanatomical information, combining xyz parameters with each structural and functional entity so that they can be successfully mapped within three dimensional reconstructions.

In some BMP files, two specific neurochemical labels are exhibited along with neuroanatomical and spatial information.

3.3. Prepare Map of Structural Organization of Human Thalamus

The main contribution here derives from the work of Larry Stensaas, described in detail in SOW 4.1, in which the entire brain stem and diencephalon, including the human thalamus were outlined at 20x magnification, digitized, aligned and displayed. For comparison purposes, we newly digitized another whole human thalamus and also made three dimensional comparisons with three reconstituted whole monkey thalami, as follows in the remainder of this section.

Jason Doctor, Marney Blair and Jessica Chou, outlined on semitranslucent tracing paper the whole human thalamus from serial sections of the entire brain stem prepared by Paul Glees, Professor of Anatomy at the University of Goettingen, West Germany. Glees had made a present of these beautifully prepared slides to the Quantitative Morphology Laboratory some years previously.

Tracings, carefully rendered by volunteers under Livingston's supervision, included the major functional groups of nuclei in the thalamus: i.e., sensory relay,

sensory association, motor association, limbic association and diffusely projecting groups, such as the intralaminar nuclei and reticularis. Several sequences of these conscientiously rendered two dimensional tracings were digitized on the Evans and Sutherland Picture System 2. The digitized sequences were aligned to establish the anatomical congruity of the reconstruction procedures. For want of time, this particular human thalamus has not yet been fully digitized and aligned. The images available on the E&S system are in the form of wireframe reconstructions.

For comparison between monkey and human thalami, we capitalized on and added to some previous work in this laboratory. Using monkey serial sections, prepared in 1947 by Yakovlev and Livingston, adjacent sections of which are in the Yakovlev Collection at the AFIP, Xu Lu-xi, Associate Professor of Anatomy at Beijing University, painstakingly outlined each of 29 identifiable thalamic nuclei at 12.5x magnification. She did this in each of three matched monkey brains sectioned at right angles to one another in the three classic orthogonal planes. The three sequences through the whole brains of these animals provided the thalamic material digitized by Xu. Since the brains were similar in size and cut in the three orthogonal planes, they each served as morphometric controls for one another, e.g., the profile of horizontal sections was used to verify the length and z-axis of the sagittal sections; the coronal series was used to verify the width and z-axis of the horizontal sections; the sagittal series was used to verify the width and z-axis dimension of the horizontal series, etc. The digitized sections were aligned on the Evans and Sutherland system using the ALIGN program of Phil Cohen.

BMP volunteers and staff developed wireframe atlases of these three thalamic renderings, including the thalamus as a whole and each of the 29 sub-structures of the thalamus. The thalami in these series were displayed both as wireframe reconstructions and as solid surface renderings, using the Reynolds CONTOUR VIEW software (See Figures 23 and 24).

3.3.1. Wireframe Maps Shall Be Based on Slides from Yakovlev Collection at USAFIP

This has been fully described in this Report in Scope of Work section 4.1. Examples of some of the completed wireframe reconstructions are given in Figures 21 and 22).

3.3.2. Relaxation of Registration Requirements

(a) Methods Employed to Align Registration of Unaligned Human Brain Sections

As presented in this Report, Stensaas' careful tracings from serial sections examined directly in the microscope at 12.5x magnification and projected onto photographic blowups of the same sections, were digitized by Stensaas and Livingston on the Evans and Sutherland system. Alignment is by the ALIGN program, written by Phil Cohen, which allows sequences of digitized sections to be represented simultaneously in three orthogonal planes of section. Thus, four to six sections, depending on the burden of total data, are projected simultaneously in profile for two of the planes of reference, and en face for the third plane of reference. With the en face projection, two sections, with any choice among the several sections exhibited in the other plane, are projected in wireframe outline of whole and sub-structural parts of whole sections. One of these Sections is taken to be the "Reference section" to which all other sections in the series will be aligned. The first group of sections is selected somewhere close to the mid-region of the entire sequence of sections so that "drift" will be minimal throughout the whole sequence. The Reference Section is held stable by the software. The section-to-be-aligned can then be rotated and translated to align its outline and internal features as closely as possible to the Reference Section. The projections in the two other planes of reference move also. Their simultaneous projection on the screen allows the operator to see the profile of the sections in those projections. This helps to avoid "drift" and other misalignment tendencies when alignment is addressed only in the en face projection. The operator has prior knowledge as to what the profiles in the various planes and projections "should" look like and can maneuver the sections undergoing alignment procedures so as to obtain "best fit" alignment by external and internal appearances from any desired point of view.

Once an adjoining section has been satisfactorily aligned, the operator indicates acceptance, and that section becomes the Reference section for the next adjacent section. Working both directions from the middle of a long sequence allows the operator to create anatomically responsible decisions throughout the entire stack. If, after completion of a long run of sections, or the entire stack, the operator can go into the series and undo and redo any desired section. When the entire stack of sections has been satisfactorily aligned, the data relating to three-space control of alignment are stabilized for each section in reference to all other sections in the stack. Whenever that three dimensional object is called up for imaging or dynamic display, the whole block of reconstructed tissue is exhibited as an intact structure. The align data constitute a separate add-on of data assigned to each section and to the whole stack of sections and these data go with the section or stack henceforth. They can be modified at any time without disturbing the internal vectors that were "immortalized"

when the section was first digitized. This means that alignment data remain separate from the detailed neuroanatomical data representing the digitized contents of each serial section.

The entire catalogue of two dimensionally accurate neuroanatomical structures drawn from serial sections of the whole human brain (excepting neocortex) by Larry Stensaas (See list of anatomical structures in Appendix B) was digitized by Stensaas and Livingston. They used the TALOS tablet and the Evans and Sutherland Picture System 2 for this purpose. There were three fiducial channels, marked by the insertion of fine needles throughout the whole brain stem. The fiducials and numerous other landmarks were used for alignment purposes with the ALIGN program implemented by Phil Cohen on this system. Although celloidin sections are remarkably stable, we still had great difficulty achieving satisfactory alignment. Once aligned, the structural outlines of numerous structures were displayed on the E&S monitor, singly and in functional groups. (Examples of this three dimensional wireframe production of human brain substructures are given in Figures 21 and 22.)

3.4. Map Structure/Function Relationships in Retina

(a) General Approach to Comprehending and Accelerating Neurosciences Progress

One of the main purposes of the BMP is to facilitate neurosciences comprehension of structure/function relations of the nervous system as-a-whole. Much of this part of BMP activity has been advanced by Floyd Bloom, Dean Hillman and Harvey Karten. Their attention has become focussed on the development of a powerful, computer-aided neuroscience database. Karten's contribution to an evolving concept of a neuroscience database as it applies to the BMP follows:

The purpose of a comprehensive neuroscience database is to provide an inventory of neurons, connections, transmitters, physiology, pharmacology, and behavioral aspects of brain structure/function organization. There is an imperative need to provide a standardized source of information, easily accessible, that will permit correlations within the rapidly growing mass of data of importance to advancing research and clinical understanding of the structure/function relations of the brain. There is at present no existing database that provides an adequate model for the development of a powerful neurosciences database. Indeed, a powerful neurosciences database would provide inspiration and contribute as a model for other life sciences. Such a database will be of immense importance to research progress in the neurosciences and to generally clarifying the role of the nervous system in normal and

pathological conditions.

The goal of this part of the BMP involves developing a format for collecting and retrieving fundamental selected ("vetted") information concerning the brain. Such information must be keyed to both structural and functional systems, component cell patterns, connections, transmitters, receptors and trophic factors, features of ontogenetic development and organization, susceptibility to pharmacological agents, neurotoxins and other deleterious agents, role in physiological, behavioral and pathological processes, and the effects of direct and indirect injury to the nervous system.

Methodological advances within the past couple of decades have provided unexpected capabilities for the collection of valuable information in each of these areas. Expanding growth of methods and data has overwhelmed existing methods for data collection and retrieval. Accelerating progress unaccompanied by adequate methods and experience in retrieval represents an undesirable handicap imposed on existing opportunities for basic and clinical research, teaching and service.

Of significant immediate help to investigators and clinician will be a universally accessible database containing information on many diverse and some neglected aspects of brain organization and function.

Establishment of a suitable neuroscience database requires development of new methods for data collection, evaluation, organization, storage and retrieval, within the framework of an "expert system."

With Floyd Bloom's leadership, initial development of such a system is being designed and tried out with respect to several brain circuits and is engaging the database development skills of a diverse group of advanced neurosciences research laboratories. For example, in the BMP, Karten is developing a database system for the retina which may become a useful prototype for database development for the nervous system as a whole.

(b) Studies on the Retina:

The retina is desirable for detailed structure/function analysis for several reasons, all pertinent to solving generic brain mapping problems. The retina is an embryologic extension of brain tissue, structurally and functionally brain. It comprises a thin, layered neuronal network with a limited number of cell types. No other brain circuit is equivalently circumscribed between input and output. There is a large body of information available regarding the anatomy, physiology, pharmacology, and psychophysical

properties of the retina. The retina is thus relatively well understood as an integrative subsystem of the brain.

Retinal features make possible quantitative spatial analysis of defined neuronal populations. Recent histochemical studies of the retina reveal an unexpected diversity of biochemically specific neuron types within the population of horizontal, amacrine and ganglion cells. Identification of neurotransmitters, important in its own right, is not enough. There are several oligopeptides that can serve modulatory as well as communicative functions in neuronal circuits. Receptors of all sorts need to be characterized functionally because different receptors can have entirely different consequences with respect to the same transmitter. What is not understood is what specific information-determining processes take place, where, and by what channels? It is known, for example, that there can be two-way communications between neuronal processes without dispatch of signals via axons. Amacrine cells lack axons; yet they play a critical role in integrative processes and information relay in the retina. It is desirable from the point of view of understanding and analyzing biochemical diversity throughout the brain that we investigate retinal cell types, make quantitatively accurate reconstructions of their circuitry, and analyze their structure/function relations with respect to their role in physiological and psychophysical functions of the eye.

Karten and his colleagues generated software for collecting information on cell density and average cell spacing. This software can be applied to any appropriately stained neural tissue throughout the brain. Procedures are employed to combine functional specificity with structural maps.

(c) Adrenergic Transmitters in Horizontal Cells

Karten is investigating both avian and mammalian horizontal cells. They mediate lateral interactions among photoreceptors. With the exception of the still disputed possibility of GABA neurotransmitters, the identify of transmitters in horizontal cells was unknown at the beginning of the BMP. On the basis of previous Golgi studies, two types of horizontal cells had been identified in the mammalian retina, Type A and Type B. A very important finding by Karton's group was the demonstration of PNMT in Type A horizontal cells. PNMT is the enzyme responsible for the final stage of synthesis of epinephrine in neural tissue. This enzyme was first found by Karten and colleagues in the ferret retina. The evidence was published in J. Neuroscience. Subsequent studies demonstrated a similar population of horizontal cells in the rat; studies have been initiated to determine whether adrenergic horizontal cells occur in the human retina.

Using morphometric methods provided by BMP technology, the number, density and regional distribution of adrenergic horizontal cells have been investigated. The feasibility and success of this discovery is due to the provision of equipment, computer facilities and software by this Contract. Details of this research were provided in the Sixth Quarterly Report, giving examples of quantitative morphology using immunohistochemical methods in a well defined brain circuit.

(d) Nicotinic Acetylcholine Receptors in Retinal Amacrine Cells

Research of the last decade has demonstrated that acetylcholine is restricted in its distribution within the retina to a limited population of amacrine and ganglion cells. The cholinergic amacrine cells consist of two distinct populations, an orthotopic group with cell bodies lying within the inner plexiform layers (IPL), arborizing in layer 1c-2, and a group of displaced amacrine cells with cell bodies in the ganglion cell layer, with dendritic arborization within layer 4 of the IPL. Cholinergic amacrine cells constitute approximately 15% of all amacrine cells (average of approximately 3,000 orthotopic and 3,000 displaced amacrine cells per square millimeter in the central retina).

(e) Gamma-Amino Butyric Acid (GABA) and GABA-A Receptors in the Retina

GABA is one of the major inhibitory transmitters of the retina, and is estimated to occur in about 40% of all amacrine cells. (Glycine, a second inhibitory transmitter, is estimated to be present in an additional 40% of retinal amacrine cells.) Identification of precise populations of these distinctive amacrine cells has proven difficult due to the generally high density of staining of dendritic arbors within the IPL and a faint and inconsistent pattern of staining of GABAergic somata. There are at least two major types of GABA receptors in the central nervous system, GABA-A and GABA-B. GABA-A receptors are better characterized and monoclonal antibodies specific to the GABA-A receptor have been generated. Current work on the monkey retina in Karten's laboratory is directed towards identifying this population of GABA-receptive neurons and obtaining quantitative data on their number and specific distribution.

(f) Ganglion Cell Transmitters and Modulators

With support of the BMP, Karten and colleagues have demonstrated substantial heterogeneity in the biochemical characteristics of ganglion cells: Approximately 1% contain a catecholamine synthesizing enzyme (tyrosine hydroxylase), 3% contain substance p, and a third population contains

cholecystokinine-octapeptide (CCK-8). The results of two studies were recently published and the analysis of CCK-8 is nearing completion.

Studies on the human retina have been initiated in collaboration with Donald Minckler of the SCRF. Despite delays in some necessary equipment and software to count cells automatically, a fullscale analysis of the distribution of various neurotransmitters, neuropeptides and receptor molecules is now making substantial progress based on methods developed for avian and mammalian studies.

Importantly, the retina provides an excellent testbed for the development and utilization of a database that could be considered prototypical for development of a more comprehensive database for the brain.

3.4.1. Specify Structure-Function Relationships Between Amacrine and Ganglion Cells

As noted above, (3.4. (d)), cholinergic amacrine cells have been identified and localized in the retina. Identification of cells receiving cholinergic input would provide important information regarding the consequences of activation of cholinergic systems in the retina. It would also tell us something about the effects of exogenous agents likely to alter the levels of acetylcholine within the retina (e.g., agents that affect the levels of acetylcholinesterase, cholinergic receptor sites, etc.).

Using monoclonal antibodies directed against specific subunits of the nicotinic acetylcholine receptors, developed by Jon Lindstrom of the Salk Institute, Karten has identified well-defined populations of retinal ganglion cells containing the nAChR, and analyzed their three-space distribution within the IPL in relationship to the location of the cholinergic amacrine cells. The nAChR positive ganglion cells constitute approximately 18% of all ganglion cells. The laminar distribution of nAChR within the IPL is sharply restricted to the same laminae that contain the acetylcholinergic dendrites of amacrine cells. Thus, unlike apparent discrepancies, referred to as "receptor mismatch," reported in other parts of the central nervous system, there appears to be a precise relationship of transmitter and receptor distribution within the retina. The results of this study are in press (Keyser, et al, in Visual Neuroscience).

Double labeling for both ChAT and nAChR demonstrated that there is no apparent co-localization of these two substances in any amacrine cell. This implies that the cholinergic amacrine cell does not receive a direct input from other cholinergic neurons. Estimates of the number of nAChR

positive ganglion cells indicates that not less than 15% and not more than 30% of ganglion cells are cholinoceptive. There is no evidence for acetylcholine in any other retinal cell types (photoreceptors, bipolar, horizontal and ganglion cells).

Collection of the quantitative data and computer plots of regional distributions were made possible through the availability of hardware and software provided by the Contract (See Figures 25 and 26).

3.4.2. Basemaps on Differential Peptidergic Identifications of Amacrine Cells These were reported in detail in previous Quarterly Reports.

4. CREATE CYTOARCHITECTURAL AND MYELOARCHITECTURAL REFERENCE BRAIN "ATLASES"

4.1. For the Human Brain:

4.1.1. Location of Major Units at 0.7mm Intervals

Stained serial myelin and Nissl sections of one representative "reference" human brain were selected by Larry Stensaas from the Yakovlev Collection at the Armed Forces Institute of Pathology. These sections were analyzed and the cytoarchitectural units (CU) of the brain stem and telecephalon were mapped, exclusive of neocortex. Serial maps were created at an interval of 0.7mm using photographic enlargements at 10x magnification. The original slide served as the negative.

Each CU was then outlined on the photographic enlargement by examining the original slide under the microscope and carefully tracing the outlines, using individual cells as landmarks. Stensaas labored through a total of six increasingly refined editions of this "Reference Atlas" in order to establish, to the best of his ability, boundaries and nomenclature that would be widely accepted by the world community of neuroanatomists.

[See Appendix B: List of Neuroanatomical Structures outlined by Larry Stensaas and digitized and aligned by Stensaas and Livingston. The location of these named structures in the three-space of the "Reference Atlas" brain was assured by the careful tracing and preservation of neuroanatomical boundaries throughout each section, at 0.7mm intervals.]

4.1.2. Alternate Celloidin Sections Stained for Myelin and Nissl

Stensaas prepared myelin stained images at 10x and 40x using 35mm photomicrographs taken at 2mm intervals. Myelin stained sections at an interval of 0.7mm were also prepared as photographic enlargements at a magnification of 10x and the principal CUs and myeloarchitectural units (Mus) were mapped with reference to each individual section, viewed by means of a light microscope. 35mm color slides of the MUs were prepared at 2mm intervals using a light microscope equipped with 10x and 40x objectives. A total of approximately 1500 35mm slides were prepared in this way.

4.1.3. Preparation of Nissl Images of Nuclei at 40x, 100x and 200x, Using 35mm Photomicrographs at 2mm Intervals

Photographic documentation of each of the CUs of the Nissl stained sections was provided using 35mm color slides which were taken with a light microscope equipped for photography using progressively higher 40x, 100x, and 200x images of the same field of view. A total of 3500 slides were prepared of this material at 2mm intervals throughout the entire brain stem.

4.1.4. Store on Optical Disk

In collaboration with David Chabolla and Luann Teschmacher, medical students at UCSD, Stensaas then documented 2600 of the total of approximately 5000 color slide images of the CUs and MUs throughout 23 representative levels of the human brain. These were organized in carousels, projected, digitized and recorded on one-inch magnetic tape with appropriate time codes. This was done in the Department of Educational Media television studio at the University of Utah.

The CU slides showing neuroanatomical details at low, medium and high magnifications were labeled both with their Latin scientific names and their common names, and the section level was indicated for each group of brain images. This provides a direct correlation between the optical disk images and each level of the "Reference Atlas."

An optical video disk was then created from the one-inch master tape by the 3M Company as part of a University of Utah teaching project. The disk was entitled A Slice of Life. Images pertaining to the mapped Yakovlev brain were put into a new order to provide a sequential progression through the brain stem and these were recorded on 3/4-inch video tape for distribution for teaching and research purposes.

4.1.5. Employ Contemporary Nomenclature and Produce Table of Equivalents

Appendix B contains the nomenclature assigned to the human brain subcortical structures by Larry Stensaas.

4.2. For Rat and Monkey Atlases, Align Photomicrographs With:

4.2.1. Digital Renderings of Whole Brain Surface

We now have complete serial sets of sections from two whole rat brains. Tissue sections from the two animals were carefully removed from the cryomicrotome blade and stored in phosphate buffer. They have not yet been mounted, stained and photographed. There are approximately 250 sections stored for each brain. The RCI's which correspond to each of these sections are available in computer tape storage.

Completion of this task is awaiting tissue staining and photomicrography for alignment with existing digital renderings of whole rat brain surfaces.

4.2.2.

4.2.3.

4.2.4. Digital Renderings of Ventricular Surface, Myeloarchitectural Units of the White Matter and Cytoarchitectural Units of Gray Matter

These digital renderings are not entirely satisfactory with respect to complete computer controlled differentiation of ventricles, myeloarchitectural and cytoarchitectural units of white and gray matter. While we have been successful in detecting the outersurface of the brain with thresholding, we have not been as successful in contouring the ventricles and white matter. Several problems have been encountered. The outersurface is more easily defined because of it's light color set against the black embedding media whereas, the video image gray level differences inside the brain are not as sharp and therefore are not as easily detected. Changes in lighting, such as the amount of background light (i.e., daylight levels), lamp movement and camera drift in light level gain over many hours of camera use, make accurate and consistent thresholding difficult to perform automatically.

Figure 1. a: Photograph of Registration Control Image (RCI) acquisition system. The long white bench-height cabinet is part of the refrigeration housing of the LKB giant cryomicrotome which is used to slice whole brain tissue sections. The microtome operates automatically, with adjustable angle of blade attack, and variable speed of sectioning, thickness of section, pause on station at selected intervals among cutting cycles, etc. The block, frozen or solidly embedded specimen, is moved by a powerful motor along a steady base track in the floor of the refrigerator. Following each cut, the knife is raised during the return course of the block and the returned to a precise setting, lowered by the incremented value of thickness of the section. Operator continuous control of cutting speed is enabled by the knee-lever with a white plastic upright blade is seen lower right. Control of microtome is set up on the black instrument control box sitting on the left top. Next to the right is the MicroVAX system terminal and keyboard by which the operator calls up the SLICE program which controls the cryomicrotome and the RCI acquisition. Immediatly over the location where the block is stationed between slices, erected on a scaffold, is the MegaVision camera and Zoom lens. Illumination is provided by lamps mounted to the same scaffold, inside the microtome chamber. The black shroud which covers lens, lamps and base of the scaffold to the sides of the microtome block traveller, has been removed. The MegaVision monitor is seen to the right, with an inverted, transilluminated whole monkey brain tissue section presented in place of the usual registration control image.

Figure 1 b: The Tissue Section Imaging Microscope (TSI Microscope) is based on a heavy granite slab that is mounted on a sturdy table. The computer controlled giant stage holds a slide with twelve whole monkey brain slices, alternately stained for fiber (a modified Weil stain) and cells (Nissl). The glass slide is slid against a right angle jig that ensures accurate replacement of the same slide on subsequent occasions. The MicroVAX computer, not shown, controls two Compumotor driven stage indexers, front and left, which accurately control the x and y positioning of the slide. Stage position verification is by quartz light scaling monitors which display these values in microns in two boxes which are not seen, sitting below the TSI Microscope table. The light column comes from a light source and condenser beneath the table, through a hole in the granite slab. The microscope has an objective turret with 2x, 4x, 10x, and 20x PlanAPO Nikon lenses and space for another objective. Focussing is by the two black handles seen at the sides of the top of the microscope support column, L and R. The light beam is split to allow operator to examine the image via traditional eyepieces in front and for controllable

light access to the Circon CCD camera, seen with its cable coming out from the top of its housing. A Panasonic video monitor, to the right, shows the center of the camera view, in this case, part of the temporal horn of the lateral ventricle and part of the hippocampus in a Nissl stained whole monkey brain section. The MegaVision monitor, not seen, is used to setup light values in the acquired image and to display the composite mosaic reconstitution of a large region or the whole of a brain tissue section, depending on size of the specimen and degree of magnification.

Figure 1

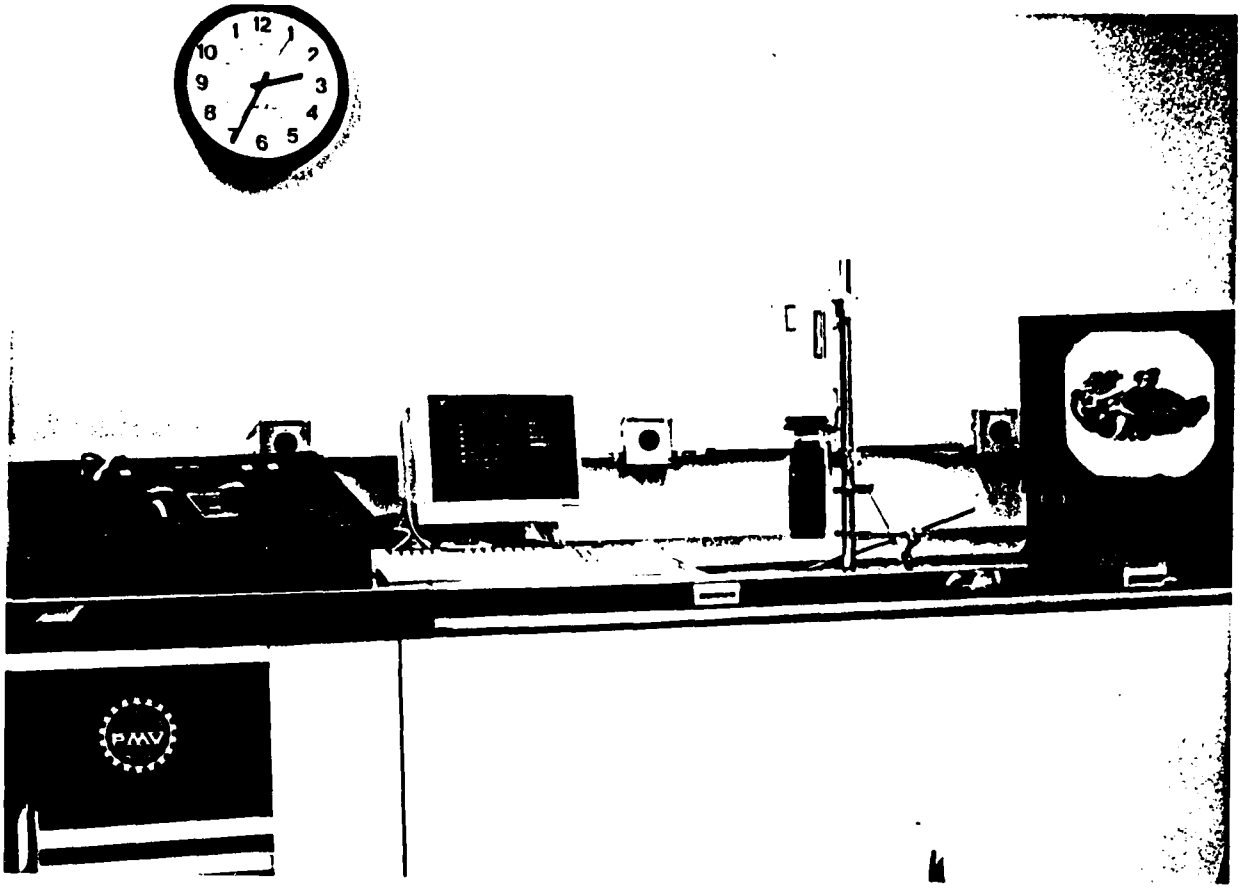

a

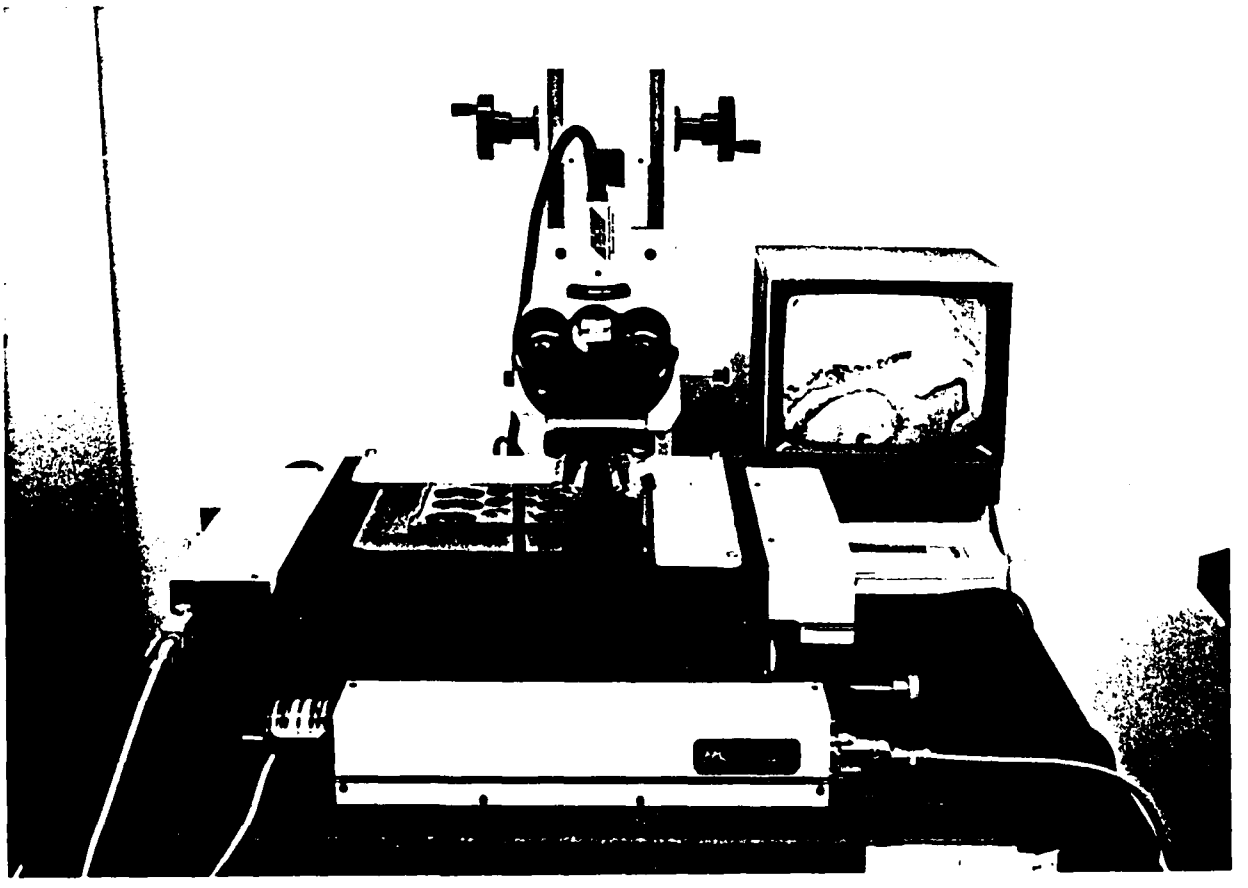

b

Figure 2. Sketch by Michele Frost of scaffold support for lights and camera mounted on the columns that support the LKB giant cryomicrotome knife. The specimen block is mounted on a travelling belt that moves back and forth (arrows) beneath the simplified representation of the knife mount. The scaffold maintains a precise distance and exact angle, normal to the blockface, so that blockface and camera are always in registration. The lamps, L&R, only one of which is illustrated, are Examatron, the macro-zoom lens on the camera is Tamron 70-210mm and the camera is the standard 1Mb MegaVision camera.

Figure 2

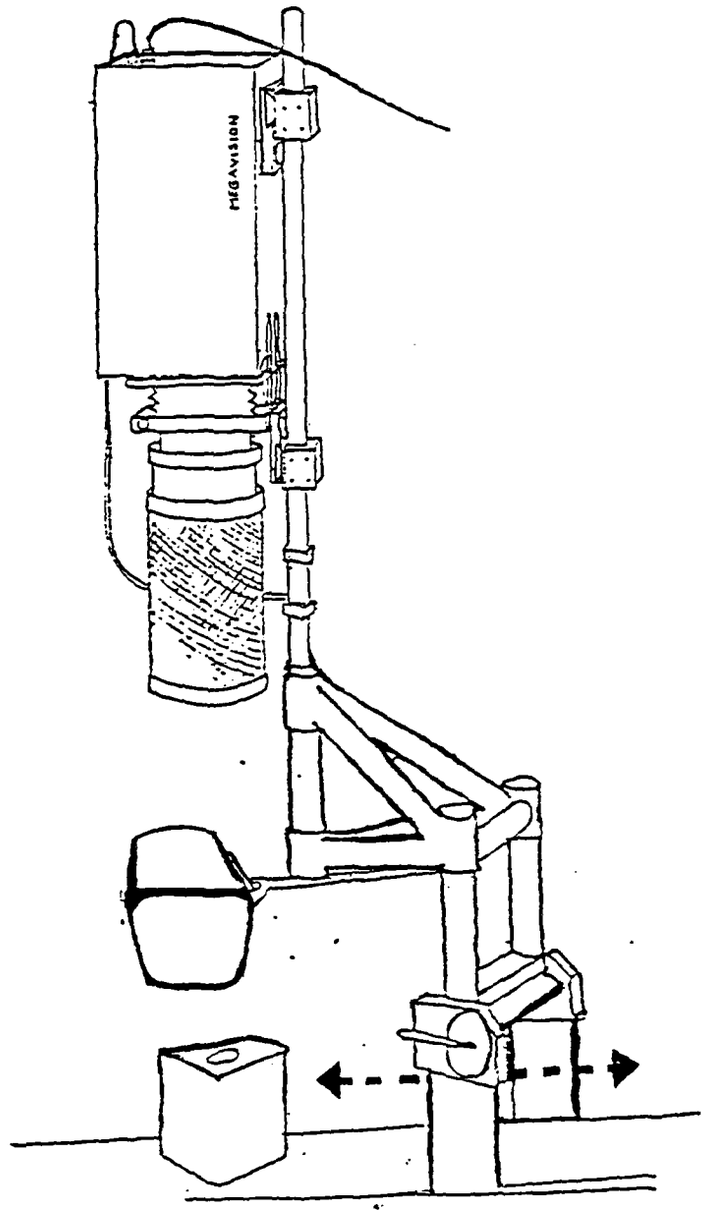

FIGURE 3

TYPICAL SPECTRAL SENSITIVITY CHARACTERISTIC

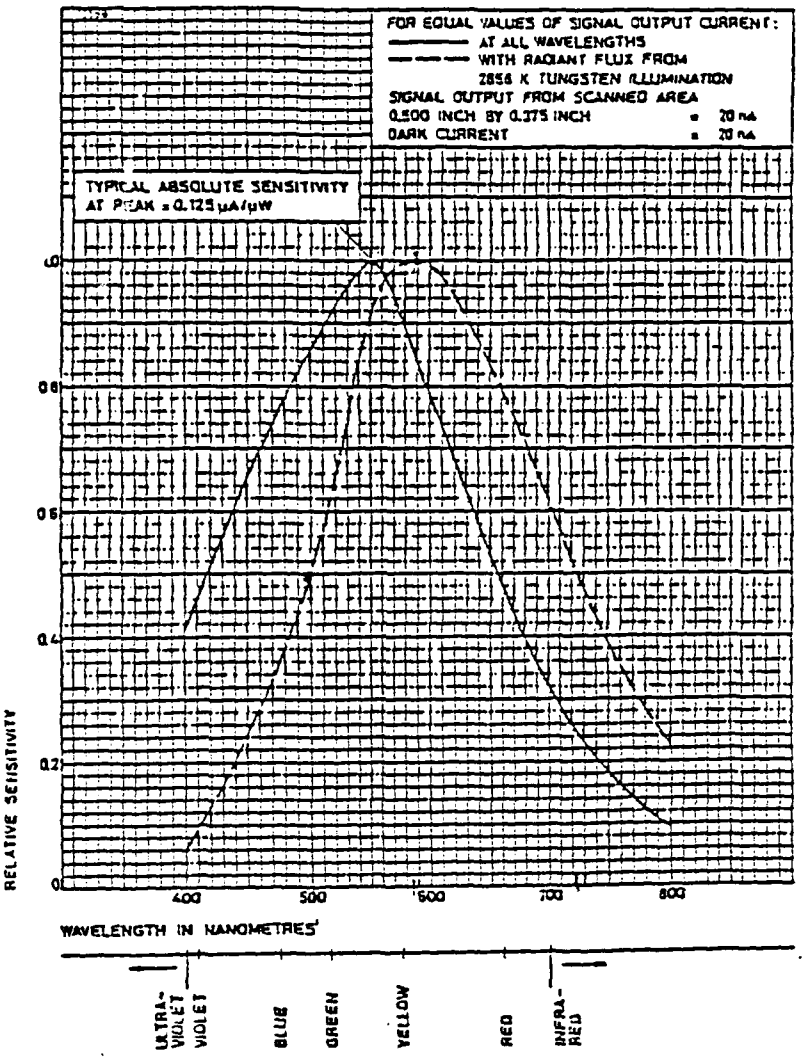

FIGURE 3

(Top) Spectral response curve of the Circon CCD camera. Note the substantial fall-off of sensitivity in those wavelengths associated with picrocarmine dyes (680nm). (Bottom) Characteristic spectral response of MegaVision camera. Note that with tungsten illumination (dashed line) the red component of the carmine stain (the gray matter) generates nearly 80% max output, while the yellow component (white matter) generates almost exactly 100%. This is a much greater degree of differentiation than available from the Circon CCD camera, and partly explains the improved contrast we see with the MegaVision-lithiumcarmine combination.

Figure 4

ABM SLICER V1.1
(c) 1987 UCSD

0 - Exit slicer

1 - Initialize scanner

2 - Change/reset environment

3 - Capture shading mask

4 - Continuous scanning

5 - Capture image

SELECT ?

test dir /monkey/monkey2, images 18 time 12:00pm

The ABM Slicer program is designed for automatic acquisition of blockface images. In the first step, the camera is initialized by adjusting the analog circuits to provide optimum use of the analog-to-digital converter range. The working directory, root filename, current sectioning depth and increment may be changed with Option 2. Option 3 provides a continuous live image. A black surface image is captured for correcting non-uniform lighting using Option 4. In Option 5, images are then captured by accumulating and dividing to reduce noise. Automatic filenaming is used in storing the images.

Figure 5

```
ABM MAPPER V1.1
(c) 1987 UCSD

    0  - Exit mapper

    1  - Start/Stop megavision

    2  - Re-initialize megavision

    3  - Change/reset environment

    4  - Initialize mapper

    5  - Convert to gpx format

    6  - Apply shading mask

    7  - Produce contour

  Select ?

srcdir /monkey/monkey3 (70) dstdir /monkey/monkey4  (3)
image  hrat12400            megavision  on          time 12:00pm
```

The ABM Mapper us designed to produce contours from the captured grey-level images. The MegaVision unit is turned off and on with Option 1. Option 2 resets the Megavision working environment to the original predetermined parameters. Option 3 allows the operator to change the working directory, root filename, depth of image in brain, sectioning increment and directory destination of the contoured image. Copies of the original grey-level images from one directory are placed into a temporary working directory in Option 4. Images in the working directory are converted to GPX format with Option 5. Option 6 corrects the images for non-uniform lighting using the pre-captured shading mask. In Option 7, contours are produced in vector format after user-interactive image editing and anatomical structure selection.

Figure 6 a1. A whole rat brain blockface in the coronal plane of sectioning has been imaged by the MegaVision system. The specimen was embedded in egg albumin with gelatin, blackened with India ink particles and carbon black to reduce spurious reflections from the cut surface of the block. The image includes the outline of the two hemispheres, the third ventricle, above and below, the lateral ventricles surrounding the dorsal hippocampus, the thalamus, internal capsule, putamen and part of the globus pallidus, optic tract, and part of the hypothalamus. These features, when examined in closer detail, exhibit a number of landmarks which can serve as control loci by which the displaced (translated, rotated, compressed, dilated, torn, folded) homologous landmarks on the corresponding tissue section image, the TSI, can be de-deformed to conform to this particular RCI. The normal microscopic view, through eyepieces and the monitor, can be used for focussing.

Figure 6 a2. Computer drawn outline of the exterior of the rat brain RCI shown in a1. This outline is obtained by use of MegaVision capabilities and BMP SLICE software. The raw RCI image is converted to a black and white silhouette around which the computer draws a tracing. Note that it did not follow in the midline into the interhemispheric cleft. BRAINMATE software enables an operator to amend such deficits in the computer drawn outlines. The corrected outlines become the basis for wireframe whole brain reconstructions. Since the RCIs are taken from the same camera position viz-a-viz the blockface, the outlines are in perfect registration.

Figure 6 b1. Similar RCI capture at a more anterior coronal section level.

Figure 5-4

a

a

Figure 6b

b_1

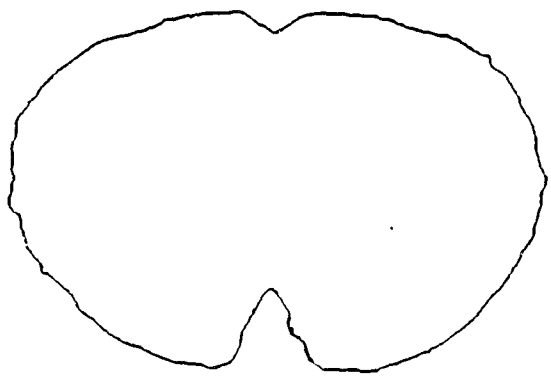

b_-

Figure 7 a. On the left is an image acquired by the MegaVision of a whole human brain horizontal section above the level of the corpus callosum, stained by the Bielschowsky method to show myeloarchitecture. On the right is the result of applying the ROTATING BAR algorithm in a system library and database package devised by Tarek El Rashidy and Glen Harding. About four-fifths of the operator's task is accomplished automatically by the computer. BRAINMATE software is used, after the stage here illustrated, to correct errors in surface following by the automatic system.

Figure 7 b. This illustrates how the operator can retrieve sections previously captured and inspect boundaries that have been traced by computer to examine them at any desired scale, with the corresponding original images presented in the same view. The two images can be simultaneously scrolled for inspection and for the application of correcting procedures, e.g. by using BRAINMATE. The automatic boundary detection in this case is preliminary, before use of CONTOUR FOLLOWER, so the boundaries exhibited are more primitive than in Figure 7 a. Ordinarily, CONTOUR FOLLOWER is applied before final operator corrections are undertaken.

Figure 7

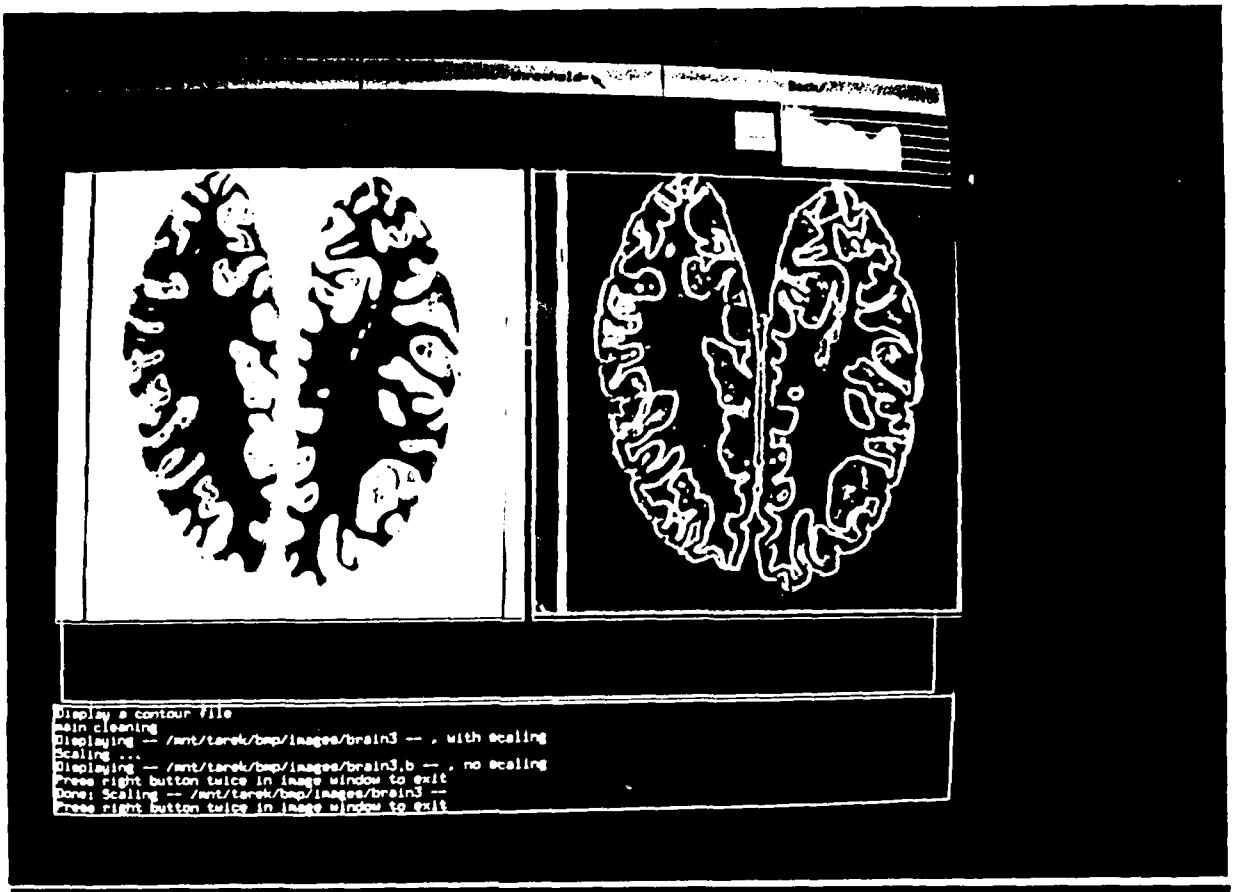
Display a contour file
Displaying -- /mnt/tarek/bmp/images/brain3 -- , with scaling
Scaling ...
Displaying -- /mnt/tarek/bmp/images/brain3.b -- , no scaling
Press right button twice in image window to exit
Done; Scaling -- /mnt/tarek/bmp/images/brain3 --
Press right button twice in image window to exit

a

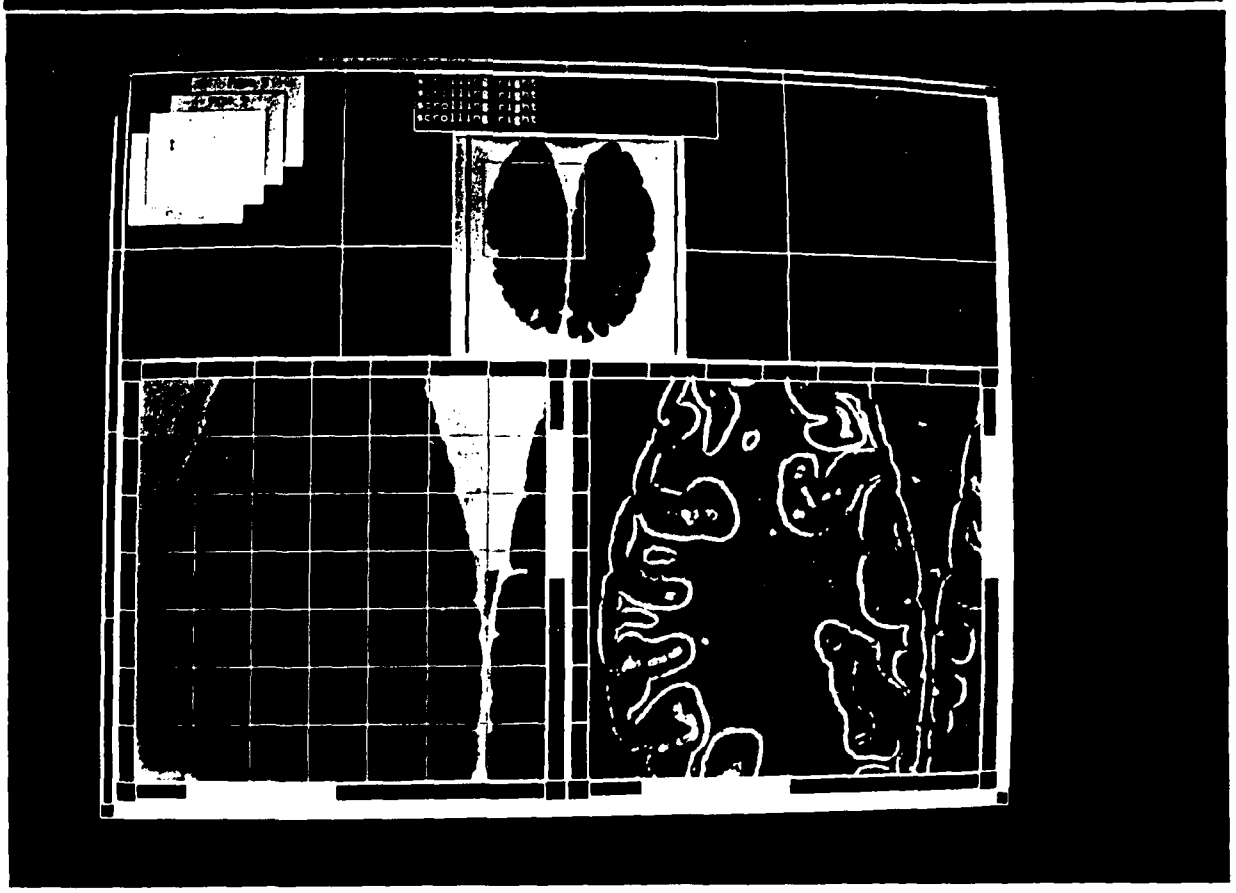
scrolling right
scrolling right
scrolling right

b

Figure 8 a1. Solid surface rendering of whole rat brain sectioned coronally and reconstructed first as a wireframe image which is then subjected to the Reynolds CONTOUR VIEW software to provide a solid surfaced, shaded, reconstruction. This is a direct posterior to anterior view, x = 0, y = 0.

Figure 8 a2. Wireframe view of the same whole rat brain sections in the same perspective, printed with a less than top quality laser printer.

Figure 8a

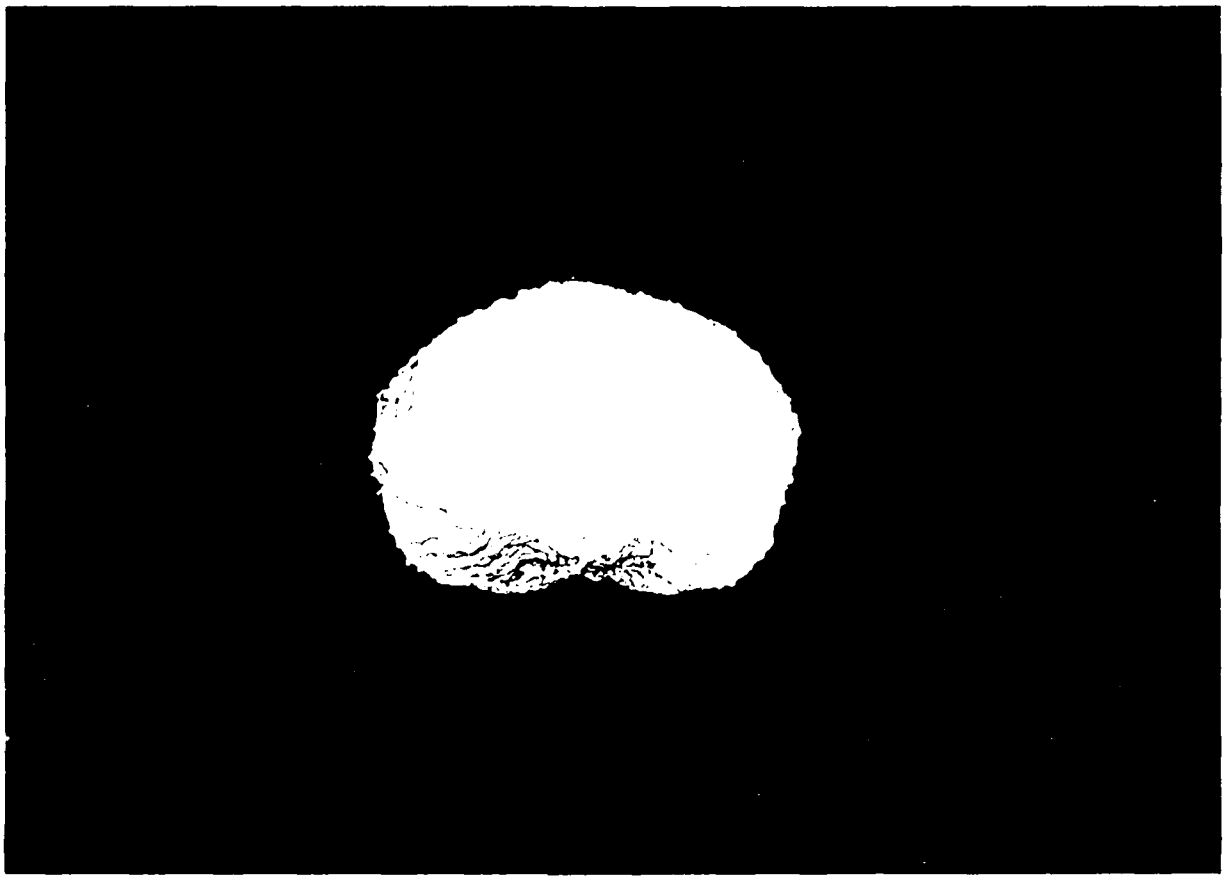

a_1

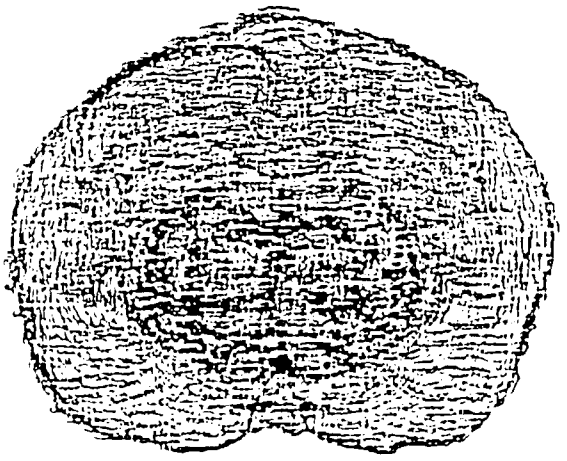

a_2

Figure 8 b1. Coronal whole rat brain reconstruction as in Figure 8a, with rotation of both x and y axes to present any desired angle of view. The mid-medullary brain stem can be seen, the cerebellum, the two hemispheres, and in the remote distance anteriorly, the olfactory bulbs. x = 35, y = 35.

Figure 8 b2. Wireframe view of the same whole rat brain but at a slightly different perspective, x = 20, y = 135. The same structures can be made out, and the perceptual advantage of solid surface modeling is obvious.

Figure 8b

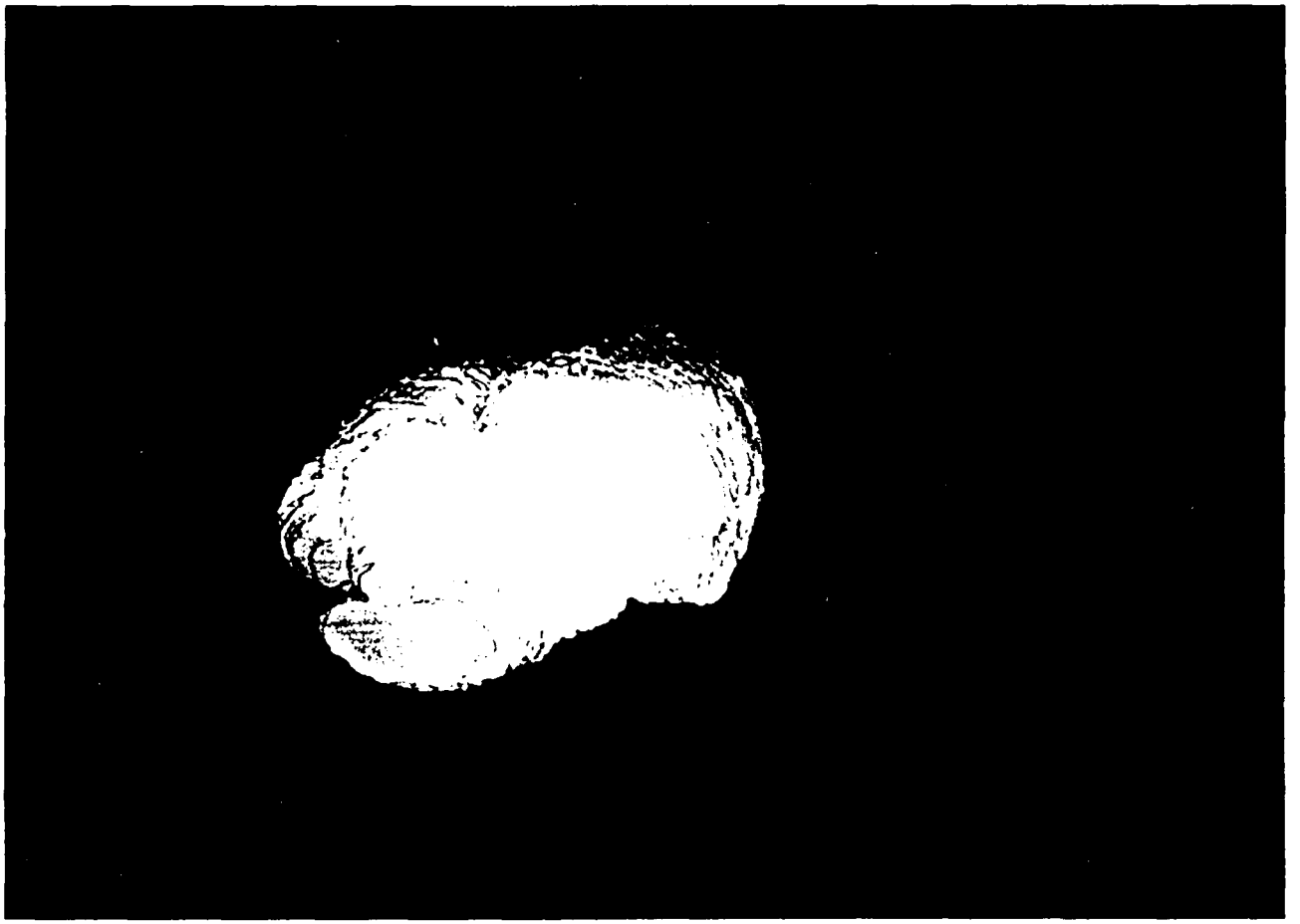

b_1

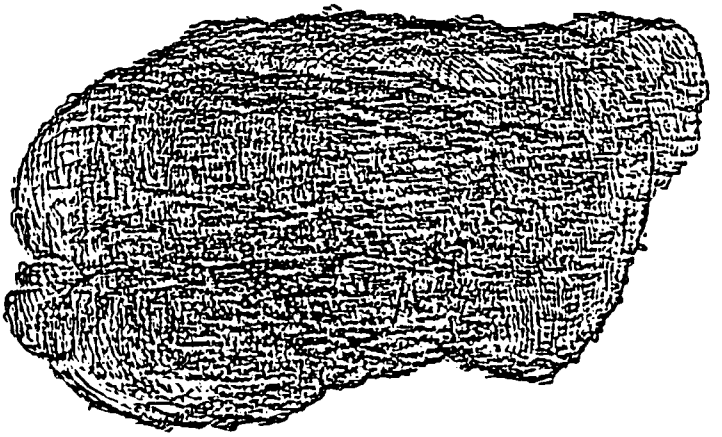

b_2

Figure 8 c1. CONTOUR VIEW representation of the same brain as in 8b, now with x = 40, y = 75. The brain stem, cerebellum, hemispheres and olfactory bulb and tract can be seen to advantage.

Figure 8 c2. Wireframe three dimensional reconstruction of the same brain, but represented in a radically different perspective. The olfactory bulbs are to the left, the brain stem toward the viewer to the lower right. Again, the advantages of CONTOUR VIEW is clear.

Figure 8c

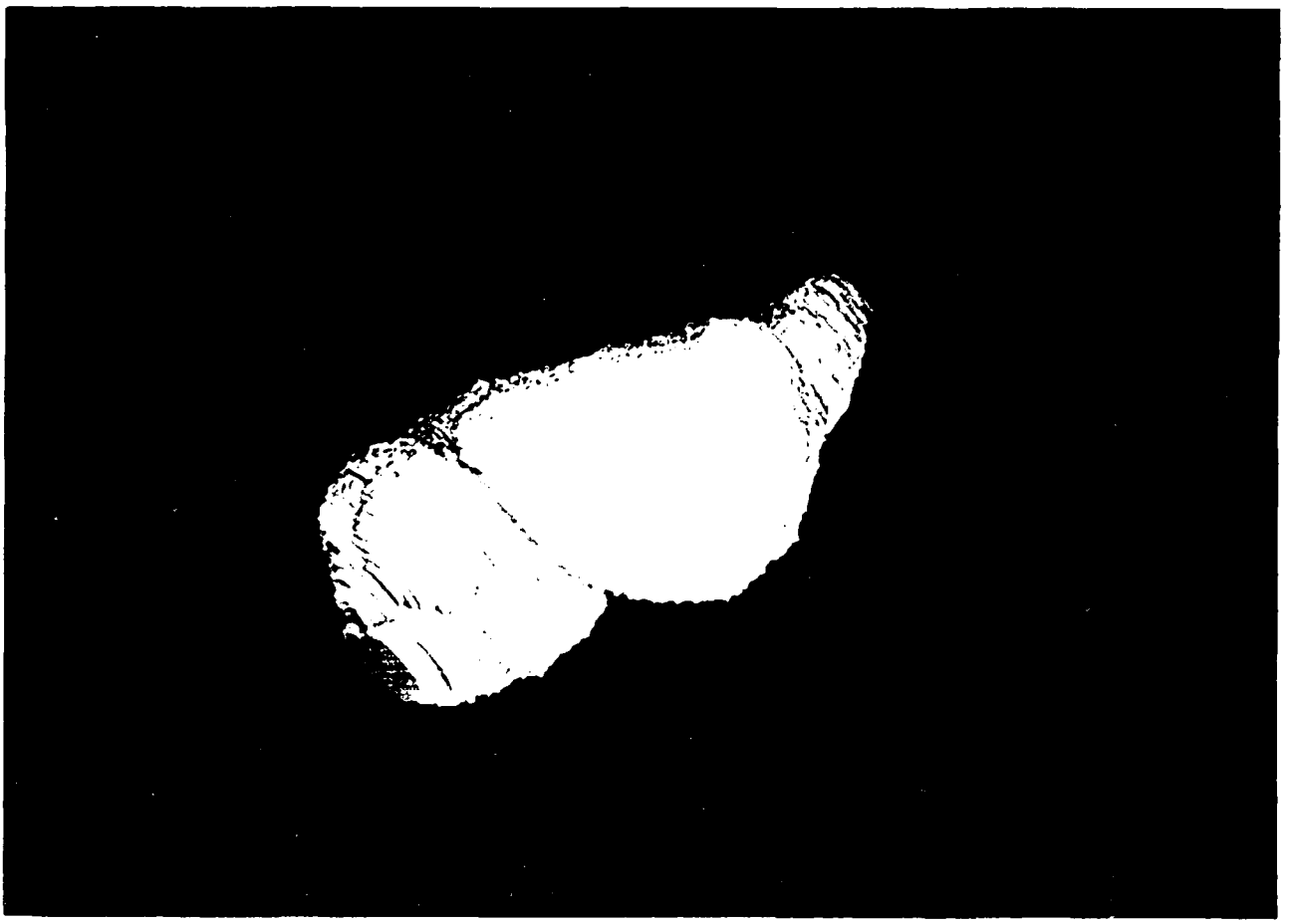

c_1

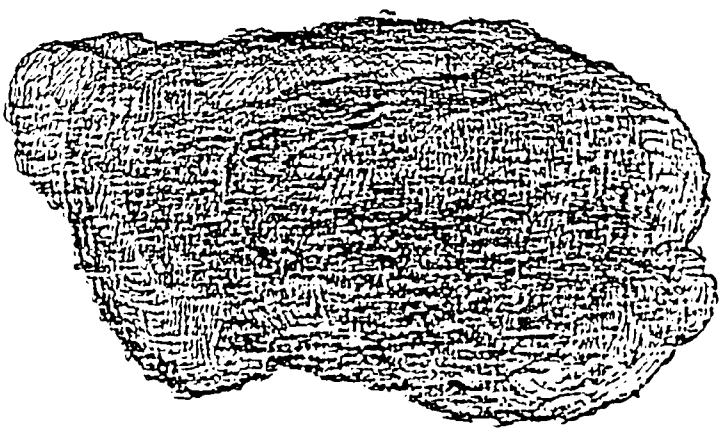

c_2

Figure 9 a. Large-scale reconstruction from whole monkey brain horizontal section, stained for cells. Anterior is toward the top. The cerebral cortex can be plainly seen, including some differentiation e.g., between the more laminar cortex posteriorly and the more granular cortex anteriorly. Moreover, this section illustrates, in the frontal lobe regions of the section, how increasingly tangential planes of cortical transection present increasingly thick appearing cortex, with layers spread out, an illusion because the cortex is simply cut tangentially. Computer reconstruction and tissue texture analysis to differentiate cytoarchitectural regions are presented some difficulty in making comparisons between such differently appearing projections. In principle, it should be possibe for future software to present serial section data at any angle desired, e.g. normal to the cortical surface, for purposes of tralditional cytoarchitectural comparisons. [The computer might do as well three dimensionally without reconstitution in a plane normal to the cortical surface, but, in that case, it should be done for the sake of the operator!] This reconstructed image consists of an array of 11 x 13 individual MegaVision images captured at 2x magnification the CCD camera mounted in the TSI Microscope. The images are acquired at full 525 x 525 pixel value but the composite reconstruction is compressed so that the overall image falls within the 1Mb projection capability of the MegaVision system.

Figure 9b. A lower level whole brain section from the same brain as in Figure 9a. This horizontal section cuts through the corpus callosum, septum, fornix, thalamus, and cerebellum near the midline, and the caudate, putamen, internal capsule, and hippocampus more laterally. This large-scale reconstruction consists of 14 x 17 mosaic elements, reconstituted and presented in drastically compressed format.

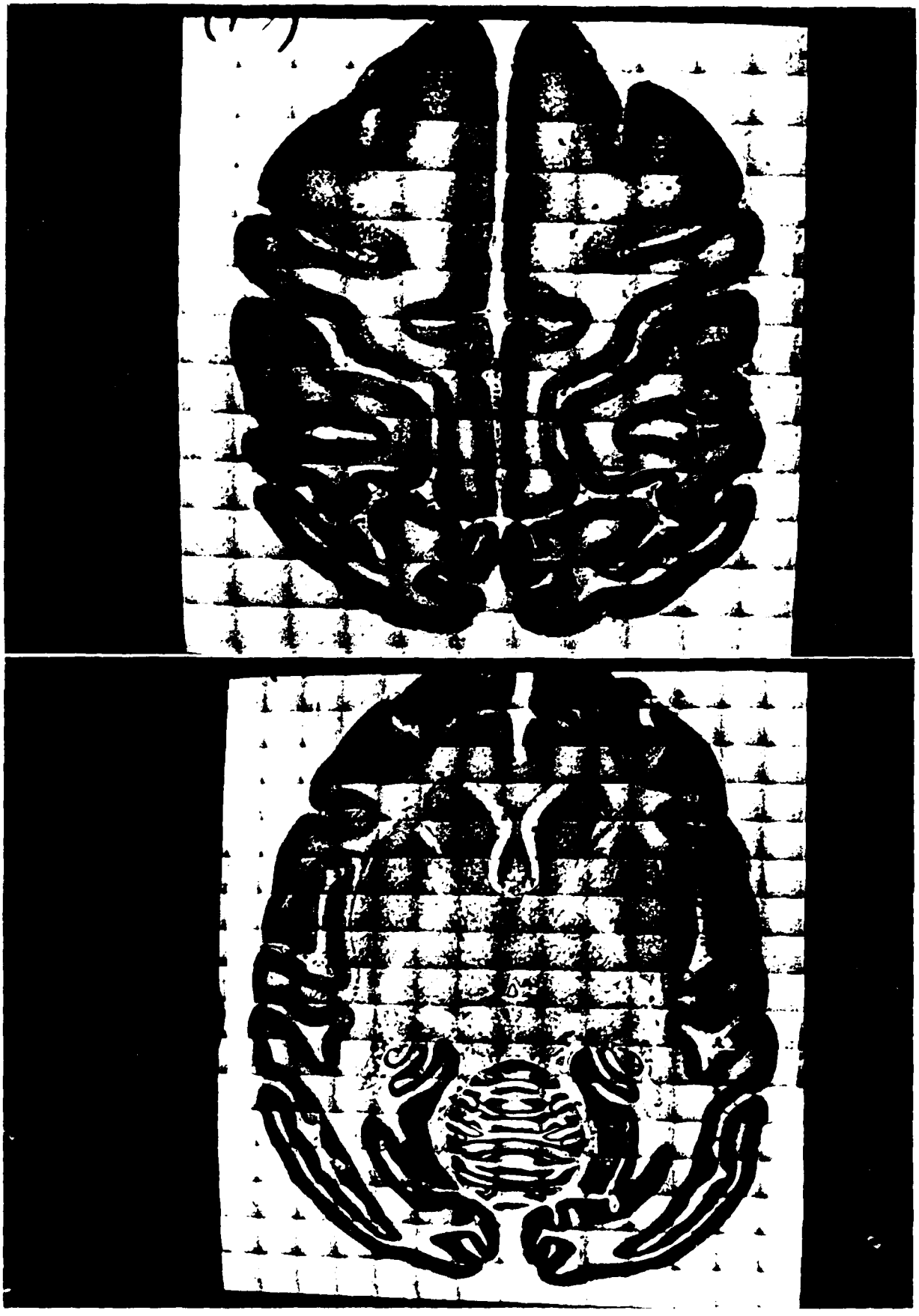

a

b

Figure 10a. Ten times magnification of a small portion of a whole monkey brain section, stained for fibers. This array consists of 16 x 16 mosaic parts reconstituted into a single, compressed-data image, which is presented in the MegaVision monitor. The section shows beneath a region of the hippocampus the medial part of the temporal pole. Magnification 4x. Coronal section, level 2260.

Figure 10b. Similar magnification of a monkey whole brain section, stained for cells. The 16 x 16 array shows part of hippocampus and temporal lobe further anterior than in Figure 10a. with delineation of cell layers in hippocampus, temporal lobe cortex and part of the amygdala. White matter is obviously pale and has only sparse cell definitions. Magnification 4x. Horizontal section, level 751.

Figure 10c. TSI Microscope mosaic reconstruction from a coronal section stained for fibers, showing the striations caused by fibers streaming across the internal capsule. Coronal section 2260 at 10x magnification. Note that the "postage stamp effect" due to non-uniform illumination of the field in each TSI captured is markedly reduced as magnification increases; the microscope is looking increasingly at the "sweet center" of the optical column.

Figure 10

a

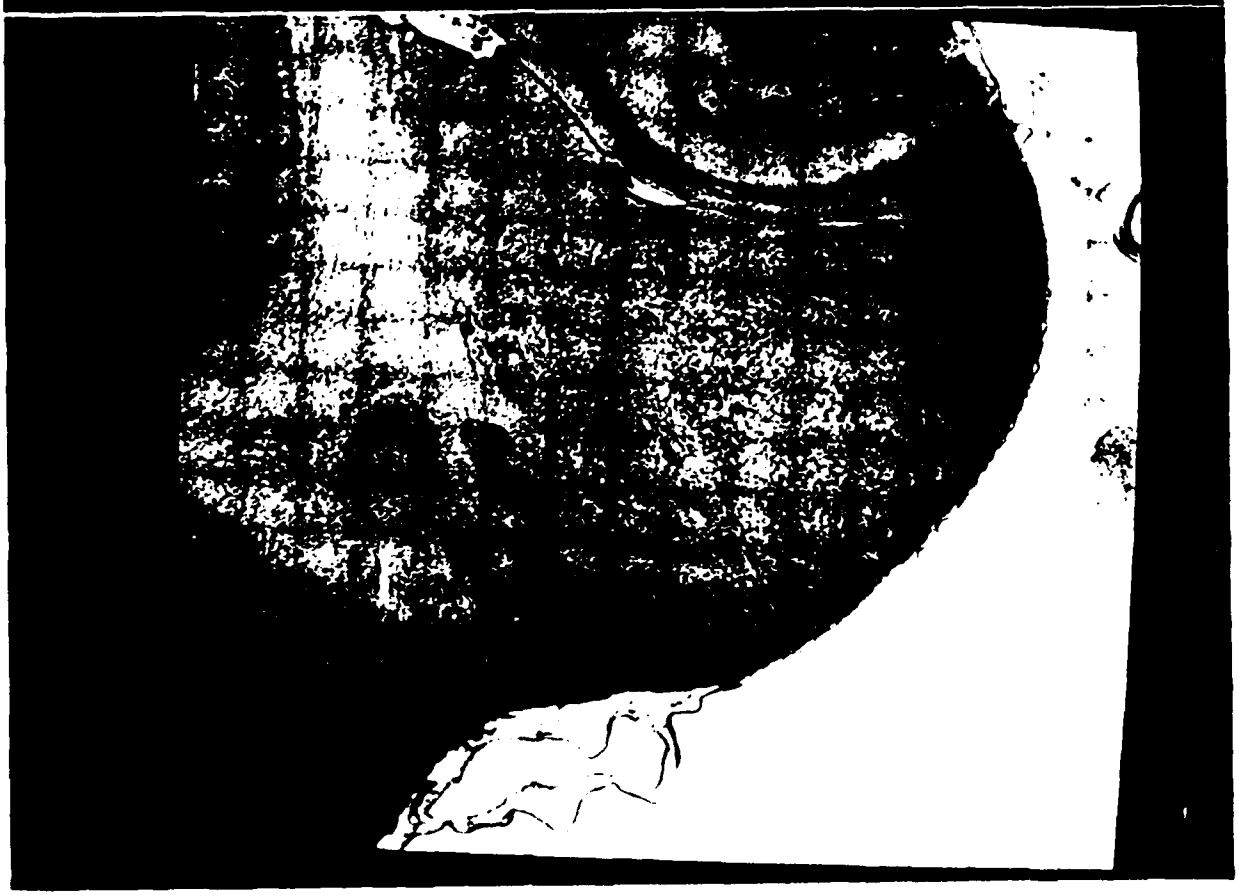

b

Figure 10c

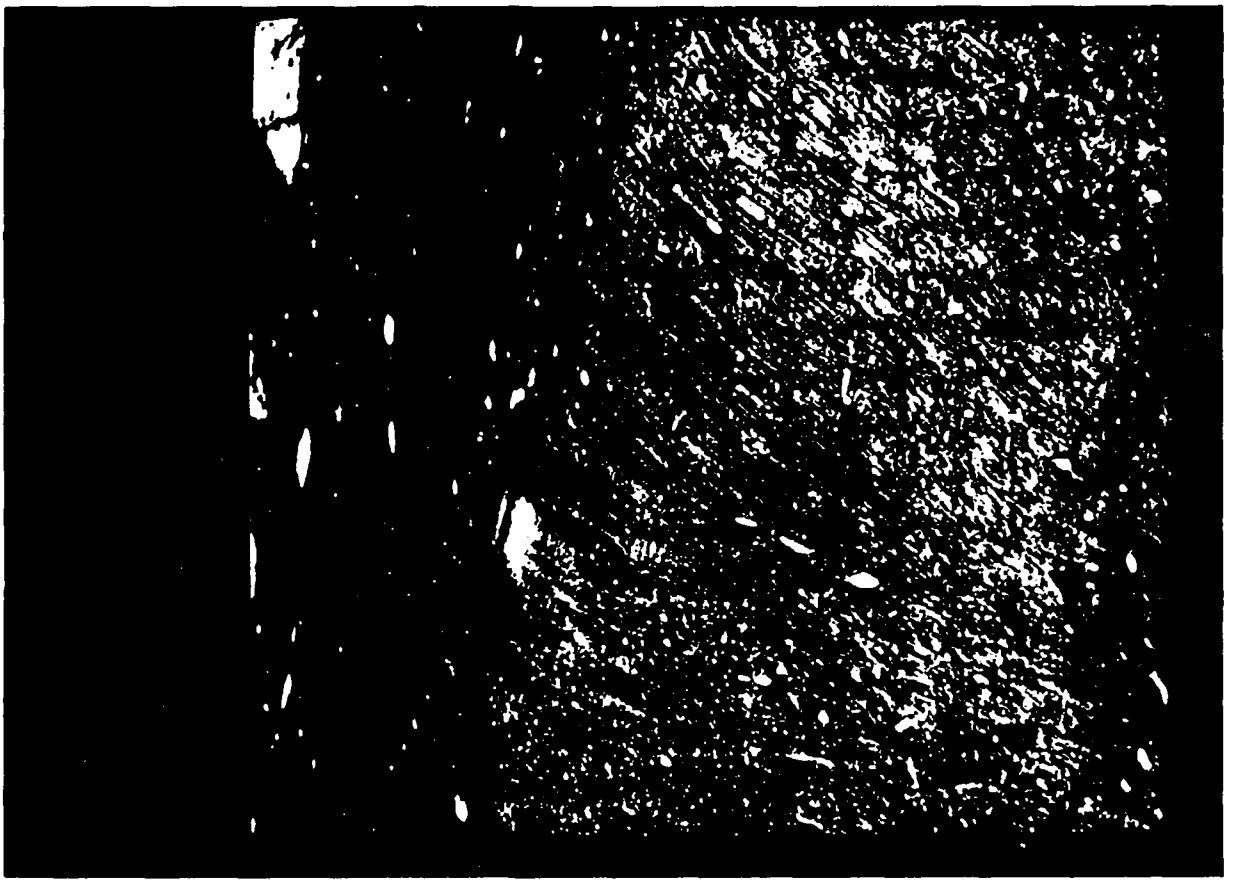

FIGURE 11

Specimen Preparation

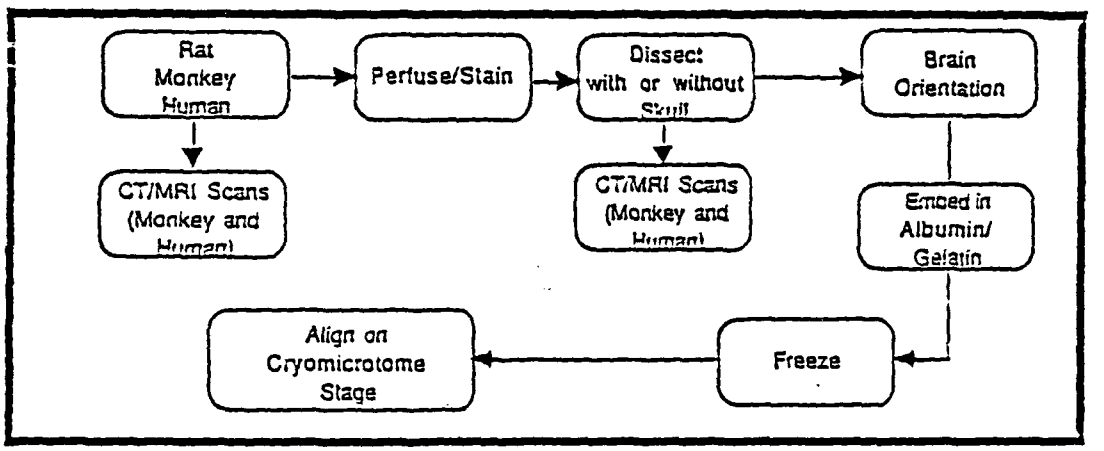

Figure 12

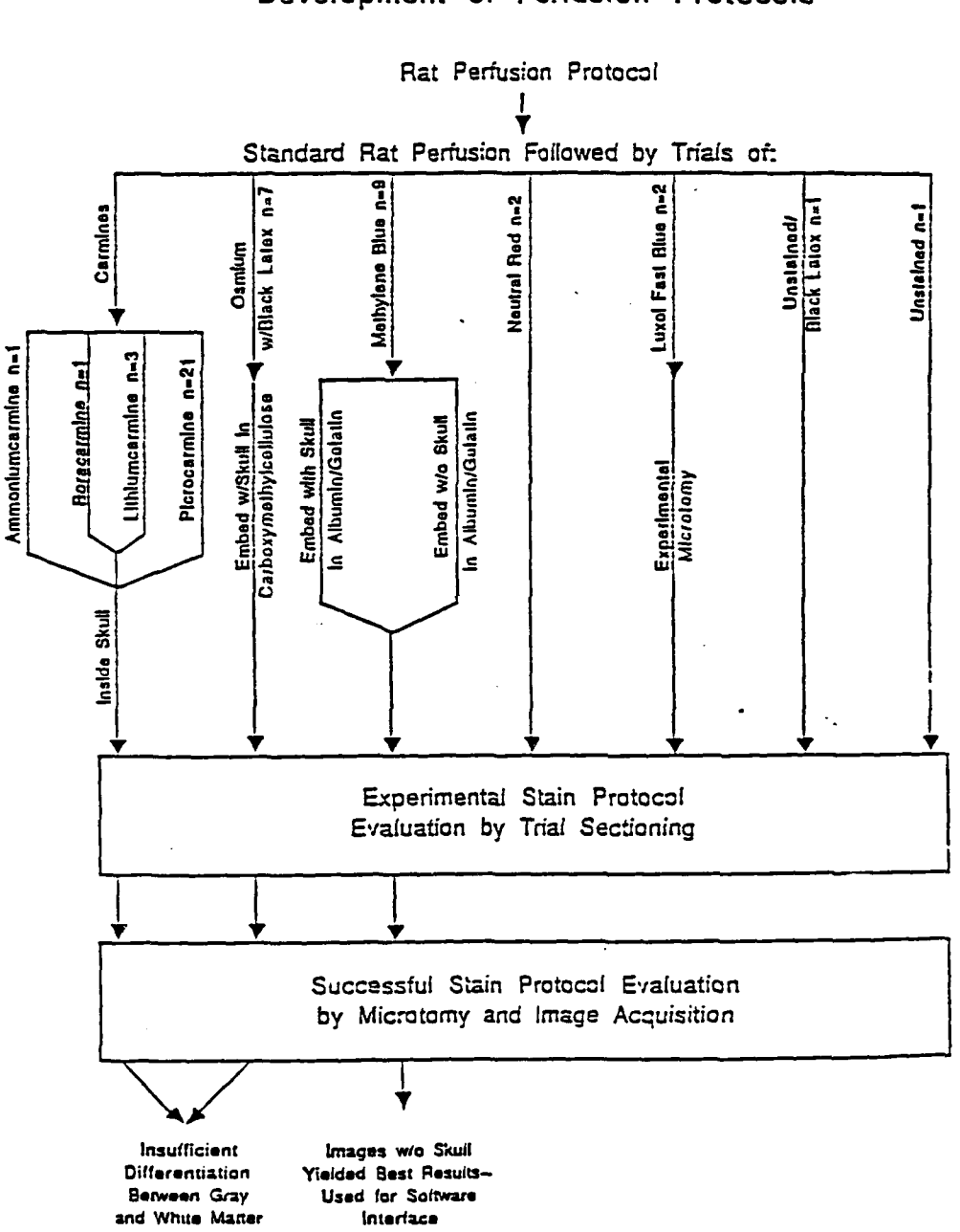
Development of Perfusion Protocols
Rat Perfusion Protocol
Standard Rat Perfusion Followed by Trials of:
Carmines
Ammoniumcarmine n=1
Borocarmine n=1
Lithiumcarmine n=3
Picrocarmine n=21
Inside Skull
Osmium w/Black Latex n=7
Embed w/Skull in Carboxymethylcellulose
Methylene Blue n=9
Embed with Skull In Albumin/Gelatin
Embed w/o Skull In Albumin/Gelatin
Neutral Red n=2
Luxol Fast Blue n=2
Experimental Microtomy
Unstained/ Black Latex n=1
Unstained n=1
Experimental Stain Protocol Evaluation by Trial Sectioning
Successful Stain Protocol Evaluation by Microtomy and Image Acquisition
Insufficient Differentiation Between Gray and White Matter
Images w/o Skull Yielded Best Results– Used for Software Interface

Figure 13. Digital images were captured by the MegaVision 1024 x 1024 camera of part of a series of whole human head MRI scans, used as controls for BMP brain registration from cadaver specimen, roughly coronal sections. The Megavision monitor displays nine images simultaneously in vastly compressed image format for operator scanning purposes. A good deal of detail can be seen even in these reduced images.

Figure 13

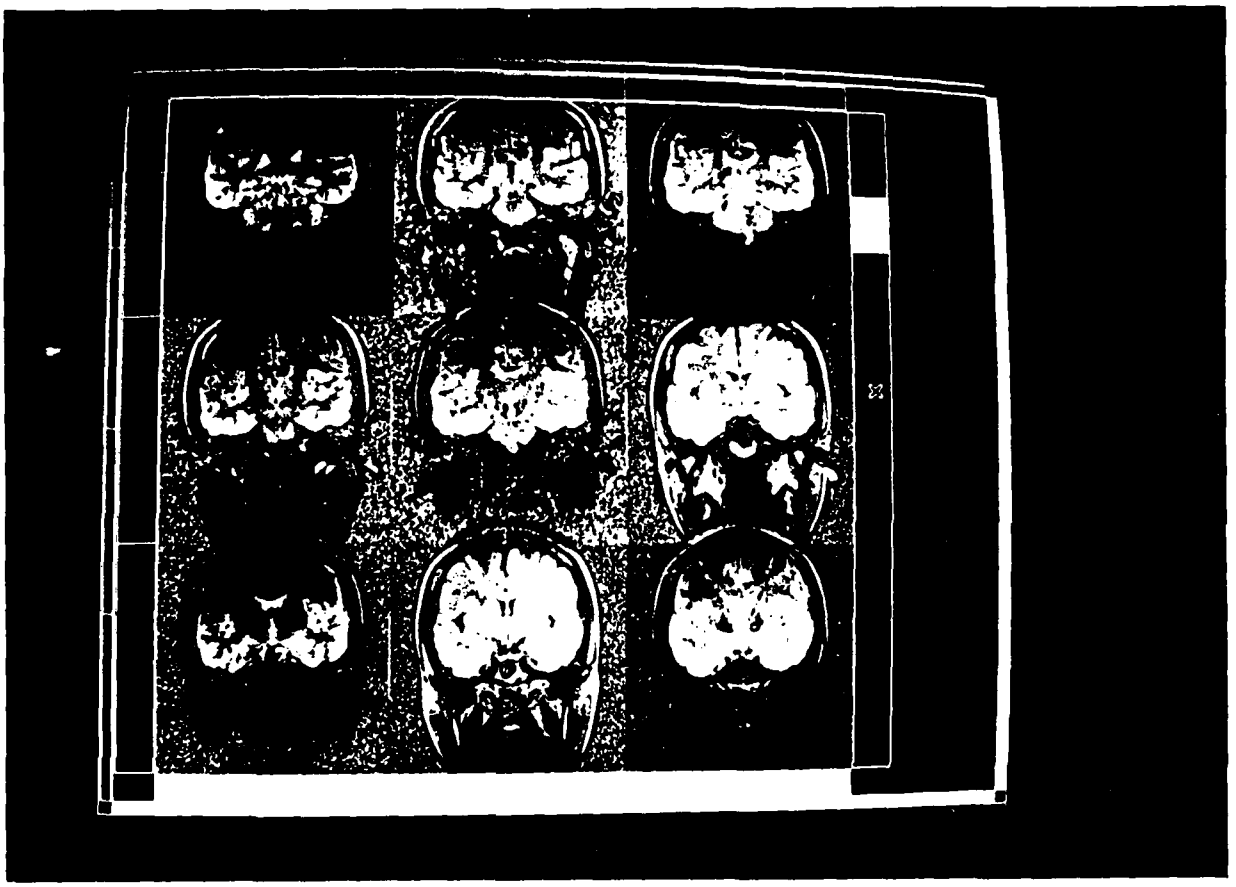

Figure 14 a. Whole monkey brain sagittal section, fiber stained, acquired by the MegaVision camera with transillumination from a lightbox. The objective of this imaging program is to obtain silhouettes of each of three entire whole brain series, cut at right angles along the classic orthogonal planes, stained for fibers and cells in alternate sections, for purposes of approximation of wireframe reconstructions. Since the monkey brains were matched for size and cut in planes at right angles to each other, each outline serves as an accurate dimensional control for outlines in the other planes of section.

Figure 14

a

b

Figure 15 a. TSI Microscope reconstruction of composite image using 15 x 10 individually acquired images. Parts of Frontal, Temporal, Parietal and Occipital lobes can be seen in this section. The putamen is prominent, as is the hippocampus lying in the floor of the temporal horn of the lateral ventricle. Part of the hemisphere of the cerebellum is also seen. The MegaVision monitor projection has some distortion and the photograph of the monitor contributes further distortion to the image which distortion, along with the enormous data reduction, reduces the quality of the reproduction. The individual original mosaic images, however, are much less distorted and their composite reconstruction is quite accurate for purposes of quantitative morphology. The problem comes with our limited means for reproduction.

Figure 15 b. TSI Microscope image of whole monkey brain coronal section image, occipital region. This shows part of the midline and lateral cerebellum on both sides below the hemispheres. The lines of Genari can be easily seen in the occipital cortex, even in this greatly compressed reconstitution.

Figure 15

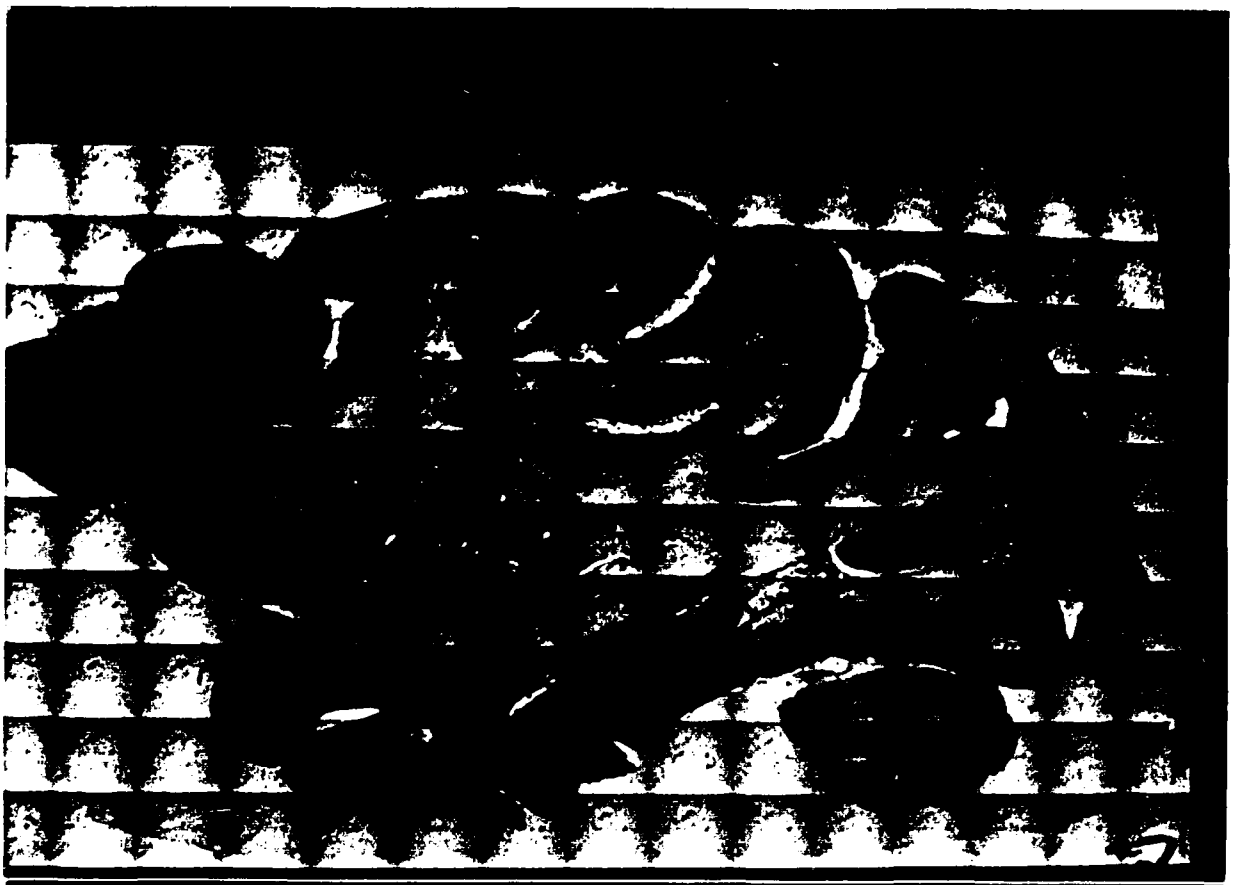

a

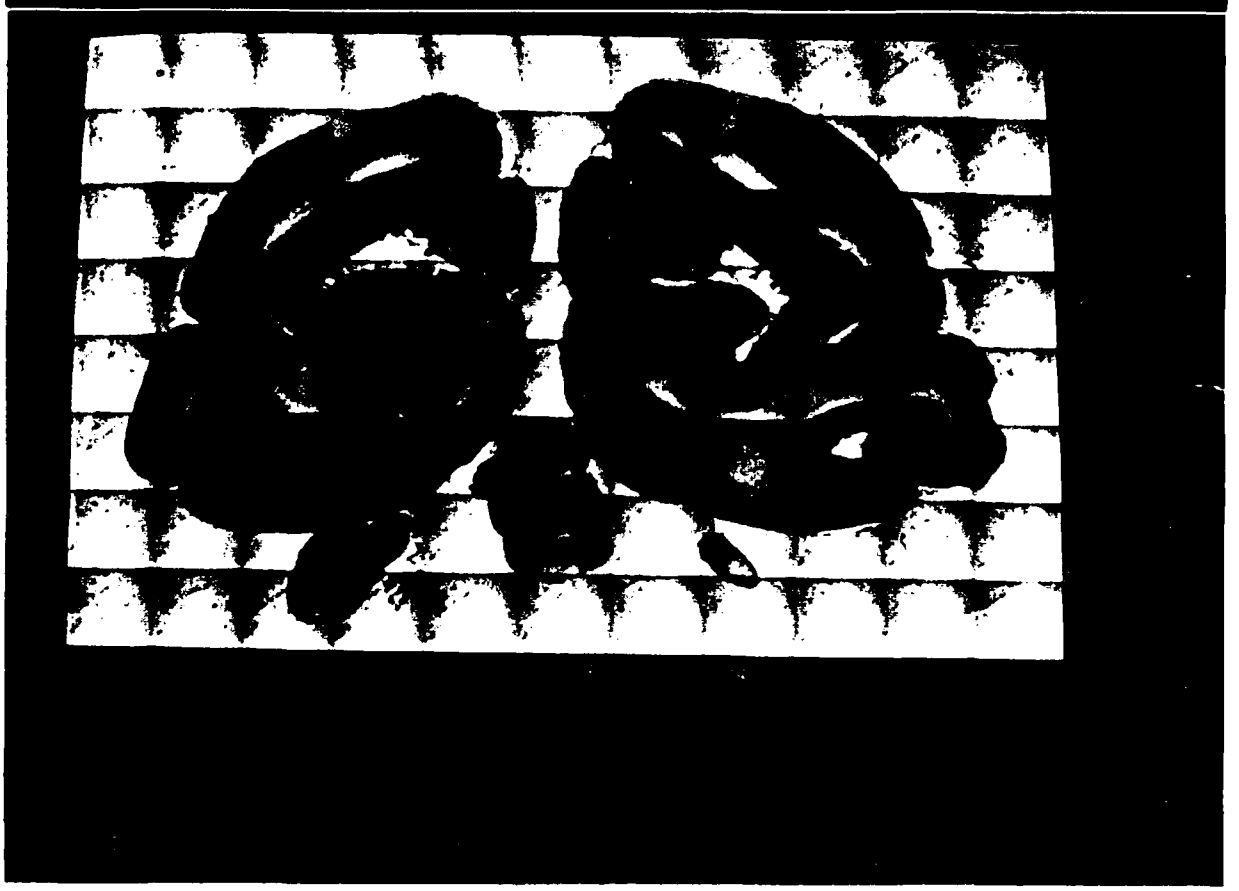

b

AD-A197 853 THREE-DIMENSIONAL COMPUTER GRAPHICS BRAIN-MAPPING PROJECT(U) CALIFORNIA UNIV SAN DIEGO LA JOLLA R B LIVINGSTON 24 MAR 88 DAMD17-86-C-6093 2/2

UNCLASSIFIED F/G 6/4 NL

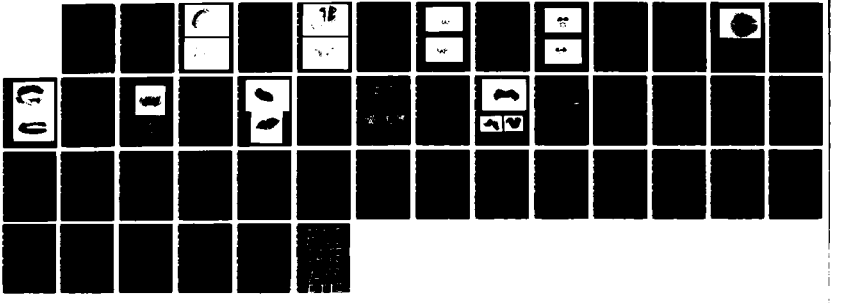

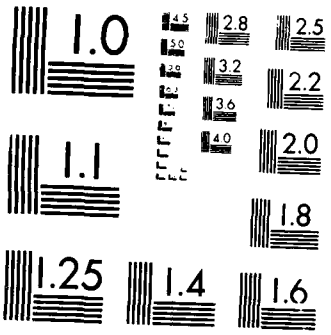

MICROCOPY RESOLUTION TEST CHART
NATIONAL BUREAU OF STANDARDS-1963-A

Figure 16 a. This and Figure 17 illustrate some of the BMP contributions made by Arthur Toga Consultant principally responsible for the reconstruction of whole monkey brains using computer graphics techniques. This image shows the stacking of outlines of successive serial coronal sections, with some of the anterior sections removed to allow a better sense of perspective. This method of stacking contours was used by Toga to provide a framework for the synthesis of the whole brain surface.

Figure 16 b. This illustrates the triangulation algorithm applied to stacked outline sections, in a different projection from 16 a. The triangulation is used to establish the basis for surface rendering. The surface rendering vastly improves the verisimilitude of whole brain reconstructions.

Figure 16

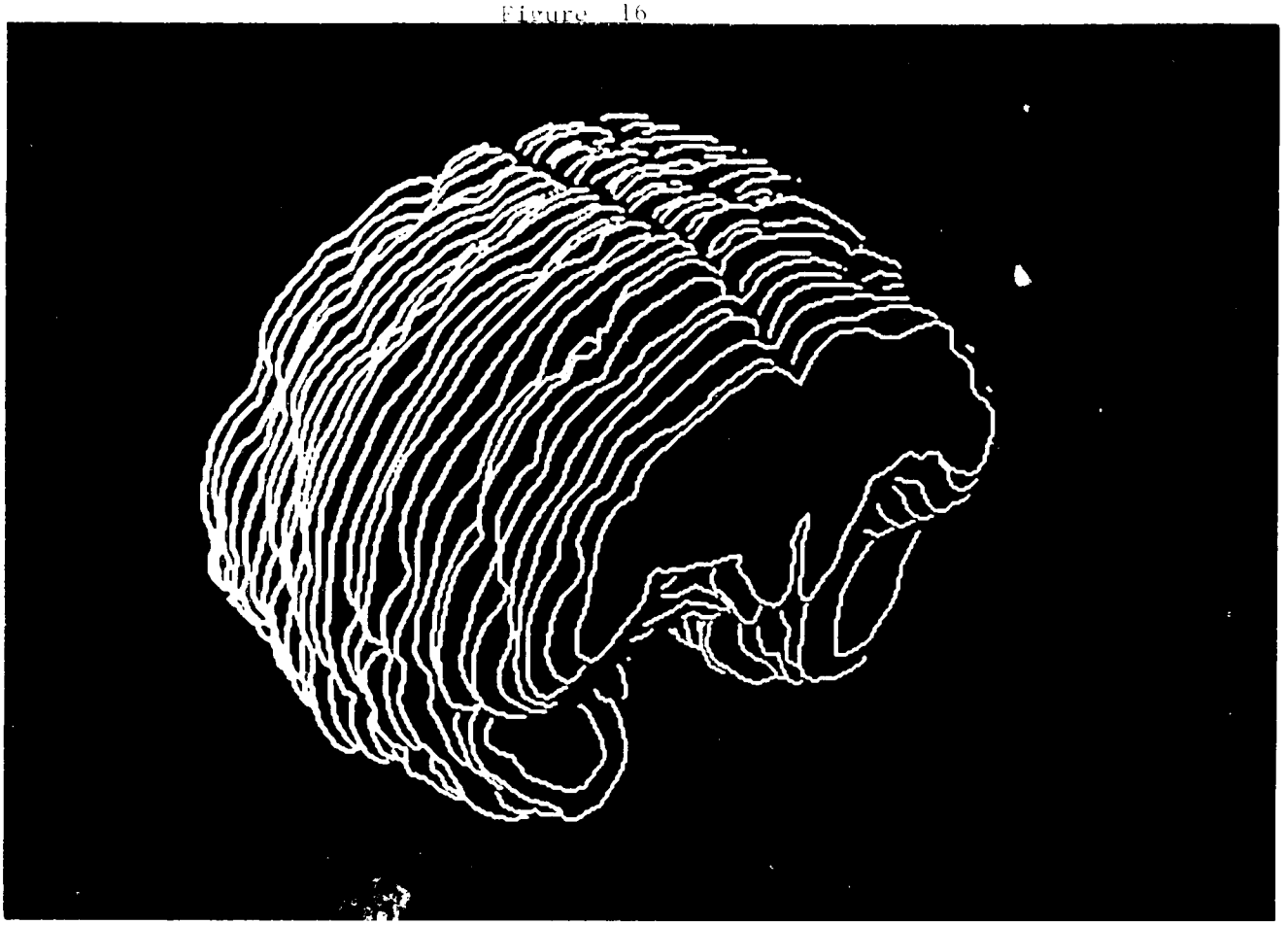

a

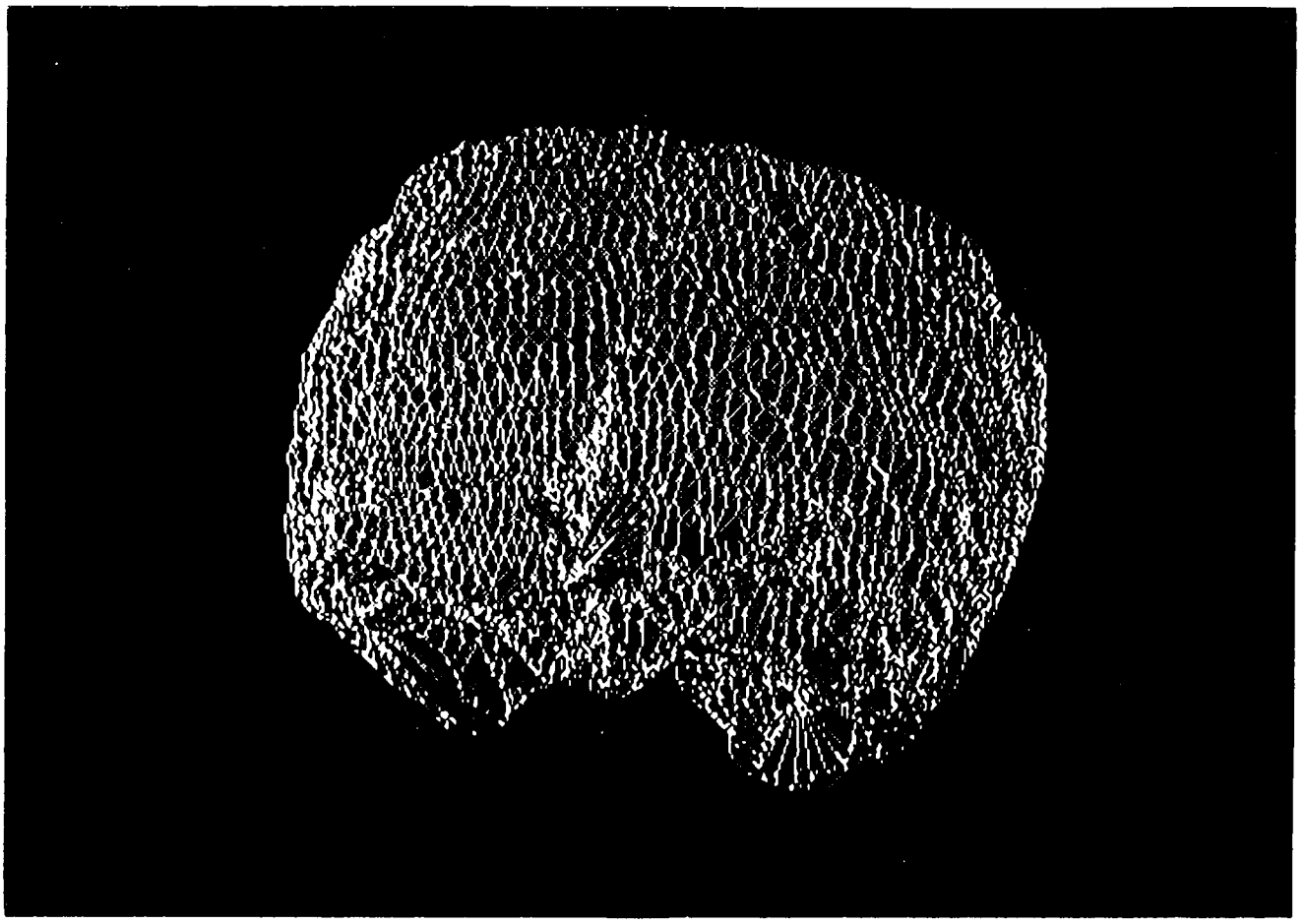

b

Figure 17 a. This illustrates a completely surfaced, shaded representation of the three dimensional reconstruction of the whole monkey brain. The shading algorithm used includes factors for specular surfacing. Note highlights of the surface, which improve the realistic appearance of the reconstruction. This Figure also shows a round object that is represented on the superior surface of the left hemisphere. This object represent a functional measure of cerebral metabolism.

Figure 17 b. The three dimensionally reconstructed whole monkey brain has been rotated and two arbitrary faces have been reprojected onto the three dimensional reconstructed block. The left hemisphere has a whole section view on which the frontal operculum, Sylvian fissue and part of the temporal lobe appear. This projection allows examination of structures underlying the frontal motor speech area, Broca's area. The coronal plane of section, because it is from the original plane of section, is somewhat more exact. It represents typical frontal white matter and cortex. This is approximately the plane of section for white matter sectioning in the now-discontinued practice of psychosurgery, frontal lobotomy. The middle of the posterior orbital surface of the frontal lobe is the only cortical area of representation of the vagus nerve.

Figure 17

a

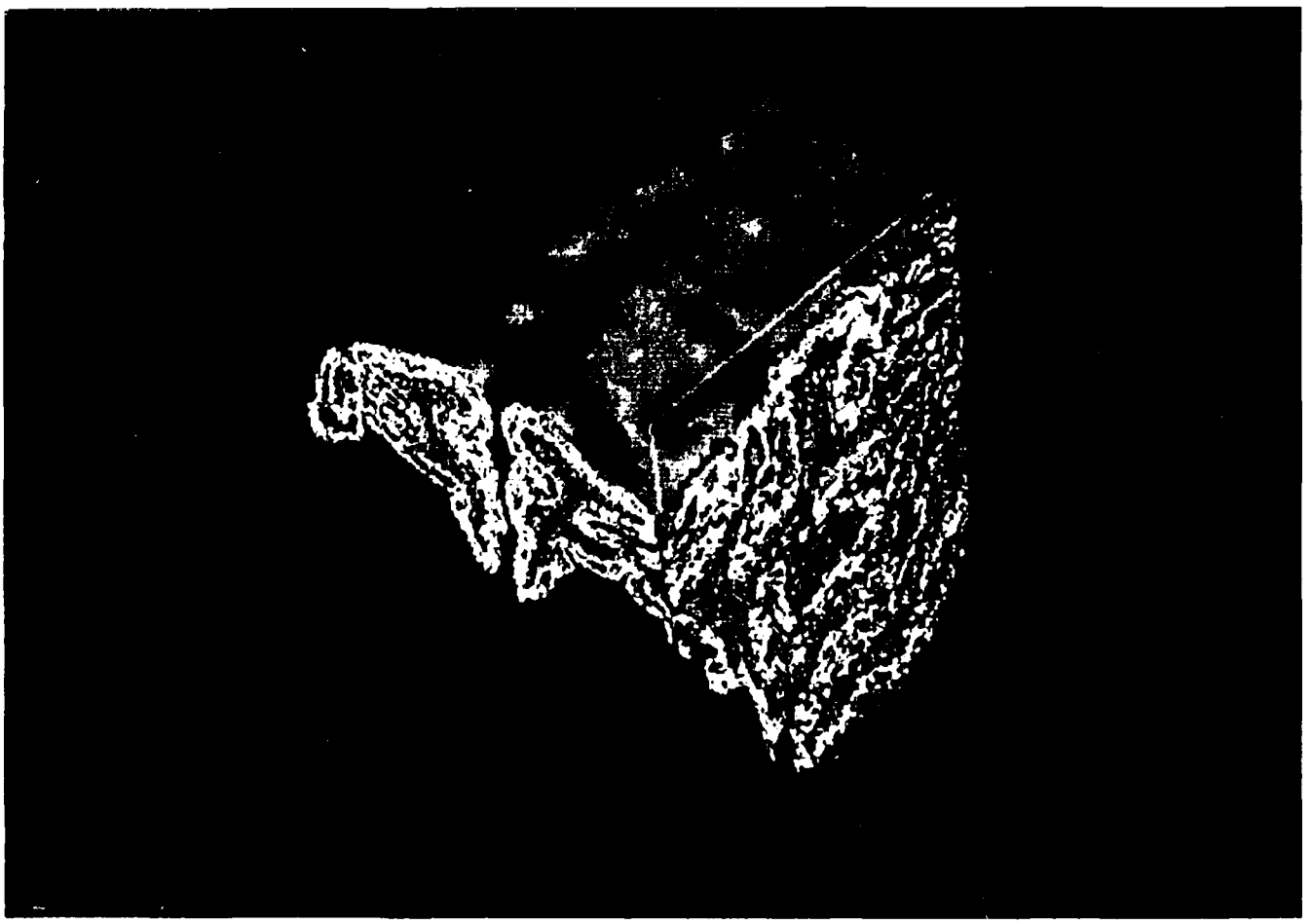

b

Figure 18 a. The images in Figures 18 and 19 come from the laboratory of Dean Hillman, Consultant principally responsible for the reconstruction of the whole rat brain. This Figure illustrates a wireframe three dimensional reconstruction of the hemispheres and brain stem of the rat (frontal projection viewed from slightly above the horizontal axis of the hemispheres). About 24 sections of the whole brain are represented in blue outline. In the same three-space, orange spheres are projected as a means of identifying all of the cells marked by monoclonal antibodies for cholineacetyltransferase.

Figure 18 b. All cells in the rat whole brain three dimensional projection of the hemispheres and brain stem which reacted to monoclonal antibodies to chonineacetyltansferase, are demonstrated by orange spheres. The projection is an anterior ventral view.

Figure 18

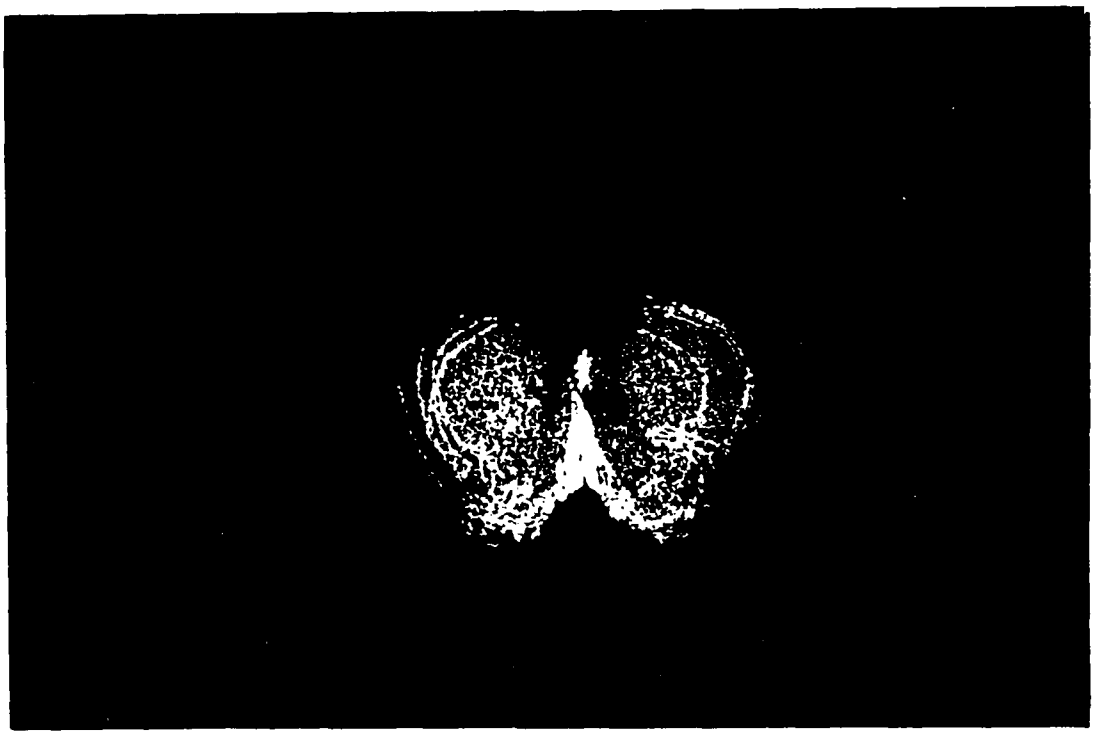

a

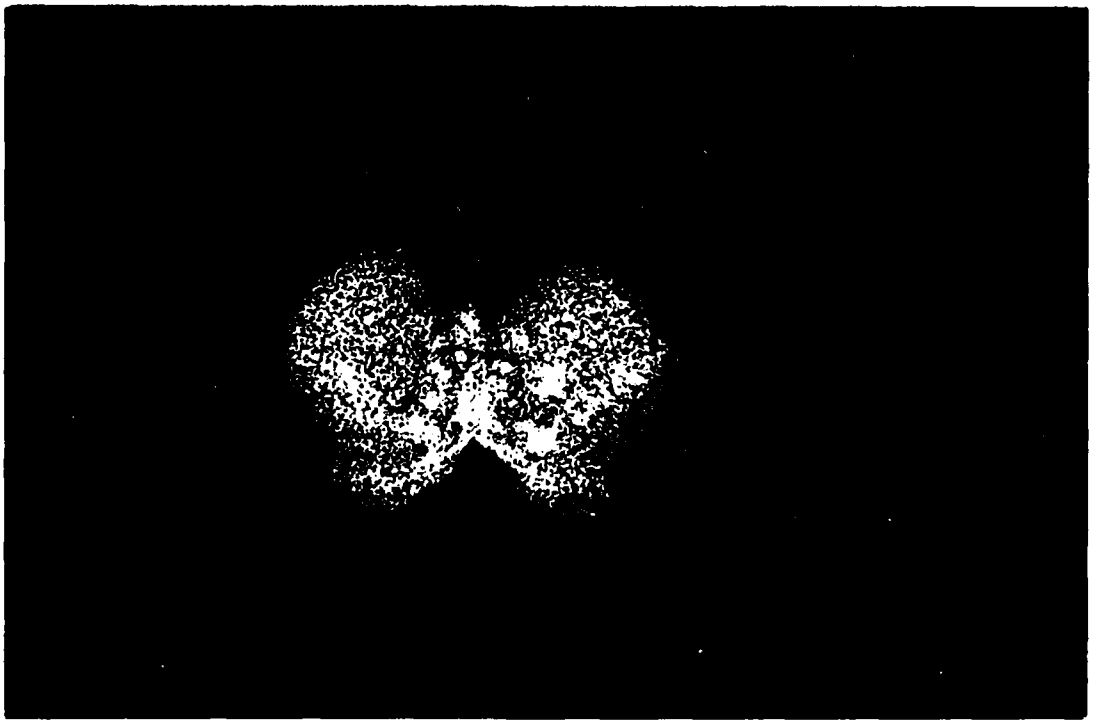

b

Figure 19 a. Wireframe three dimensional reconstruction of rat forebrain, hemispheres and brain stem in a dorsal, somewhat posterior view. The hemisphere and brain stem surfaces are represented by blue contours. Within the same three-space, orange spheres (whitened by superposition with blue lines) represent all cells marked by monoclonal antibodies to cholinacetyltransferase.

Figure 19 b. Three dimensional reconstruction of accurate three-space location of all cells in the rat forebrain which reacted to monoclonal antibodies for cholineacetyltransferase. The view is anterior, tilted slightly "nose up" compared to the posterior "nose down" view seen in Figure 19 a.

Figure 19

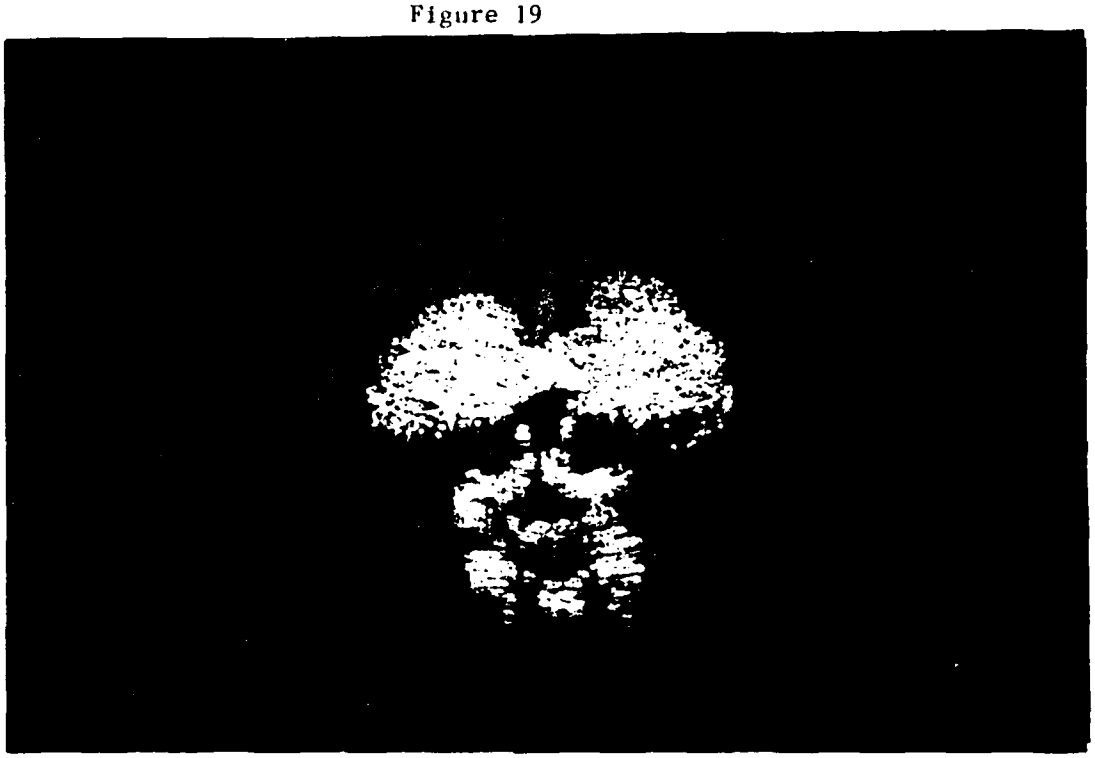

a

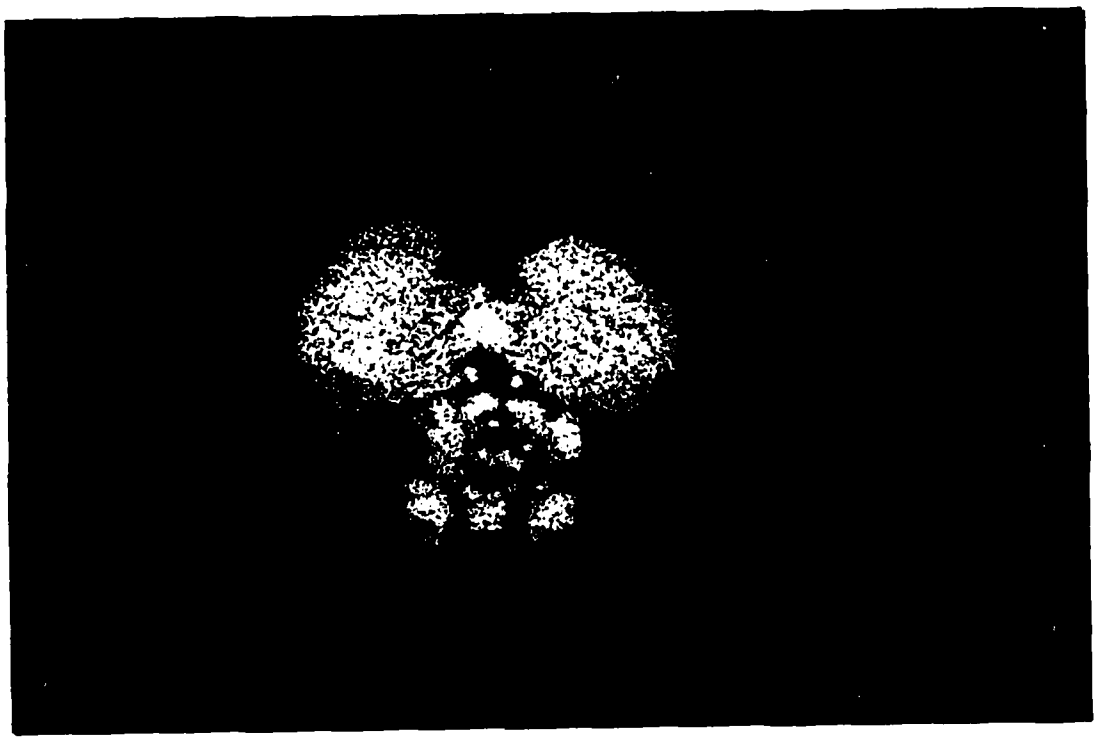

b

Figure 20

Primate Perfusion Protocol

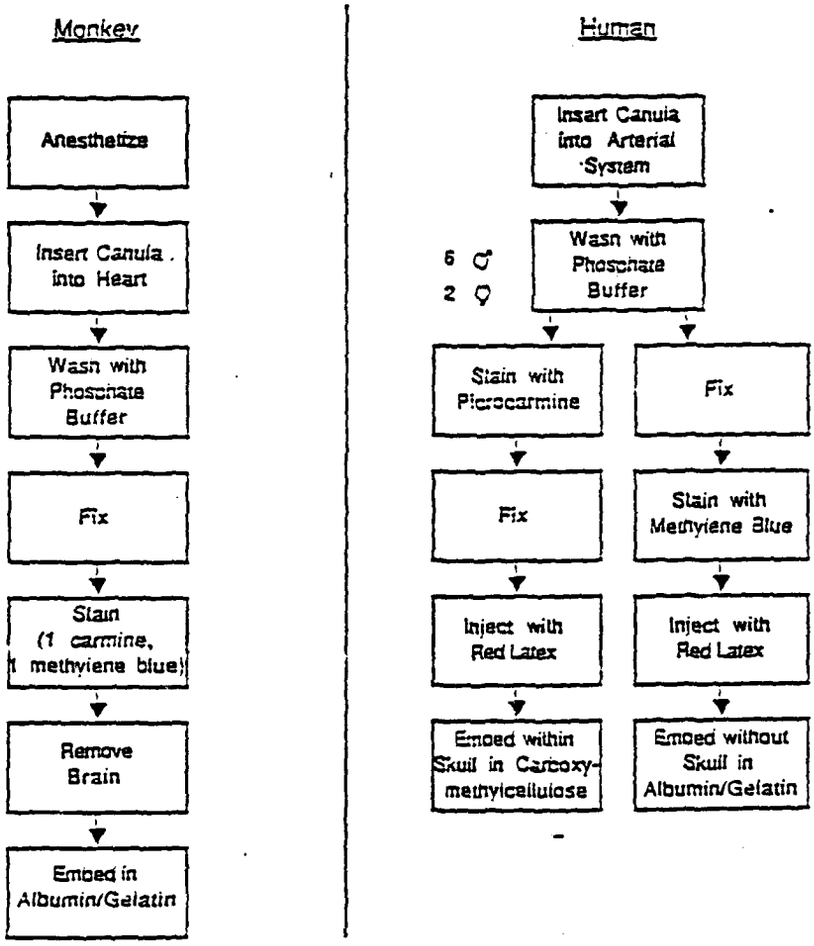

Figure 21 a. CONTOUR VIEW of top sequence of sections, taken at 1.1mm of a whole human brain, top view, anterior to the left. Reconstructions of this kind, detailed by hand digitization, are too labor-intensive to enable much science to be performed. When robust methods are worked out to enable fast, accurate machine reconstructions, it will be possible to make quantitative comparisons between brain and beteen the two hemispheres in the same brain. Asymmetries of this kind appear to be far more common than presently appreciated, where examination has been largely limited to measurements in areas of cerebral representation of language function. x = 0, y = 0.

Figure 21 b. This is a standard laser printer output for the same contours that were used for solid surface, shaded representation in Figure 21 a. x = 0, y = 0.

Figure 21

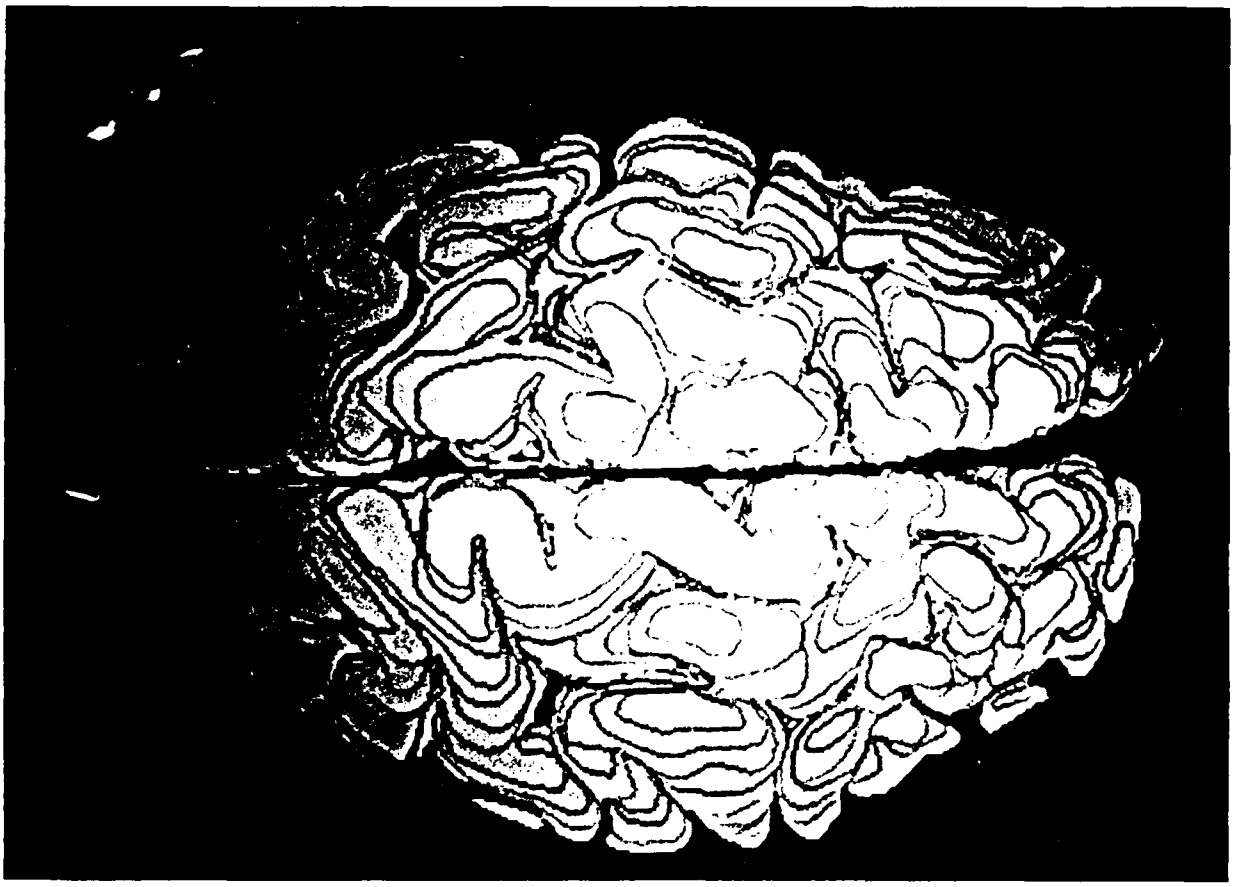

a

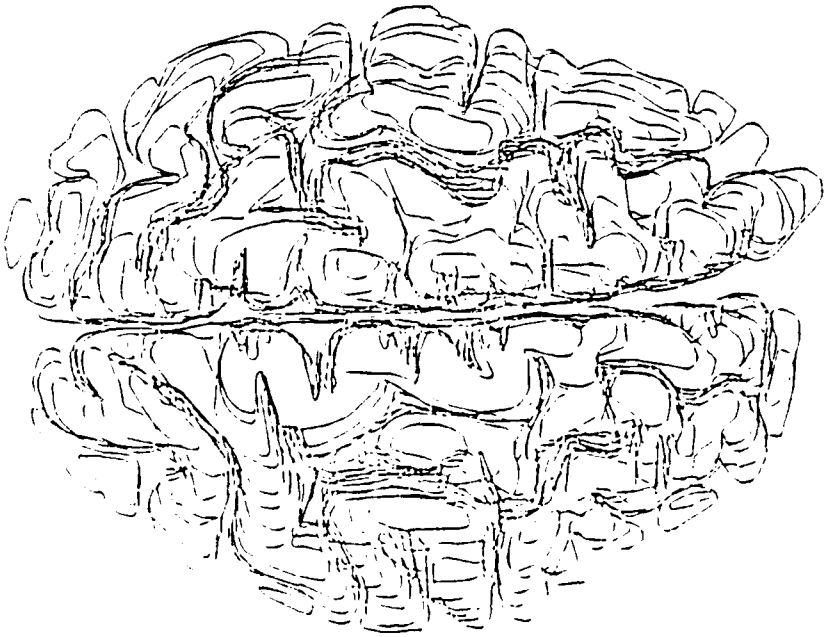

b

Figure 21 c. CONTOUR VIEW of a sequence of the lowermost representations of the cerebral hemispheres, seen from slightly to the left of midline, from below. Note that CONTOUR VIEW has some difficulties in tracing vector contours, made obvious by the straight lines. This difficulty is being corrected by Anthony Reynolds of Phildelphia, from whom we obtained the software. z = 210, y = 0.

Figure 21 d. Another view of the same data presented in Figure 21 c. The rotated view shows how some contours are effectively represented and how, when the straightline trouble begins, it can be appreciated in a variety of views. x = 120, y = 0.

Figure 21 (cont.)

c

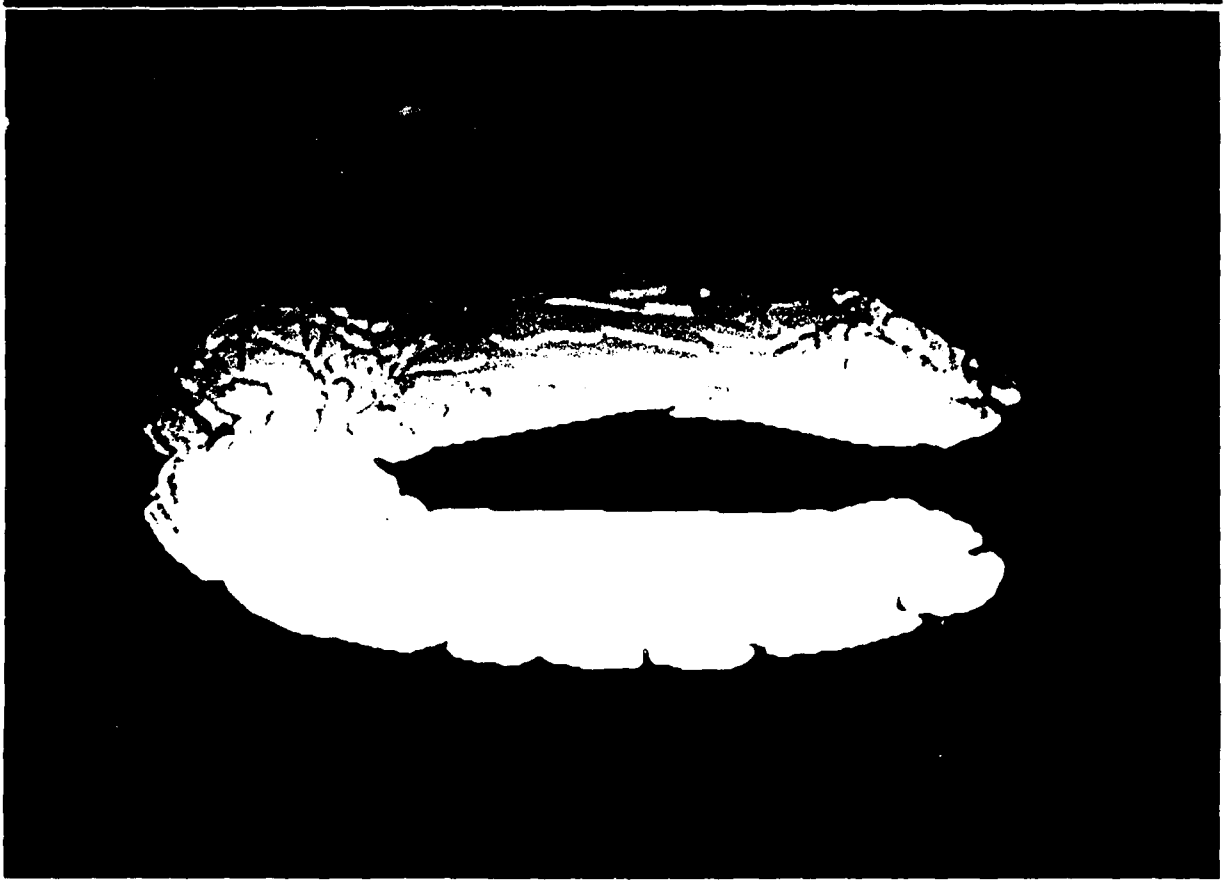

d

Figure 22 a. CONTOUR VIEW of three dimensionally reconstructed whole human cerebellum, perspective from x = 0, y = 0.

Figure 22 b. Wireframe three dimensional reconstruction of the same whole human cerebellum, same perspective.

Figure 22

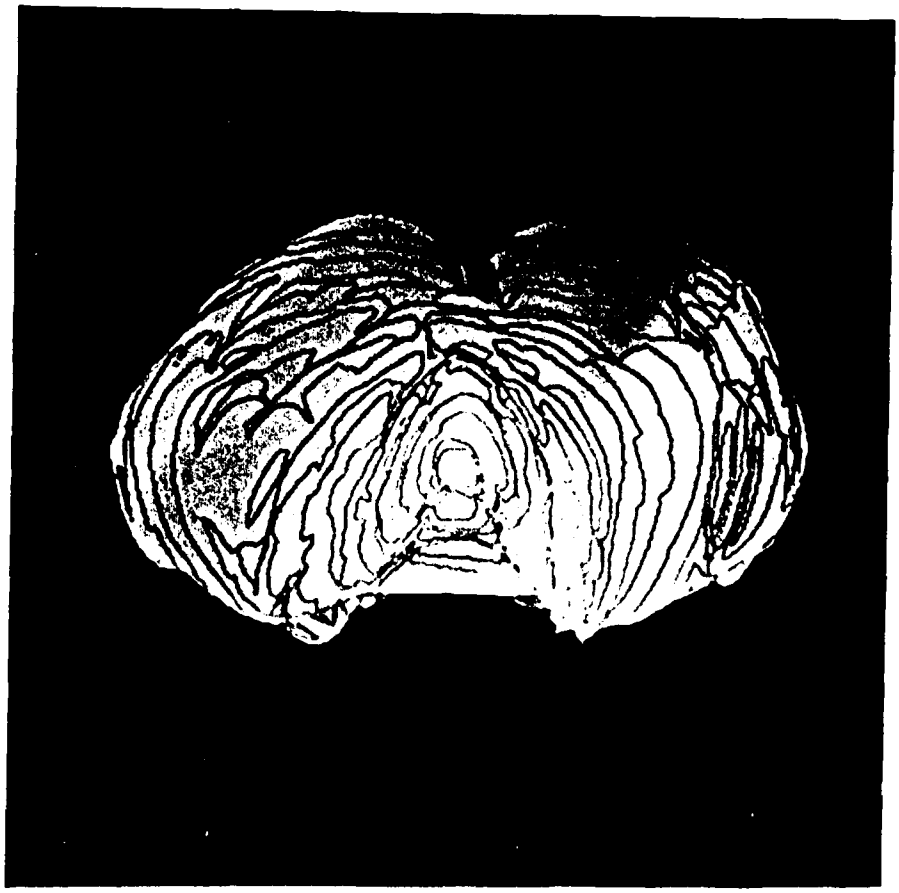

a

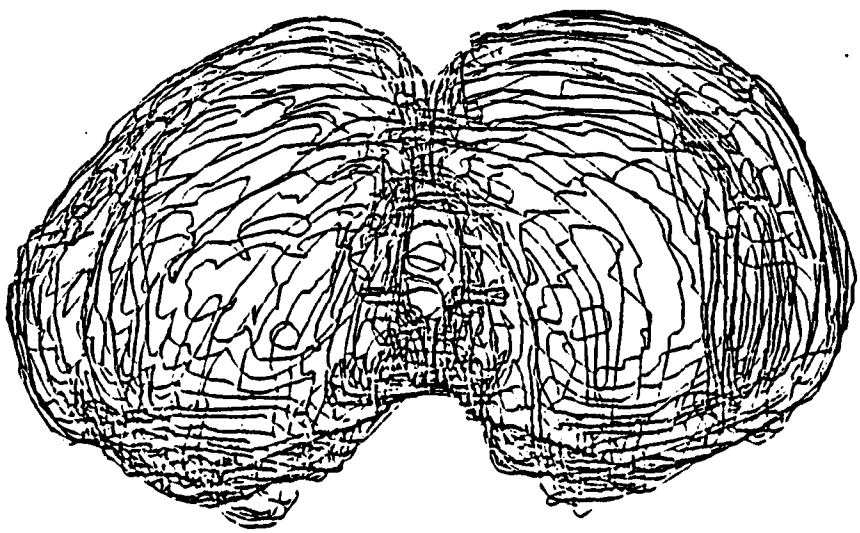

b

Figure 22 c. CONTOUR VIEW of whole human cerebellum, perspective x = 60, y = 120.

Figure 22 d. CONTOUR VIEW of uppermost sequence of layers of cerebral cortex, perspective x = 180, y = 60.

Figure 22 (cont.)

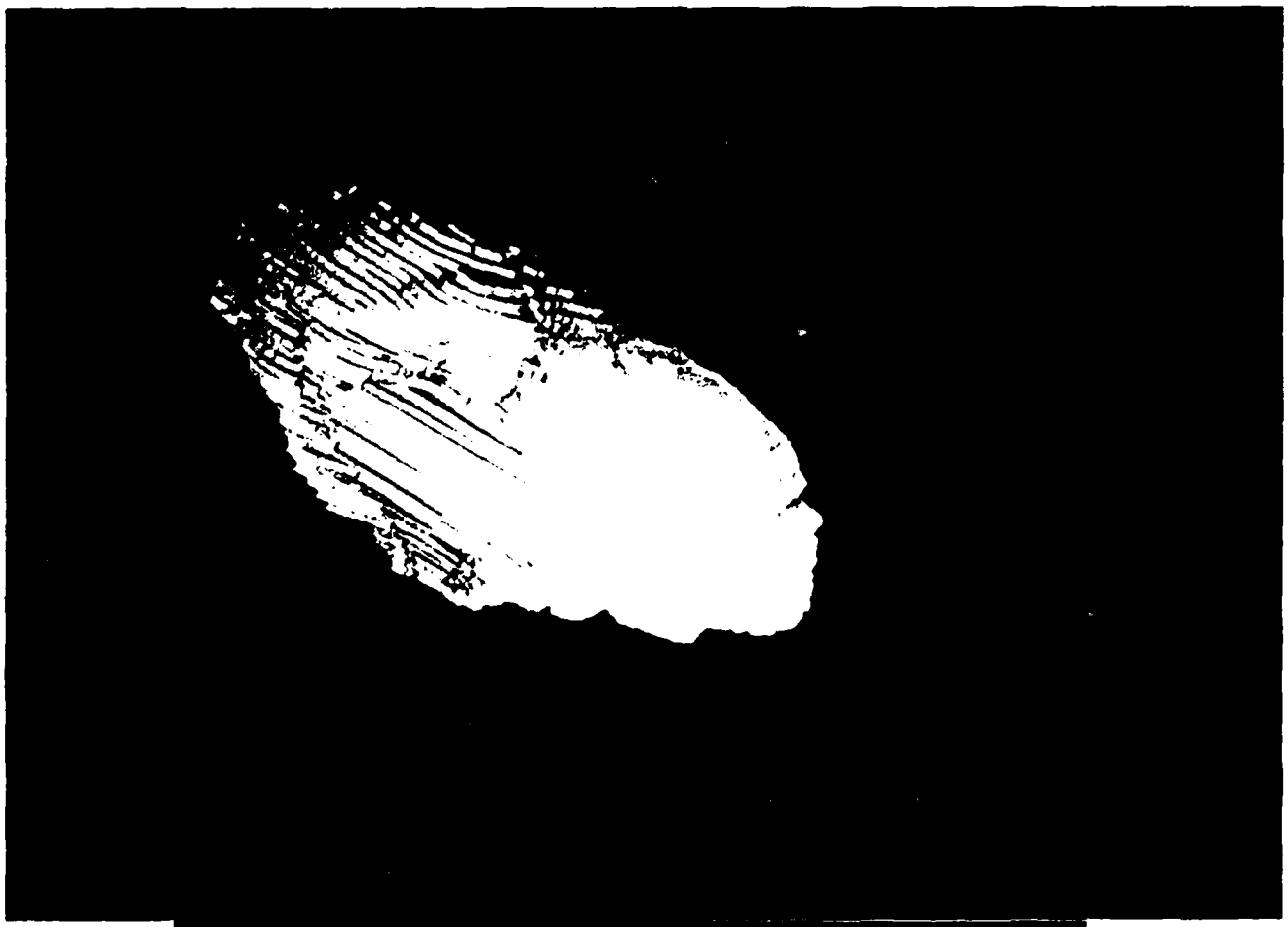

c

d

Figure 23 a. Wireframe three dimensional reconstruction of whole monkey thalamus, digitized from coronal sections by Xu, Luxi, Associate Professor of Anatomy, Beijing UNiversity School of Medicine, in the BMP laboratory. The midline surfaces of the reproduction do not mismatch, the ambiguity arises from the fact that the third ventricle was slightly curved. The domed surface at the top represents the bulge produced by the anterior nuclear group, limbic relay association nuclei. The inferior "horns" are produced by the lateral geniculate nuclei. Some other features can be made out on closer inspection, even from the wireframe reconstructions.

Figure 23 b. Similar wireframe view of whole monkey brain reconstruction based on horizontal sections, digitized by Xu. The thalamus is almost entirely inverted. The lateral geniculate bodies are seen at the upper right. Left is anterior. Perspective x = 130, y = 135.

Figure 23 c. Wireframe reconstruction from a third monkey, horizontal sections seen from below. A perspective of x = 0, y = 0. Although the thalamus represents only a small percentage of the whole brain, it has systemmatic two-way connections with all parts of the hemispheres and with subcortical structures and with hypothalamus and brain stem, so that it represents a miniature brain. Quantitative morphology of the whole thalamus will provide an excellent test bed for investigation of the whole brain.

Figure 23

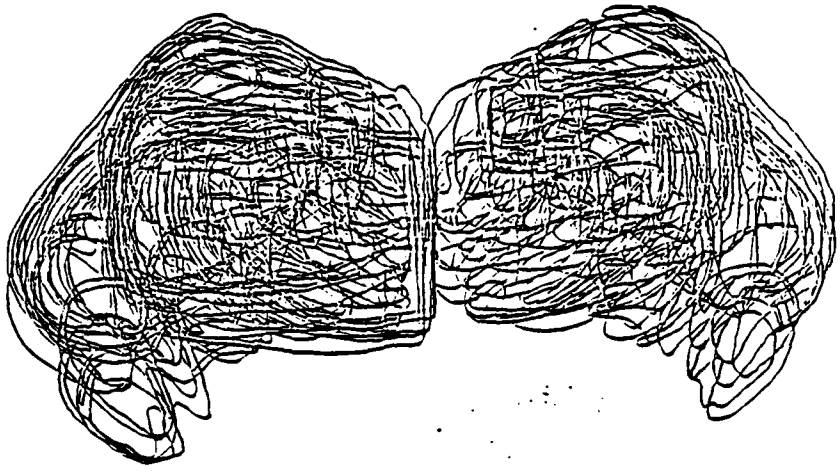

a

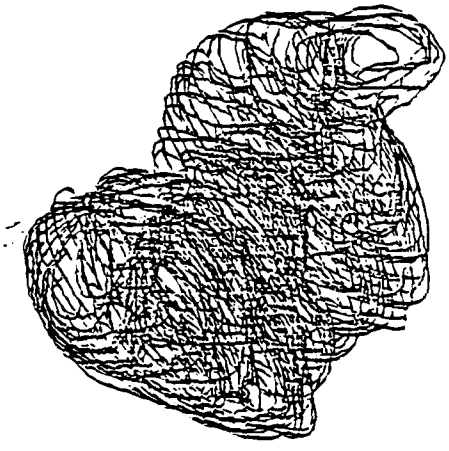

b

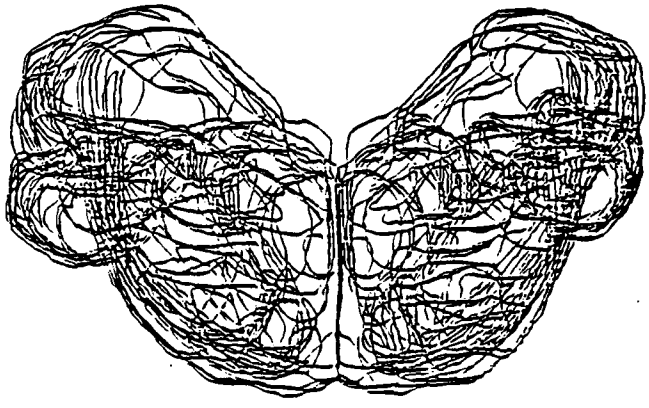

c

Figure 24 a. CONTOUR VIEW three dimensional reconstruction of whole monkey thalamus, digitized by Xu, coronal sections, posterior view, x = 0, y = 180.

Figure 24 b. Superior, angulated view of CONTOUR VIEW reconstruction of whole monkey thalamus, digitized by Xu. Perspective x = 200, y = 250.

Figure 24 c. CONTOUR VIEW of whole monkey thalamus seen from below. The lateral geniculate bodies are projected in the direction of the viewer, the right side, nearest, looks correspondingly paler because of the depth shading. Xu digitized 29 clearly identified sub-structures of the monkey thalamus in each of these animals. Programs allow rapid calculations of volume, surface area, centroid, spine, and other features of any given vector displayed structure. Perspective, x = 25, y = 165.

Figure 24

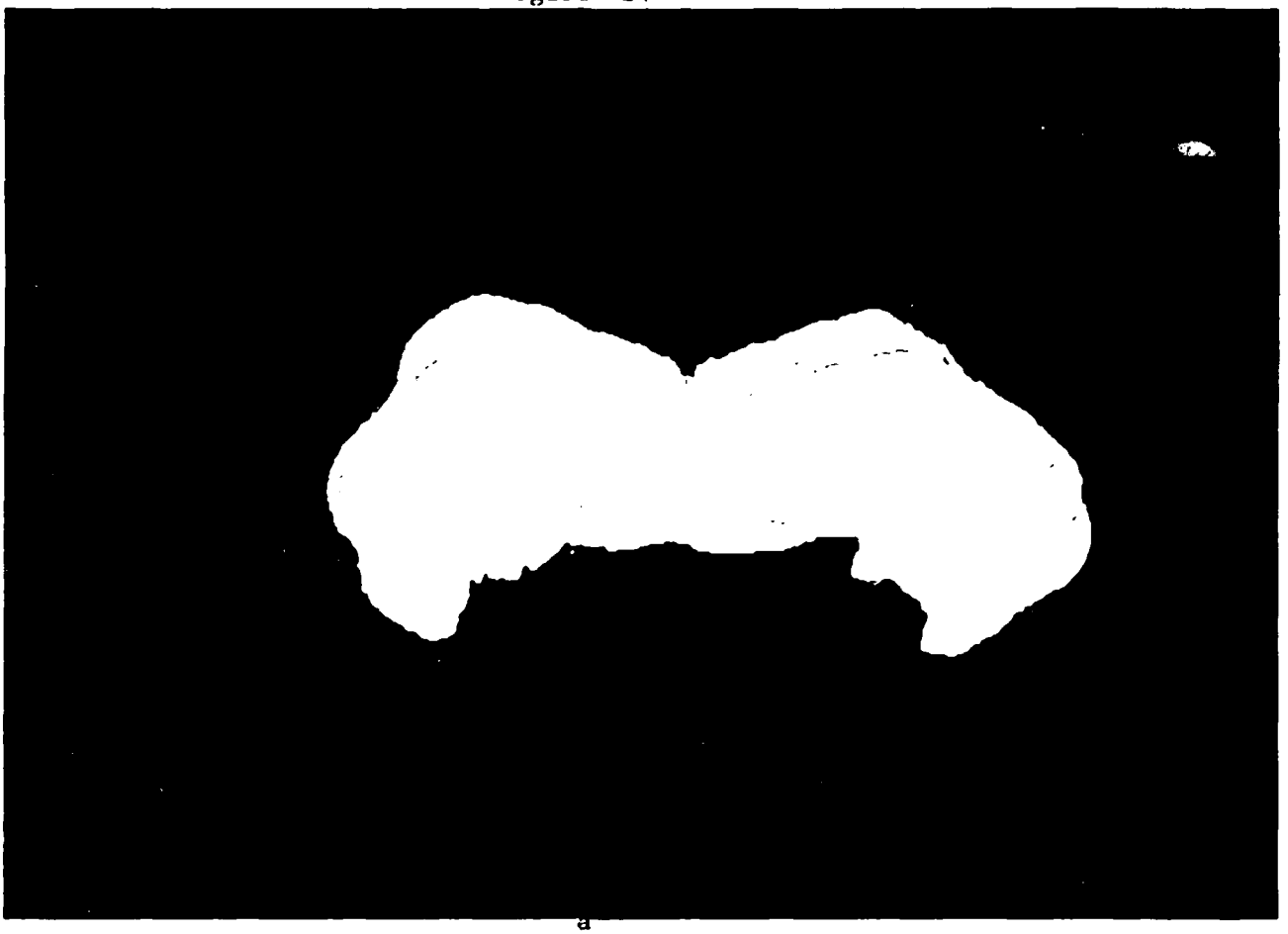

a

b

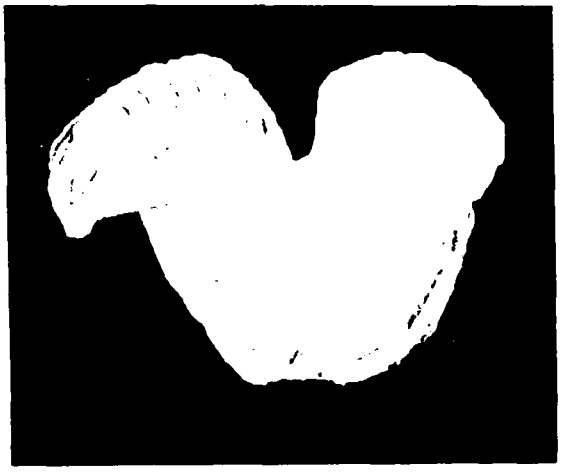

c

Figure 25:
Density of nAChR-positive ganglion cells in the chick retina. All numbers should be multiplied by 10 for density at each point. Circle indicates fovea. Scale bar = 1mm

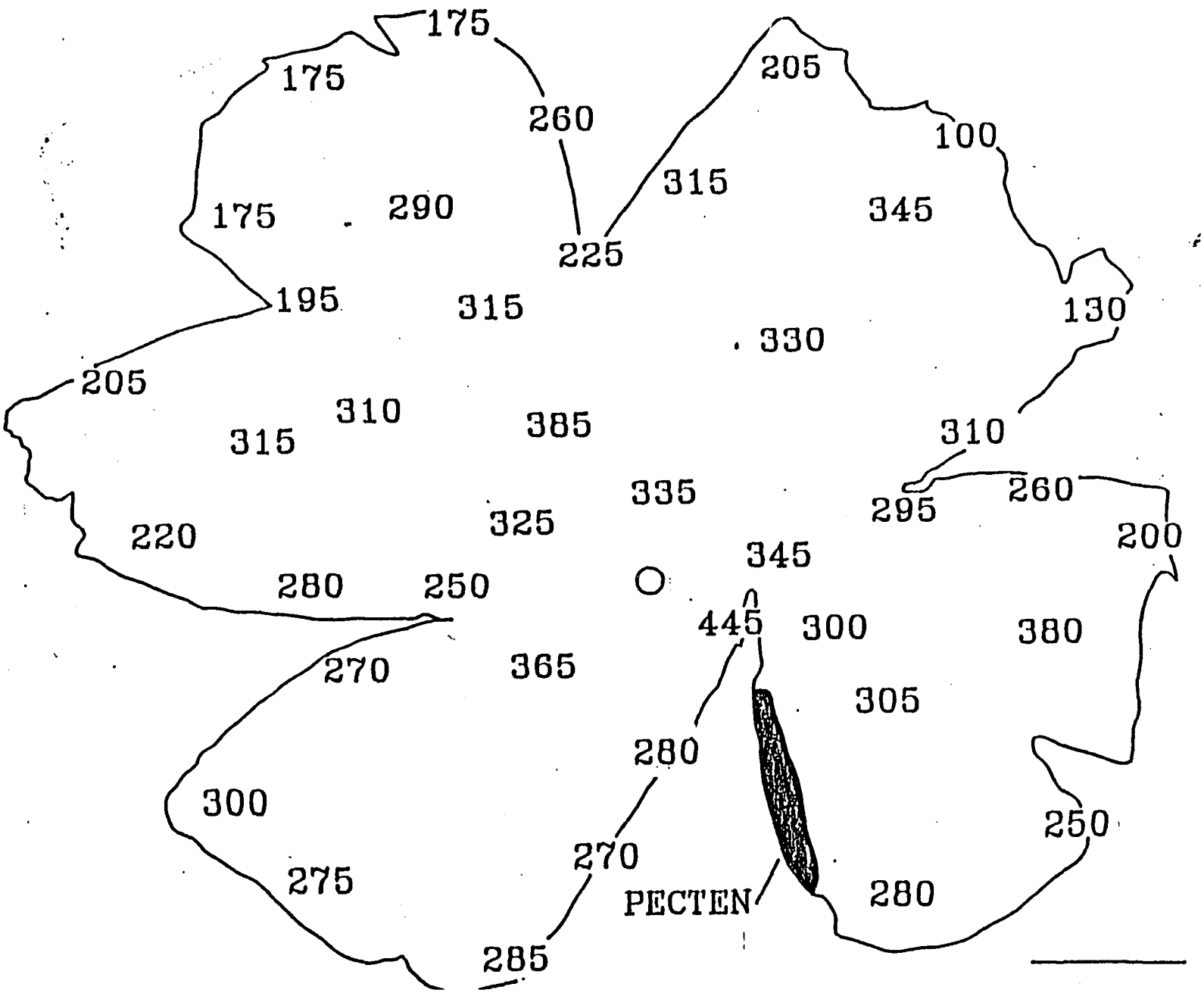

Figure 26:
The distribution of nAChR-positive displaced ganglion cells in the chick retina. Each dot corresponds to 1 cell. Scale bar = 1mm

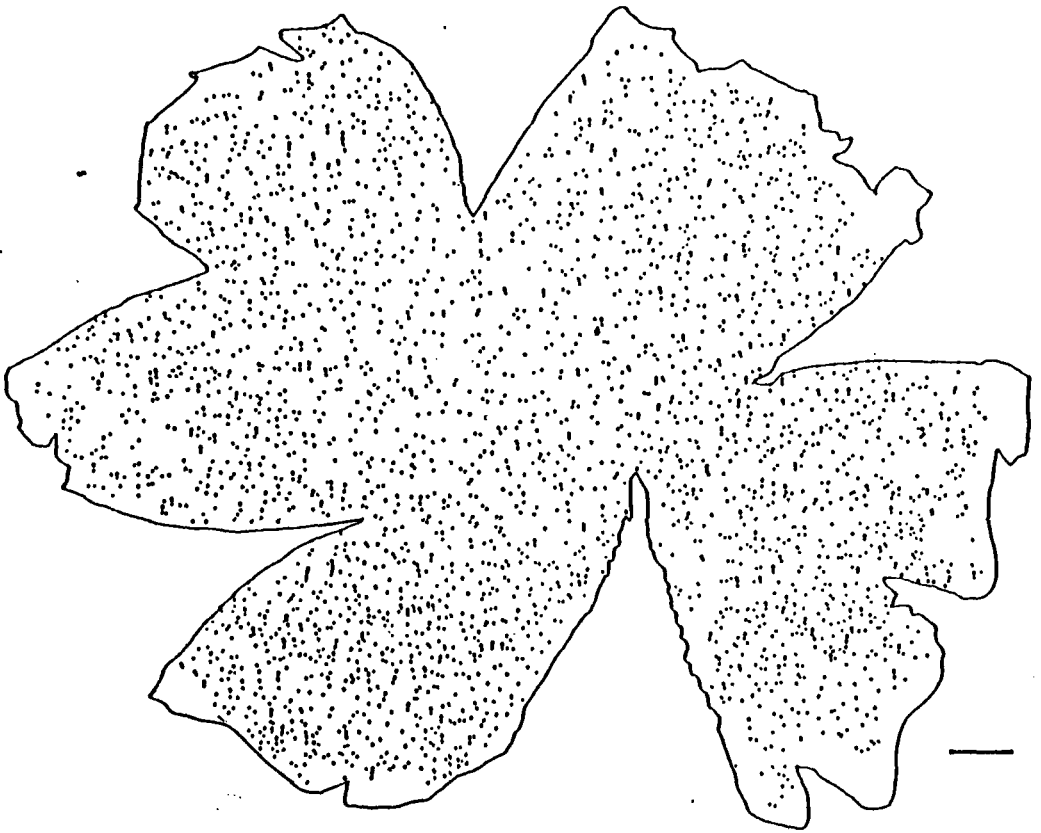

APPENDIX A

Participants in Task Definition Workshop

David Armstrong
Robert Barnhill
Floyd Bloom
Charles Bridgeman
Harry Carter
Shankar Chatterjee
Enrique Chung
Diana Clark
Wes Clark
Richard Colvin
Robert De Teresa
Jay Fillmore
John Folin
Michele Frost
Yuan-Cheng Fung
Sheldon Furst
Craig Goff
Sam Goldwasser
Glen Harding
Richard Hegge
John Hesselink
Dean Hillman
Harvey Karten
David Koons
Robert Livingston
Bruce McCormick
Don McEachron
Ted Melnechuck
Charles Molnar
John Morrison
Hossan Mostefair
Robert Nathan
Arthur Olson
Thomas Porter
R. Anthony Reynolds
Donald Roberts
Daniel Schlusselberg
Wade Smith
Larry Stensaas
David Talton
Arthur Toga
Bud Tribble III
John Williams
Donald J. Woodward
Michael Yen
Warren Young

Project Volunteers

Gary Berkowitz
Marney Blair
David Chabolla
Jessica Chou
James Conner
Jason Doctor
Deborah Forster
Carolyn Gennrich
Brian Hays
Margo Hoover
James Kapin
Erika Karagouri
Donald Knepper
John Konstanzer
Adar Pelah
Smadar Pelah
Arthur Shapiro
Richard Sharp
Luann Teschmacher
Lawrence Weber

Appendix B

A list has been compiled of the brain objects that were completed from Dr. Stensaas' work in the winter quarter of 1987. The objects were hand contoured from the drawings of brain number 118, the Yakolev collection. Then raw data files were aligned and made into objects.

When naming the structures we found that the program would only accept names of 14 characters or less. This list will help in identifing the structure to its actual name from the raw drawing list.

Brain SP-118 Objects

Actual Object Name	New E&S Version
N. anterioris thalami = Anterior Thalamic Nucleus	antthaln.ob 001
N.anterodorsalis thalami = Anterodorsal Thalamic Nucleus	antdorthl.ob 002
N.dorsalis superficialis thalami = Dorsal Superficial Thalamic Nucleus	dorsupthl.ob 003
N.centralis thalami = Centre Median of Luys	cenmedluy.ob 004
N.commisuralis = Reuniens Nucleus	reuniens.ob 005
N.ventralis oralis = Ventral Oral Thalamic Nucleus	venorthl.ob 006
Ventralis intermedius thalami = Ventral Intermediate Nucleus	venintmed.ob 007
N. paralemniscalis = Paralemniscal Thalamic Nucleus	paralemthl.ob 008
N. parafascicularis = Parafascicular Thalamic Nucleus	parafasthl.ob 009
N.geniculatus lateralis pars magnocellularis = Lateral Geniculate Large Cell Component	latgenlrg.ob 010
N. geniculatus medialis pars magnocellularis = Magnocellular Medial Geniculate Nucleus	magmedgen.ob 011

N. geniculatus medialis = Medial Geniculate Nucleus	medgen.ob 012
N. dorsalis posterioris thalami = Dorsal Posterior Thalamic Nucleus	dorposthl.ob 013
Ventralis intermedius thalami = Ventral Intermediate Nucleus	venintmed2.ob 014
N. dorsalis anterior thalami = Dorsal Anterior Thalamic Nucleus	dorantthl.ob 015
N. ventralis anterior thalami = Ventral Anterior Nucleus	venantthl.ob 016
N.medialis thalamic = Medial Thalamic Nucleus	medthl.ob 017
N. peripeduncularis = Praegeniculate Nucleus	praegenic.ob 018
N. pulvinaris = Pulvinar Nucleus	pulvinar.ob 019
N. reticularis principalis = Reticular Thalamic Nucleus	retthl.ob 020
N. faciculosus = Faciculous Nucleus	faciculosus.ob 021
N. ventralis posterior internus = VPI	venposint.ob 022
N. ventralis posterior pars medialis = VPM	venposmed.ob 023
N. endymalis = Endymalis Nucleus	endymalis.ob 024
N. periventricularis(paramedian) = Midline Thalamic Nucleus	midlinethl.ob 025
N.ventralis posterior thalami pars lateralis = VPL	venposlat.ob 026
N. zona incerta = Zona Incerta Principal Nucleus	zonincprn.ob 027
N. limitans = Supragenicuiate Nucleus	supragenic.ob 028

N. parataenialis = Nucleus of Stria Medullaris (check #039)	striamedul.ob 029
N. subhabenularis = Subhabenular Nucleus	subhabenul.ob 030
N.ventralis oralis thalami pars internis = VOI	venorint.ob 031
N. cucullaris = Central Superior Thalamic Nuclei	censupthl.ob 032
N. intralamellaris = Internal Medullary Lamina	intmedlam.ob 033
N. intralamelaris pars compacta = Large Cell Groups of the Internal Medullary Lamina	celgrpiml.ob 034
N. habenularis lateralis = Lateral Habenular Nucleus	lathabenul.ob 035
N. habenularis mixtocellularis = Intermediate Habenular Nucleus	inthabenul.ob 036
N. habenularis medialis = Medial Habenular Nucleus	medhabenul.ob 037
N. geniculatus lateralis pars mediocelluaris = Lateral Geniculate Medium Cell Layers	/#38 not found in archive/
N. zona incerta caudalis (submedialis) = Zona Incerta Caudal Nucleus	caudalzone.ob 040
041 is used as a registration mark	fuducial.ob 041

The objects in the table include the amygdala structures.

Brain SP-118 Objects

Actual Object Name	New E&S Version
N.basalis amygdali pars amgnocululari = Basal Large Cell Amygdaloid Nucleus	baslrgamy.ob 101
N. basalis amygdali = Basal Amygdaloid Nucleus	basamy.ob 102
N. lateralis amygdalii = Lateral Amygdalois Nucleus	latamy.ob 103
N. endopyriformis amygdali = Endopyriform Nucleus	endopyri.ob 104
Cortex periamygdaloidius = Periamygdaloid Cortex	periamycor.ob 112
N. corticalis amygdali (presubiculum) = Cortical Amygdaloid Nucleus	cortamy.ob 113
N. centralis amygdali = Central Amygdaloid Nucleus	cenamygd.ob 133
N. intercalatus amygdali = Intercalate Amygdaloid nucleus	interamygd.ob 134
N.medialis amygdali(prosubiculum) Medial Amygdaloid Nucleus	medamy.ob 117
Periamygolaloid (enter transition area)	tranperamy.ob 179

Cortex prepiriformis posteriorus = Posterior Olfactory Cortex	posolfcor.ob 125
N. accumbens septi Accumbens Nucleus	accumbens.ob 126
N. stria terminalis = Stria Terminalis Principal Nucleus	strtrmprn.ob 127
N. stria terminalis pars pericapsularis = Pericapsular Nucleus of Stria Terminalis	perstrtr.ob 128
N.stria terminalis pars commisuralis = Commisural Nucleus of Stria Terminalis	commisstri.ob 129
N. septi medialis pars ventralis = Medial Septal Nucleus	medseptal.ob 130
N. taenia tecta = Taenia Tecta	taentecta.ob 131
N. olfactorius anteriorus = Olfactory Trigone	olftrigone.ob 132
Cortex insularis = Insular Cortex (no match in archive)	insularcor.ob 135
N. septic lateralis = Lateral Septal Nucleus	lateralsep.ob 136
N. commisuralis anterior = Anterior Commissure Nucleus	antcommis.ob 137
N. septi triangularis = Triangualar Septal Nucleus	triseptal.ob 138
N. septi dorsalis interna = Dorsal Septal Nucleus	dorsalsep.ob 139
Basalis pars compacta Nucleus of Meynert	basparcom.ob 140
terminal vein (anterior)	terantvn.ob 141
terminal vein (posterior)	terposvn.ob 142
septal vein	septalvein.ob 143
great emmissary vein	gremmisvn.ob 144

stria terminals	striaterm.ob 145
taenia tecta (anterior)	taentecta.ob 146 131 149
fornix	fornix.ob 147
dorsal medial septal nucleus	dormsepta.ob 147
taenia tecta (posterior)	taentecta.ob 146 131 149
posterior horn of lateral ventricle 150 151 152 lateral surface ventricle III	latvenhorn.ob
subarachnoid space temporal lobe	tempsubara.ob 153
ventricular choriod plexus of posterior horn	vechplexu.ob 154
pineal body (exterior surface) 155 156	pinealbody.ob
subventricular zone of caudate nucleus	subvcaudat.ob 157
ventricular Neuroepithelium	venneuroep.ob 158
no archive extra-ventricular Neuroepithelium	159
no archives Neuroepithelial Peduncle (NeP.VentIV)	160
Globus Pallidus (outer)	glopallid.ob 161 166

The objects in the table are a continuation of the Telecephalic (forebrain) cu's.

Brain SP-118 Objects

Actual Object Name	New E&S Version
N. anterior Comm (posterior)	antecomm.ob 162
Posterior cerebral Artery (posterior temporal)	poscerebar.ob 163
Anterior cerebral Artery (Anterior temporal)	antcerebar.ob 164
Aqueduct of Slyvus(IV Ventricle)	ventrice??.ob 165
Globus Pallidus (inner)	see 161
Nucleus Basalis (medial)	nucbasal.ob 167
Nucleus Basalis (anterior)	nucbasal.ob 168
subarachnoid space (anterior)	antsubarac.ob 169
olfactory tuberole (posterior)	olfatubero.ob 170
claustrum (medial)	see 108 171
subarachnoid space (velum interpostion thalamic?)	velumsubar.ob 172
claustrum (anterior)	see 108 173
N. commisuralis anterior (most anterior)	see 137 174
N. centralis amygdali no match	175
N. intercalatus (anterior-medial)	cenamygd.ob 176/182/134

Anterior Comm see 162	antecomm.ob 177
Basalis pars compacta Nucleus of Meynert	basparcom.ob 178/140
cornu ammonic Hippocampus	corammonhi.ob 180
transitional subiculum	transsubic.ob 181
N. intercalatus	cenamygd.ob 182/134/176
subarachnoids pons & cerebral	see 190 183
middle cerebral artery	midcerebar.ob 184
posterior cerebral (anterior)	postcereba.ob 185
pituitary posterior	pituitarpo.ob 186
subiculum horn (anterior) 114/119	subiculum.ob 187
internal carotid artery	intcarotid.ob 188
Basilar Artery	basilarart.ob 189
cerebellum	cerebpons.ob 190/183
posterior pituitary	pituitarpo.ob 191
hippocampal basal	hippobasal.ob 192/153
posterior inferior cerebellar artery	picaart.ob 193
vertebral artery	vertebrala.ob 194

This list compiles all the hypothalamic cu's from brain 118.

Brain SP-118 Objects

Actual Object Name	New E&S Version
N. infundibularis = Infundibular Nucleus	infundibul.ob 201/216
N. paraventricularis = Paraventricular Nucleus	paraventnu.ob 203
N. prothalamicus principalis = Preoptic Nucleus	preoptic.ob 204/216
N. latrealis hypothalamicus = Lateral Hypothalamic Nucleus	lathypotha.ob 205
N. mammilaris medialis = Medial Mammilary Nucleus	medmammil.ob 206
N. mammilaris lateralis = Lateral Mammilary Nucleus	latmammil.ob 207
N. posterioris hypothalami = Ventral Tegmental Area of Tsai	ventegtsa.ob 208
N. dorsomedialis hypothalami = Dorsomedial Hypothalamic Nucleus	dorhypothl.ob 209
N. supraopticus = Supraoptic Nucleus	supraoptic.ob 210/218
N. tuberis lateralis = Lateral Tuberal Hypothalamic Nucleus	lattubhyp.ob 211
N. tuberomamillaris = Tuberomamillary Nucleus	tuberomam.ob 212
N. ventromedialis hypothalami = Ventromedial Hypothalamic Nucleus	venmedhyp.ob 213
N. parafornicalis = Perifornical Nucleus	periforn.ob 214 (nomatch)
N. ovoideus prothalamicus = Ovoid Preoptic Nucleus	ovoidpreop.ob 215
N. infundibularis = Infundibular Nucleus (nomatch, possibly is #201)	infundibul.ob 216/201

N. prothalamicus principalis = anterior projection	preoptic.ob 217/124
N. supraopticus = Supraoptic Nucleus (lateral)	subraoptic.ob 218/210
Mamilothalamic tract no archive	mamiloth.ob 219
Suboptic neurohemal area no archive	subopneur.ob 220
N. Suprachiasmaticus no archive	supramatic.ob 221

This list compiles all the mesencephalic cu's from brain 118.

Brain SP-118 Objects

Actual Object Name	New E&S Version
N. interstitialis Cajal's = Cajal's Nucleus	cajalsnuc.ob 301
N. colliculi inferioris = Inferior Colliculus	infcollic.ob 302
N. colliculi superioris = Superior Colliculus	subcollic.ob 303
N. cuneiformis Cuneiform Nucleus	cuniform.ob 304
N. intracapsularis = Intracapsular Nucleus	intracapsul.ob 305
N. substantia nigra pars compacta = Substantia Nigra	subnigcom.ob 306
N. paranigralis = Paranigral Nucleus	paranigral.ob 307
N. parabrachialis pigmentosus = Parabrachial Pigmented Nucleus	parabrach.ob 308
N. trochlearis = IV Nucleus (no match see 401)	trochlearis.ob 309
N. Edinger-Westphal = Edinger Westphal Nucleus	edingerwes.ob 310
N. oculomotorius caudalis centralis = Caudal Oculomotor Nucleus	caudoclmot.ob 311
N. oculomotorius principalis Oculomotor Nucleus	oculomotor.ob 312
Grisium centrale mesencephali Periaqueductal Gray	peraqdctal.ob 313
no number 314	
N. linearus posteralis = Linear Posterior Nucleus	linearpos.ob 315

N. ruber Red Nucleus	rednuc.ob 316
Griseum centrale mesencephali subnucleus dorsalis = Dorsal Periaquctal Gray	dorpraqdct.ob 317
no number 318	
N. trigemini mesencephalicus Mesencephalic V Nucleus	mesenphal.ob 319
N. parabrachialis pigmentosos Posterior Medial	parabracme.ob 320
N. Edinger-Westphal Anterior Medial	edinwespha.ob 321
##### ######	#####.ob 322
##### ######	#####.ob 323
##### ######	#####.ob 324
##### ######	#####.ob 325
##### cerebellar hemisphere	#####.ob 340

This list compiles all the ponscytoarchitectural cu's from brain 118.

Brain SP-118 Objects

Actual Object Name	New E&S Version
N. trochlearis = Nucleus IV same object as 309	trochlearis.ob 401
N. pontis centralis oralis = Central Oral Pontine Nucleus	ceoralpon.ob 402
N. centralis superior = Central Superior Nucleus	censupnuc.ob 403
N. dentatus = Dentate Nucleus of Cerbellum	dencerebel.ob 404
N. globusus Globuse Nucleus	globosenu.ob 405
N. emboliformis = Emboliformis Nucleus	embolifnu.ob 406
N. fastigialis = Fastigial Nucleus	fastigial.ob 407
N. cochlearis dorsalis Dorsal Cochlear Nucleus	dorcochle.ob 408
N. cochlearis ventralis Ventral Cochlear Nucleus (see if this object is made)	vencochle.ob 409
N. locus coerulus Locus Coerulus	loccoerul.ob 410
no number 411	
N. subcoerulus Subcoerulus Nucleus	subcoerul.ob 412
N.pedunculopontinus tegmenti subnucleus dissapatus Pedunculopontine Nucleus	pedunculpon.ob 413
N. facialis = Facial Nucleus	facial.ob 414

QML	Object List
N. interpeduncularis subnucleus dorsalis = Dorsal Interpeduncular Nucleus	dorintped.ob 415
N. interpeduncularis subnucleus medialis = Medial Interpeduncular Nucleus	medintped.ob 416
N. lemnisci lateralis Nucleus of Lateral Lemniscus	latlemnsc.ob 417
N. ovalis Oval Reticular Nucleus	ovalretic.ob 418
N. parabrachialis lateralis/sagulum = Lateral Parabrachial Nucleus	latparbrch.ob 419
N. parabrachialis medialis = Medial Parabrachial Nucleus	medparbrch.ob 420
N. Gudden = Nucleus of Gudden	gudden.ob 421
N. griseum pontis = Pontine Gray	pontinegry.ob 422
N. preipositus hypoglossi = Prepositus Nucleus	prepositus.ob 423
N. interpeduncularis subnucleus lateralis = Lateral Interpeduncular Nucleus *(no match)*	latintped.ob 424
N. raphe pontis = Raphe Pontis	raphepont.ob 425
N. raphe dorsalis/supratrochlearis = Raphe Dorsalis	raphedors.ob 426
N. papillioformis Raphe Magnus	raphemag.ob 427
N. olivaris superior medialis = Medial Superior Olive	medsupolv.ob 428
no number 429,430,431	
N. tractus spinalis trigemini oralis = Spinal V Oralis	spinalvor.ob 432
N. trigemini sensibilis principalis Principal Sensory V Nucleus	prncsensv.ob 433

	N. trigemini motorius Motor Nucleus V	motornucv.ob 434
	Griseum centrale pontis = Central Pontine Gray	cenpongry.ob 436 (no 435)
	N. vestibularis superior = Superior Vestibular Nucleus	supvestib.ob 437
	N. vestibularis medialis = Medial Vestibular Nucleus	medvestib.ob 438
	N. vestibularis lateralis = Lateral Vestibular Nucleus	latvestib.ob 409
	N. vestibularis spinalis = Spinal Vestibular Nucleus	spinvestib.ob 409
	N. olivaris superior lateralis Lateral Superior Olive	latsupolv.ob 409
	N. trapezoidalis = Trapezoid Nucleus	trapezoid.ob 445
	N. supragenicularis = Supragenicular Nucleus	supragenic.ob 446
	no number 447,448	
	N. vestibularis subnucleus "Z" = Vestibular Nucleus Z	vestib2.ob 449
	N. corporis pontobublaris Accessory Pontine Gray	accpongry.ob 450
	the following structures are unclear names	
6)	N. raphe dorsalis Anterior Dorsal	raphedors.ob 451 (see #42
	N. vestibularis interstitialis = Interstitial vestibular nucleus(subnucleus "rabbit")	#####.ob 453
	no 447 or 542	
	N. abduscens = Nucleus VI	#####.ob 454
	the following names are all unclear	
	????? ?????	##.ob 455
	no 456 ?????	##.ob 454

Dentate Nucleus Cerebellum ##.ob 457
?????

Anterior Ver ##.ob 458
?????

Post Ver????? ##.ob 459
?????

This list compiles all the rhombencephalon cu's from brain 118.

Brain SP-118 Objects

Actual Object Name	New E&S Version
N. ambiguus/retroambiguus = Nucleus Ambiguus	ambiguus.ob 501
N. centralis medullai oblongatae = Central Reticular Nucleus of Medulla	cenretmed.ob 502
N. gigantocellularis = Gigantocellular Nucleus	gigantocell.ob 503
N. cuneatus = Cuncate Nucleus	cuneatus.ob 504
N. gracilis = Gracile Nucleus	gracile.ob 504
N. hypoglossi = XII Nucleus	xiinuc.ob 504
N. olviaris inferior principalis = Inferior Olive	infolive.ob 504
N. olivaris inferior accessorius dorsalis = Dorsal Accessory Olive	doraccolv.ob 504
N. olivaris inferior accessorius medialis = Medial Accessory Olive	medaccolv.ob 504
N. lateralis medullae oblongatae,subnucleus ventralis = Lateral Ventral Reticular Nucleus of Medulla	lvretmed.ob 504
N. parvocellularis = Parvocellular Reticular Nucleus	parvoretnu.ob 512
N. raphe obscuris = Raphe Obscuris	rapheobscu.ob 514
N. Roller Nucleus of Roller	nuclroller.ob 515

N. supraspinalis = Supraspinal Nucleus	supraspinal.ob 516
N. tractus spinalis trigemini caudalis,subnucleus gelatinosus = Spinal V Gelatinosa	gelatinosa.ob 517
N. tractus spinalis trigemini caudalis,subnucleus magnocellularis = Spinal V Magnocellular	magnocellv.ob 518
N. tractus spinalis trigemini caudalis,subnucleus zonalis = Spinal V Zonalis	zonalisv.ob 519
N. tractus spinalis trigemini interpolaris = Spinal V, Interpolaris	interpolis.ob 520
no number 521	
N. raphe pallidus = Raphe Pallidus	nraphepal.ob 522
N. cunteatus lateralis = External Cuneate	extcuneate.ob 523
N. tractus solitarii Solitary Nucleus	solitarnuc.ob 524
N. dorslais motorus vagi Dorsal Motor X	motdorsalx.ob 525
Area postrema Area Postrema	postrema.ob 526
N. centralis medullae oblongatae subnucleus neuromelanosum = Central Pigmented Reticular Nucleus of Medulla	cenreimed.ob 527
no numbers 528-535	
Stratum gliosum subepedymale medullae oblongatae = Ventricular Gray of Medulla not found on list	vengramed.ob 536
N. paragigantocellularis Paragigantocellular Nucleus	pargigantce.ob 542

Ventricle IV see tele*object 165	ventricle5.ob
N. cunceatus laterlis = Ventral Accessory and ventre-medial accessory	venmedlat.ob 544/545
Vertebral Artery check #tele*194	vertebral.ob 546

APPENDIX C

REFERENCES BASED ON ADVANCEMENTS DEVELOPED DURING THE PERIOD OF ARMY SUPPORT OF THE BRAIN MAPPING PROJECT

Armstrong, D.M., Hersh, L.B. and Gage, F.H., Morphologic alterations of cholinergic processes in the neocortex of aged rats, Neurobiol. Aging, [In Press], 1988.

Armstrong, D.M., Terry, R.D., Deterera, R.M., Bruce, G., Hersh, L.B., and Gage, F.H. Response of septal cholinergic neurons to axotomy, J. Comp. Neurol., 264:421-436, 1987.

Britto, L.R.G., Keyser, K.T., Hamasswaki, D.E., and Karten, H.J., Catecholaminergic subpopulation of retinal displaced ganglion cells projects to the accessory optic nucleus in the pigeon (Columba livia). J. Comp Neurol., 269:109-117, 1988.

Buzsaki, G., Bickford, R., Armstrong, D.M., Ponomareff, G., Chen, K.S., Ruiz, R., Thal, L., and Gage, F.H., EEG activity in the neocortex of freely moving young and aged rats, J. Neurosci., [In Press], 1988.

Campbell, M.J., Lewis, D.A., Benoit, R., and Morrison, J.H., Regional heterogeneity in the distribution of somatostatin-28 and somatostatin-28(1-12)-immunoreactive profiles in monkey cortex, J. Neuroscience, 7:1133-1144, 1987.

de Lima, A.D., Bloom, F.E., and Morrison, J.H., Synaptic organization of serotonin-immunoreactive fibers in primary visual cortex of macaque monkey, J. Comp. Neurol., [In Press], 1988.

Ehrlich, D., Keyser, K., and Karten, H.J., Distribution of substance P-like immunoreactive retinal ganglion cells and their pattern of termination in the optic tectum of the chick (Gallus gallus). J. Comp Neurol., 266:220-233, 1987.

Ehrlich, D., Keyser, K., Manthorpe, M., Varon, S., and Karten, H.J., Differential effects of axotomy on substance P-containing and nicotinic acetylcholine receptor-containing retinal ganglion cells: Time course of degeneration and effects of nerve growth factor. Neuroscience. [Submitted] 1988.

Gage, F.H., Armstrong, D.M., Williams, L.R., and Varon, S., Morphological response of axotomized septal neurons to nerve growth factor, J. Comp. Neurol., [In Press], 1988.

Gage, F.H., Chen, S.H., Buzsaki, G., and Armstrong, D.M., Experimental approaches to age-related cognitive impair-

ments, Neurobiol. Aging, [In Press], 1988.

Higgins, G.A., Lewis, D.A., Bahmanyar, S., Goldgaber, D., Gajdusek, D.C., Young, W.G., Morrison, J.H., and Wilson, M.C., Differential regulation of amyloid beta-protein messenger RNA expression within neuronal subpopulations of the hippocampal formation in Alzheimer's Disease, Proc. Natl. Acad. Sci. (USA), 85:1297-1301, 1988.

Keyser, K., Karten, H.J., Katz, B., and Bohn, M.C., Catecholaminergic horizontal and amacrine cells in the ferret retina. J. Neurosci., 7:3996-4004, 1987.

Keyser, K.T., Hughes, T.E., Whiting, P.J., Lindstrom, J.M., and Karten, H.J., Cholinoceptive neurons in the retina of the chick: an immunohistochemical study of the nicotinic acetylcholine receptors. Visual Neuroscience. [In Press], 1988.

Lemere, C.A., Wurtz, C., and Livingston, R.B., Whole-brain mapping: strategies for the construction of "nested" computerized atlases, Neurosci. Abstracts, 13:146.19, 1987.

Lewis, D.A., Campbell, M.J., Terry, R.D., and Morrison, J.H., The laminar and regional distributions of neurofibrillary tangles and neuritic plaques in Alzheimer's Disease: A quantitative study of visual and auditory cortices, J. Neuroscience, 7:1799-1808, 1987.

Lewis, D.A., Higgins, G.A., Young, W.G., Goldgaber, D., Gajdusek, D.C., Wilson, M.C., and Morrison, J.H., The distribution of amyloid beta-protein messenger RNA in human cerebral cortex: Relationship to neurofibrillary tangles and neuritic plaques, Proc. Natl. Acad. Sci. (USA), 85:1691-1695, 1988.

Toga, A.W., and Arnicar, T.L., Digital image reconstruction for the study of brain structure and function, Journal Neurosci. Methods, 20:7-21, 1987.

Toga, A.W., and Arnicar-Sulze, T.L., Three dimensional reconstruction of brain physiology, Innovation et Technologie en Biologie et Medecine, 8(1):92-103, 1986.

Toga, A.W., Arnicar, T.L., and Samaie, M., Three dimensional reconstruction and display of subcortical seizure processes, Neurosci. Abstracts, 12:111, 1986.

Toga, A.W., Samaie, M., Arnicar-Sulze, T.L., and Studt, J.W., Digital rat brain: A computerized stereotaxic atlas, Neurosci. Abstracts, 13:529, 1987.

END
DATE
9-88
DTIC